

History of Deep-Inelastic scattering (Collinear PDFs from past, present and future data)

E. Tassi

Universita' della Calabria and INFN-Cosenza

First European Summer School on the Physics of the Electron-Ion Collider
18-22 June 2023 – Corigliano-Rossano, Italy

Outline (Lecture 2)

Pre-history...

- Part I (Fixed-target Experiments)
 - Quark model
 - SLAC-MIT Coll.
 - Parton model
 - Gargamelle
 - pQCD and QCD-improved parton model
- Part II (HERA and LHC)
 - Highlights
 - PDFs and LHC
- Part III (EIC)
 - Studies on collinear PDFs

Pre-History (1909-1960)

- Rutherford scattering
- Atomic nucleus
- Protons and neutrons
- Magnetic moments (p & n)
- Strong force
- Form factors



See supplementary material



Nobel prize 1908

Rutherford Scattering

“The most famous fixed-target experiment of all time:”

Rutherford taught us the most important lesson:
the use of a scattering process to investigate the structure of matter

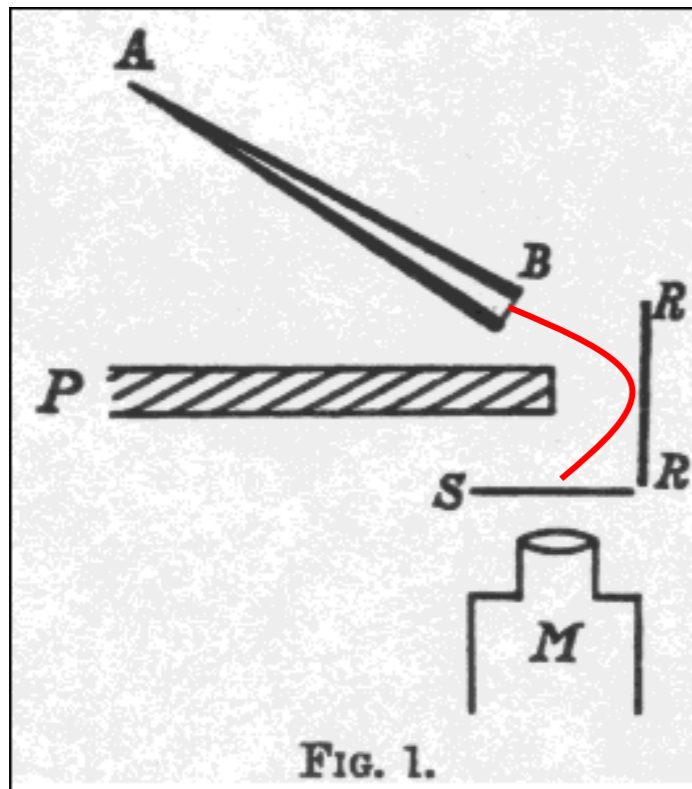
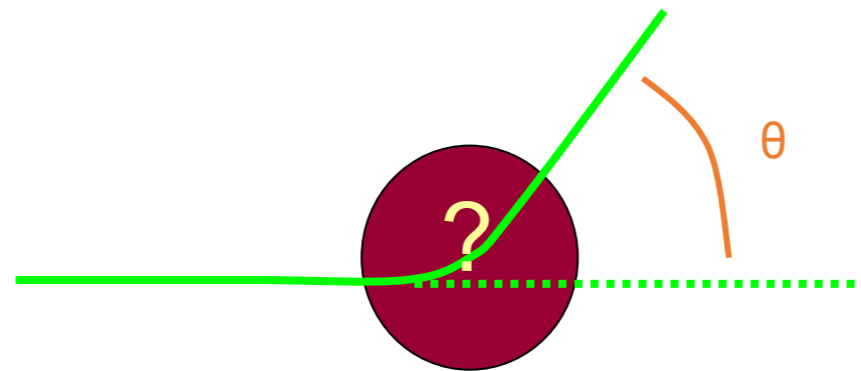


FIG. 1.

H. Geiger and E. Marsden observed the high-angle scattering ($\theta > 90^\circ$) alpha particles deflected by a thin gold foil.

Proc. Roy. Soc. **A 82**, 495, 1909

Rutherford interpreted the results as due to the scattering of alpha particles from a massive central charge

$$\sigma(\theta) = \frac{z^2 Z^2 e^4}{16E^2} \frac{1}{\sin^4 \frac{1}{2}\theta}$$

Phil. Mag. **21**, 669, 1911

Ernest Rutherford



“In our laboratory today we live in an atmosphere deemed with the flying fragments of exploding atoms and on this occasion I wish to say a few words on the methods and ideas employed to break up atoms and realize...the old dream of alchemists of transmutation of one element into another...”

You tube Link. : https://www.youtube.com/watch?v=zBHD8ksx_Sg

Linacs at the Stanford University

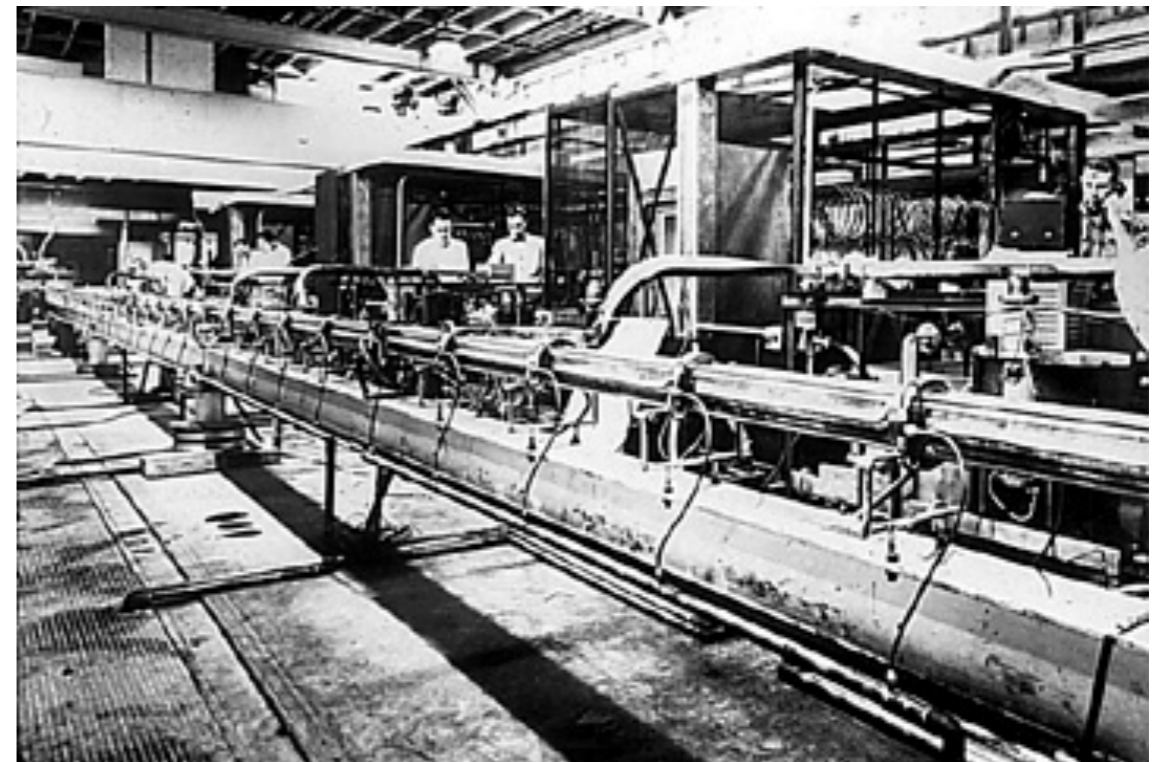


In the mid-1930s, the Varian brothers (research assistants at the microwave department of Stanford University) developed the 'klystron' using a special electromagnetic cavity (Rhumbatron) invented by W. Hansen.

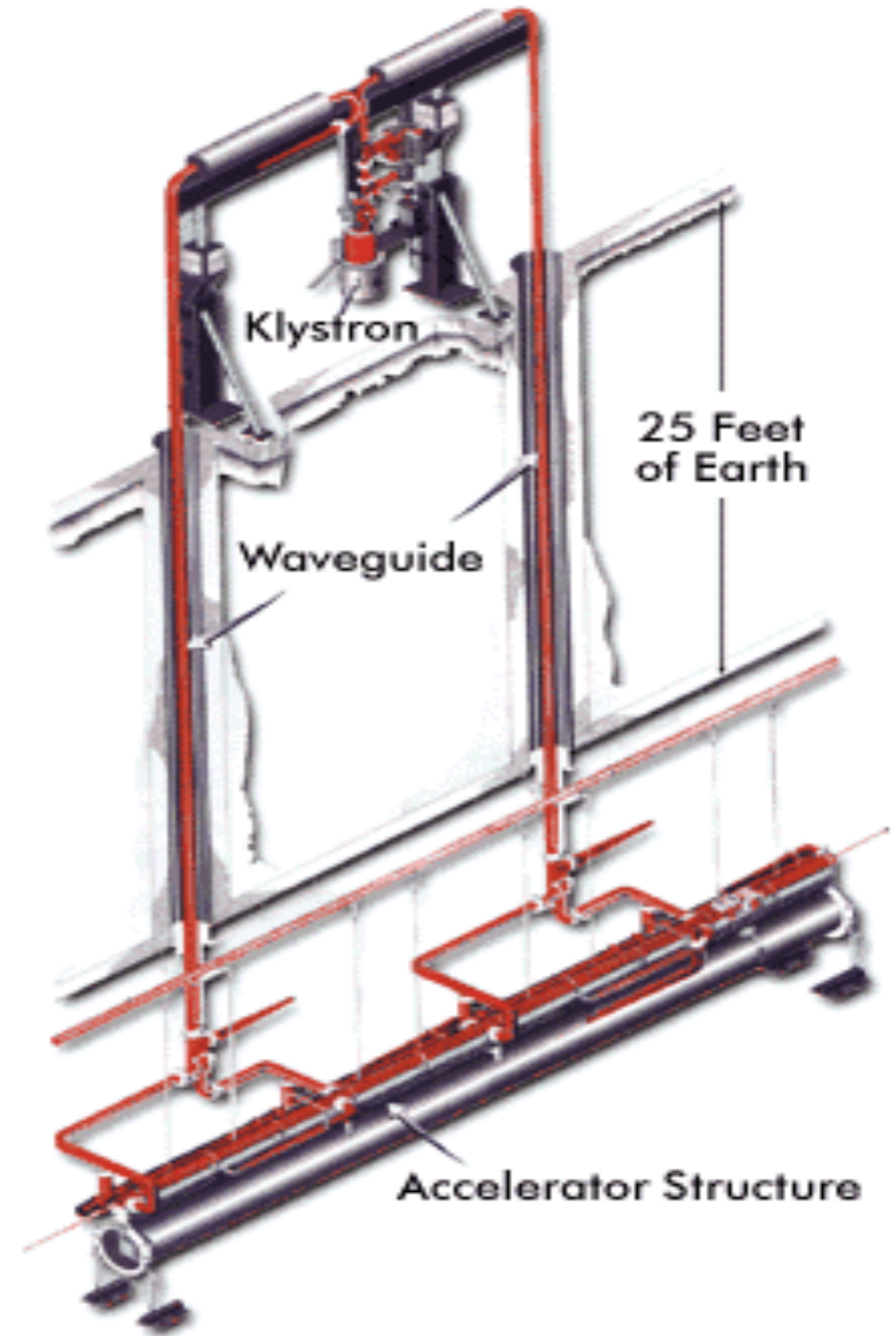
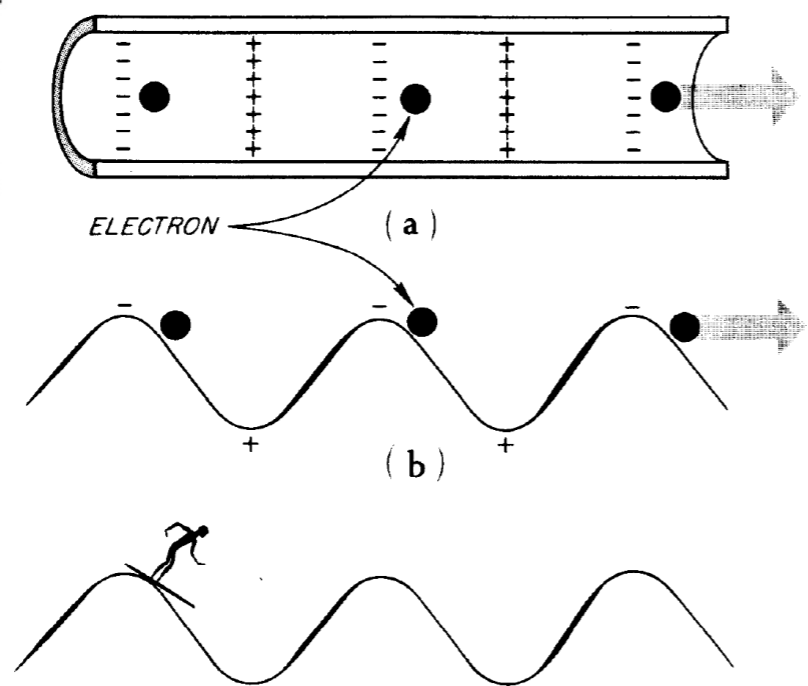
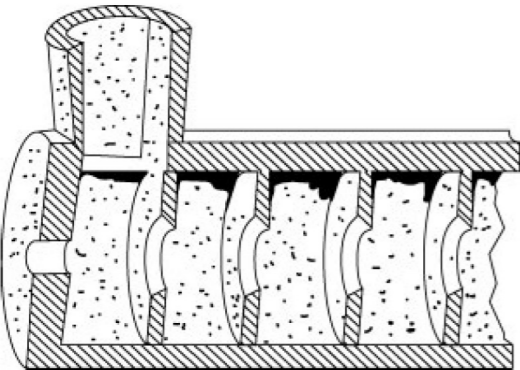
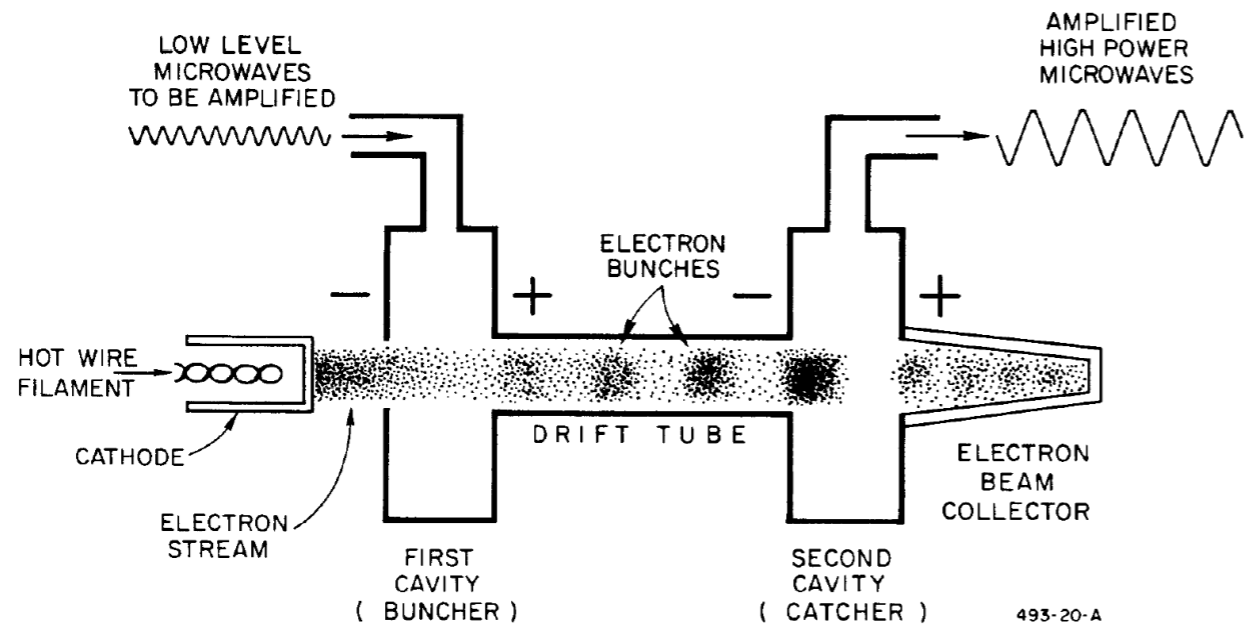
This device allowed Stanford's HEPL to play a leading role in the development of linear accelerators...

Under the direction of E. Ginzton HEPL began the construction of a series of 'small-scale' linacs (MARK I,II,III...).

MARKIII was to be fundamental for the realisation of R. Hofstadter's experiments on e-N and e-p elastic scattering.



Klystron



Nuclear Form Factor

Stimulated by accelerators technology advances and fully mature QED various theoreticians (Rose (48), Elton(50)) started to calculate cross sections for elastic electron-Nucleus scattering

$$\frac{d\sigma}{d\Omega} = \left(\frac{d\sigma}{d\Omega} \right)_{\text{Mott}} |F(\mathbf{q})|^2$$

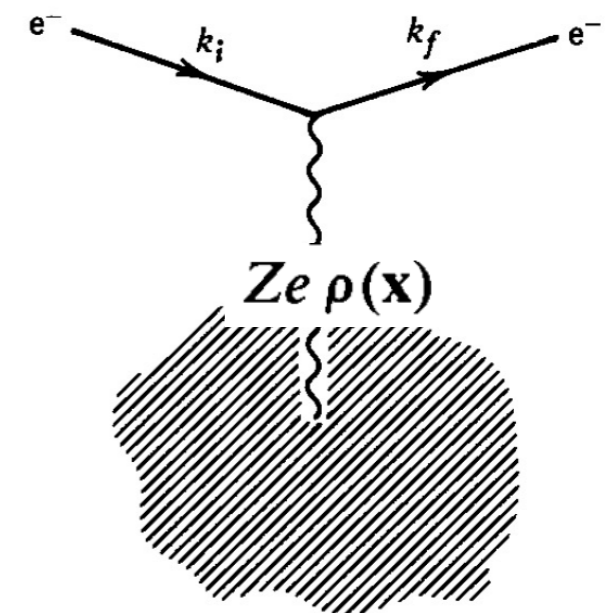
$$F(\mathbf{q}) = \int \rho(\mathbf{x}) e^{i\mathbf{q} \cdot \mathbf{x}} d^3x$$

$$\left(\frac{d\sigma}{d\Omega} \right)_{\text{Mott}} = \frac{(Z\alpha)^2 E^2}{4k^4 \sin^4 \frac{\theta}{2}} \left(1 - v^2 \sin^2 \frac{\theta}{2} \right)$$

$$F(\mathbf{q}) = \int \left(1 + i\mathbf{q} \cdot \mathbf{x} - \frac{(\mathbf{q} \cdot \mathbf{x})^2}{2} + \dots \right) \rho(\mathbf{x}) d^3x$$

$$= 1 - \frac{1}{6} |\mathbf{q}|^2 \langle r^2 \rangle + \dots,$$

$$r_m^2 = -6 \left. \frac{dF(\mathbf{q})}{d(|\mathbf{q}|^2)} \right|_{|\mathbf{q}|=0}$$



Nucleon Form Factors

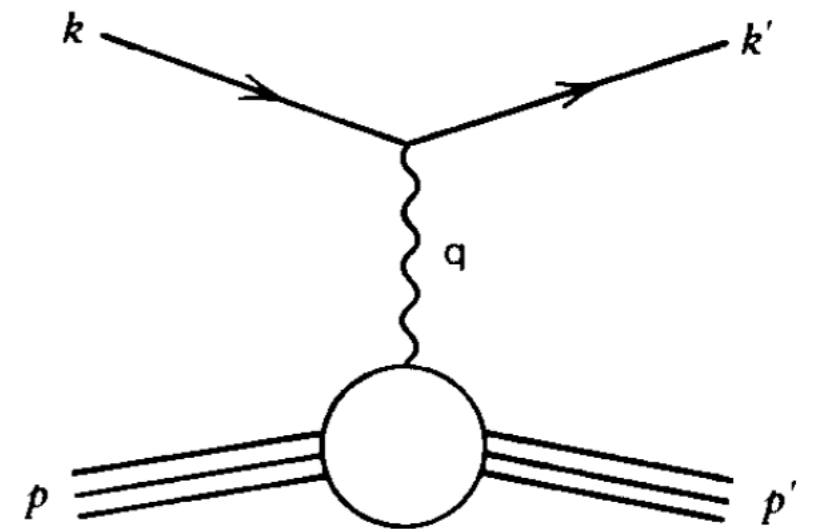
$$\frac{d\sigma}{d\Omega} = \frac{\alpha^2}{4E^2 \sin^4 \theta/2} \frac{\cos^2 \theta/2}{1 + (2E/M) \sin^2 \theta/2} \times \left\{ (F_1^p(t))^2 - \frac{t}{4M^2} \left(4M^2 (F_2^p(t))^2 + 2(F_1^p(t) + 2M F_2^p(t))^2 \tan^2 \frac{\theta}{2} \right) \right\}$$

$$G_E^p(t) = F_1^p(t) + \frac{t}{2M} F_2^p(t)$$

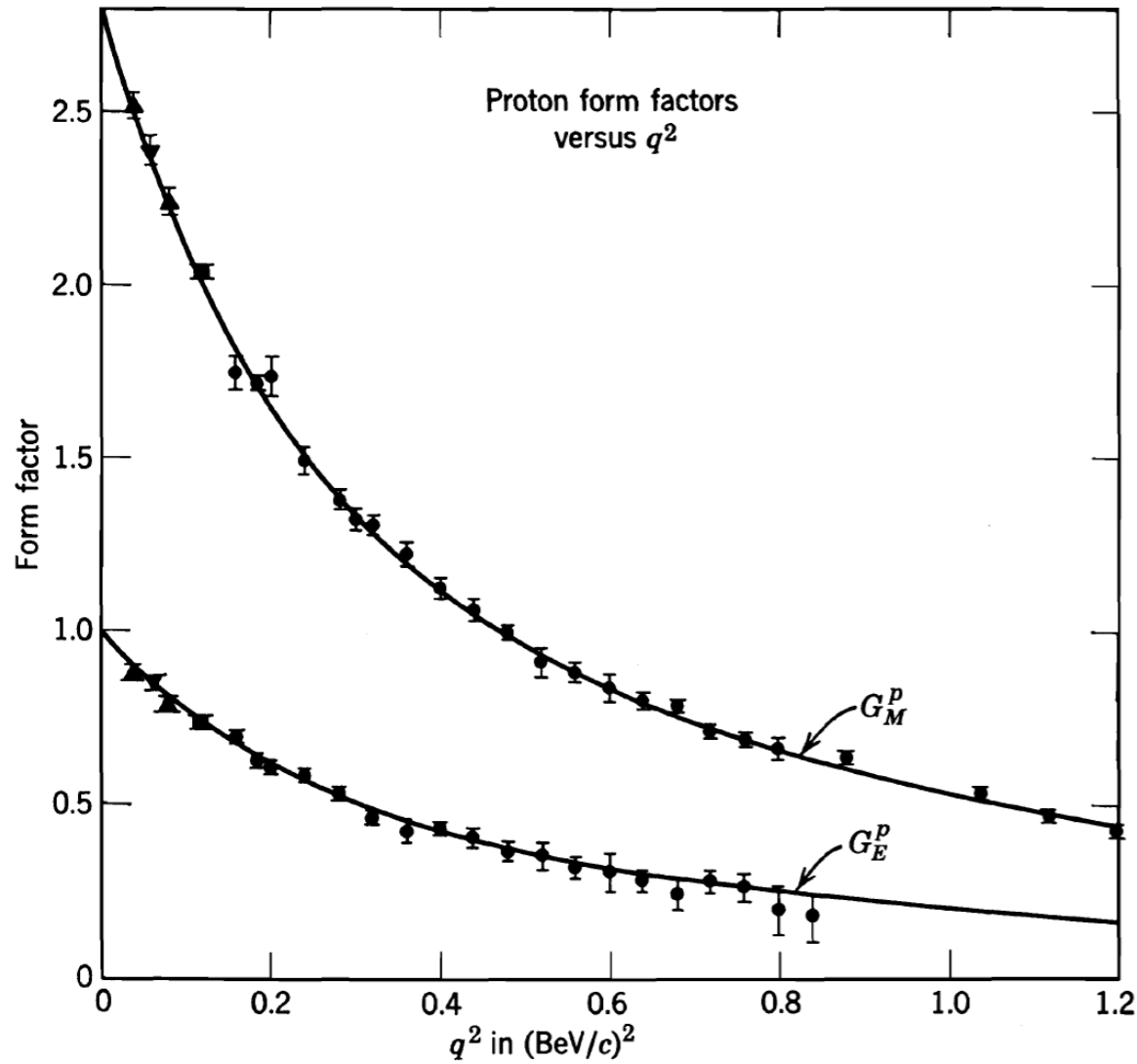
$$G_M^p(t) = F_1^p(t) + 2M F_2^p(t)$$

$$\frac{d\sigma}{d\Omega} = \left(\frac{d\sigma}{d\Omega} \right)_{\text{Mott}} \left\{ \frac{(G_E^p(t))^2 - \frac{t}{4M^2} (G_M^p(t))^2}{1 - t/4M^2} - \frac{t}{2M^2} (G_M^p(t))^2 \tan^2 \frac{\theta}{2} \right\}$$

$$\left(\frac{d\sigma}{d\Omega} \right)_{\text{Mott}} = \frac{\alpha^2}{4E^2 \sin^4 \theta/2} \frac{\cos^2 \theta/2}{1 + (2E/M) \sin^2 \theta/2}$$

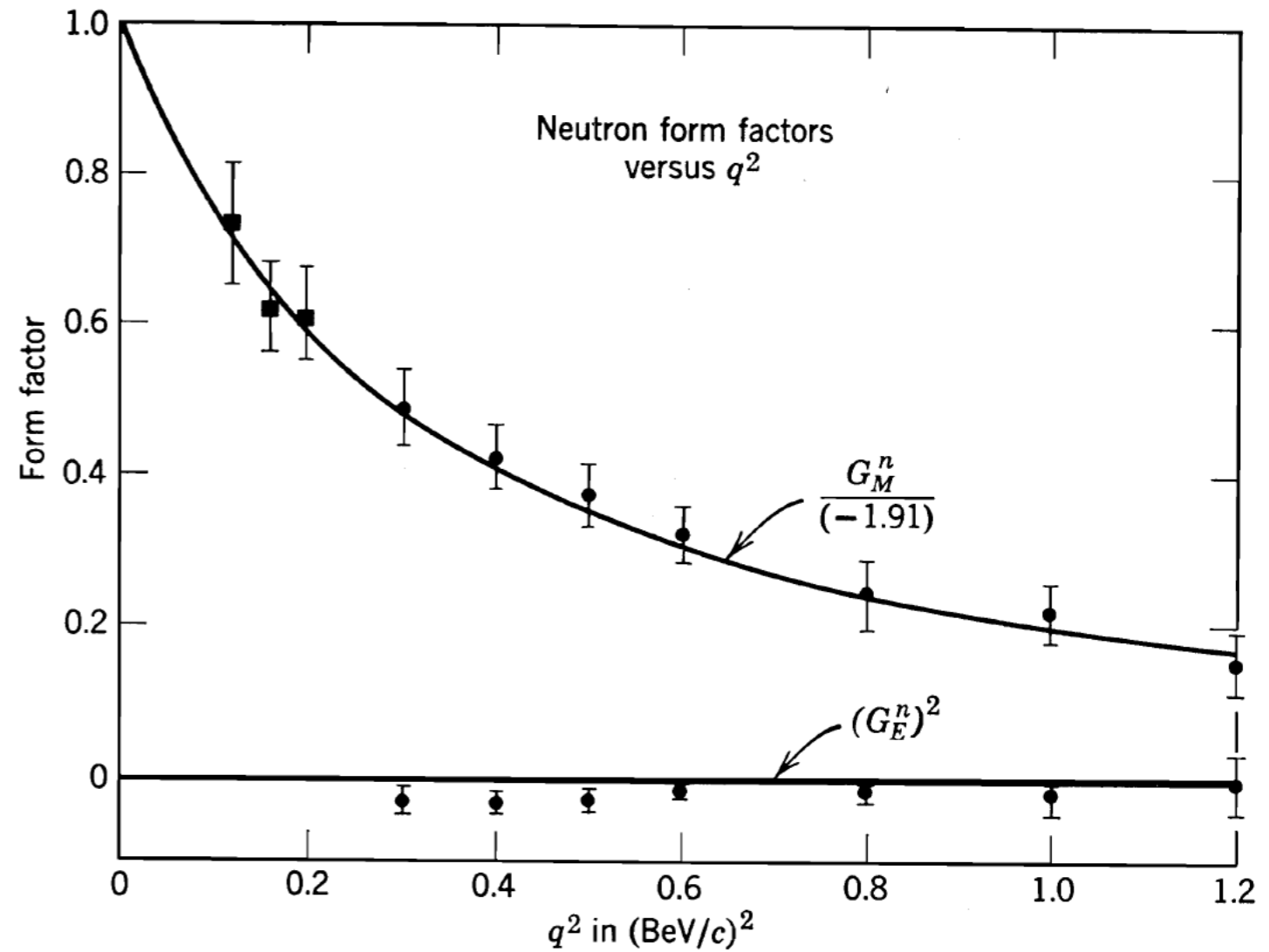


Nucleon Form Factors



$$G_E^p(0) = 1$$

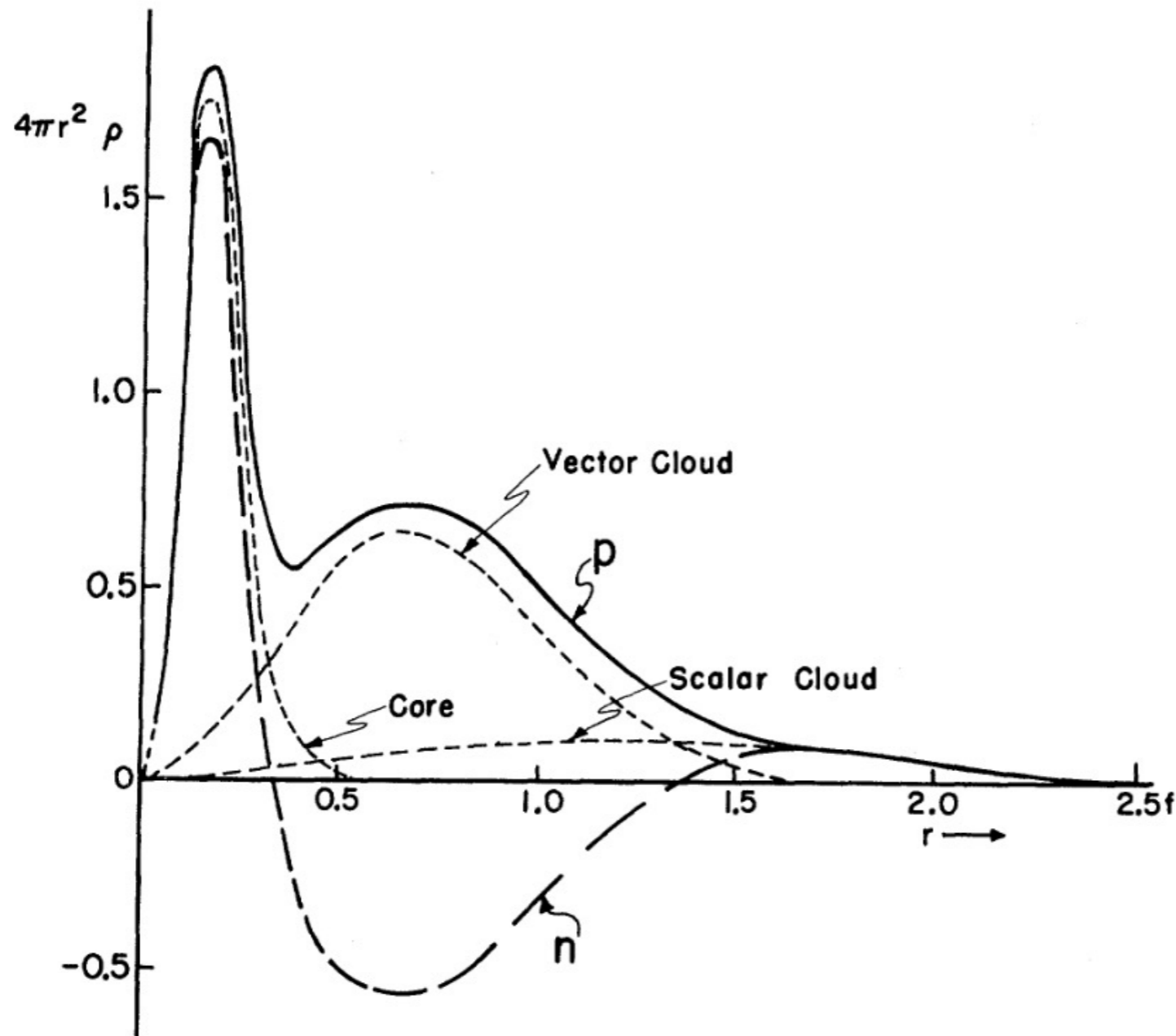
$$G_M^p(0) = 1 + \mu_p \cong 2.79$$



$$G_E^n(0) = 0$$

$$G_M^n(0) = \mu_n \cong -1.91$$

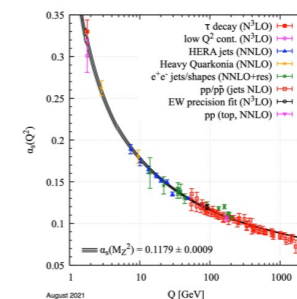
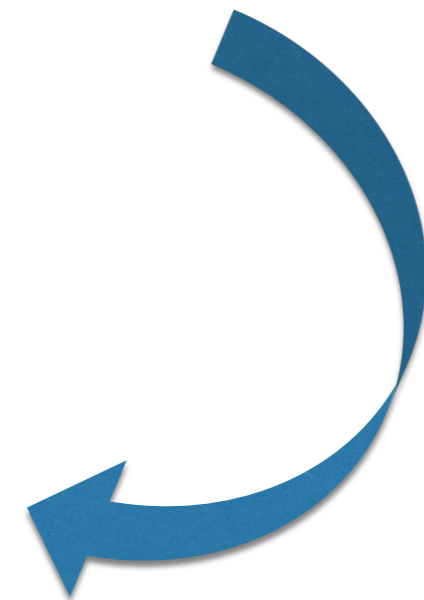
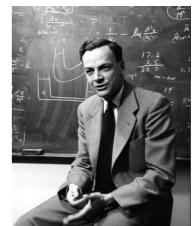
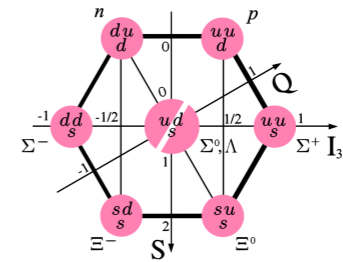
Nucleon Form Factors



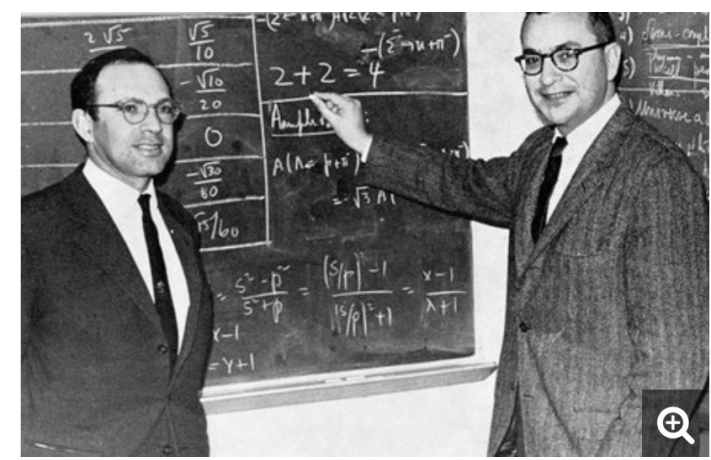
D. N. Olson, H. F. Schopper, and R. R. Wilson
Phys. Rev. Lett. 6, 286 (1961)

Part I

- Quark model
- SLAC-MIT
- Parton Model
- Gargamelle
- pQCD



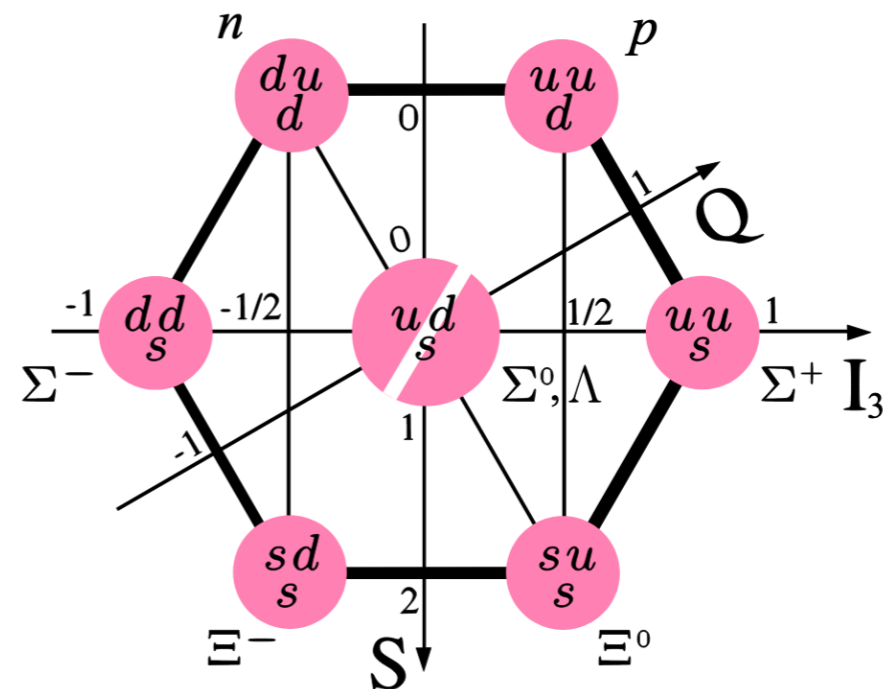
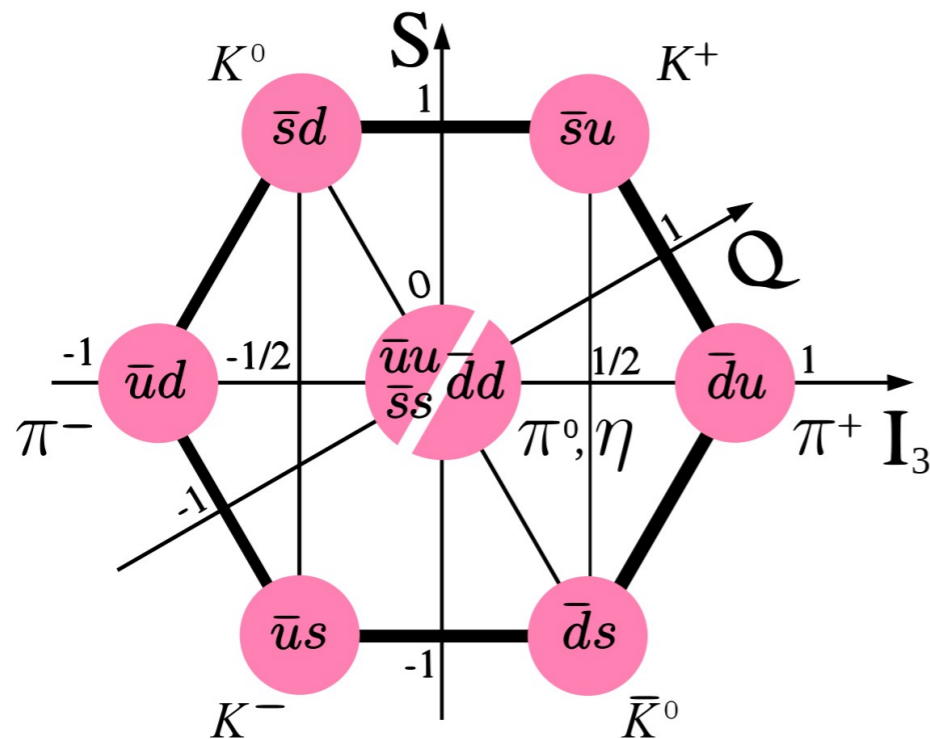
The Eightfold Way

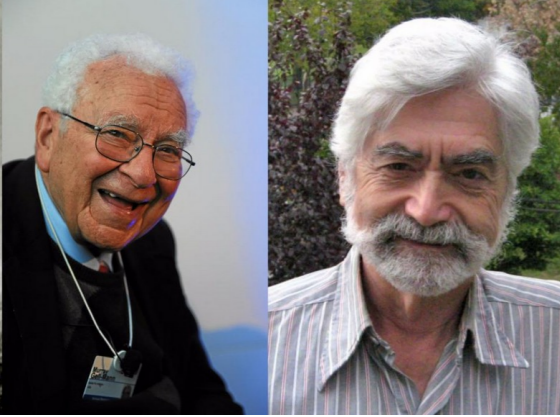


By the early 1960s, many particles (mesons and baryons) had been discovered thanks to the use of accelerator machines and new detectors.

In 1961 M. Gell-mann and Y. Ne'eman introduced a scheme for the classification of mesons and baryons into families/multiplets.

Mathematical Framework: Irr. representations of the SU(3) group



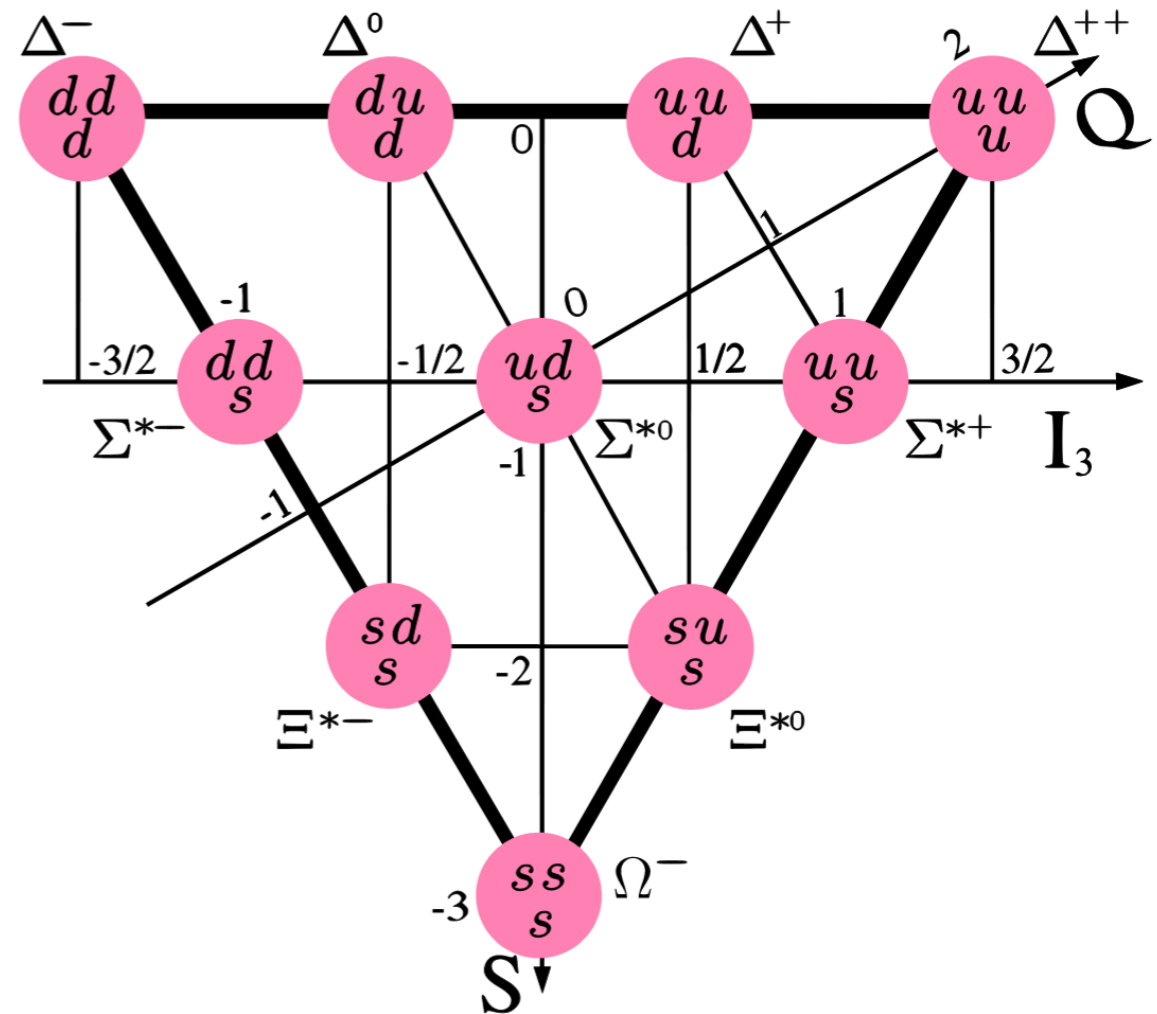


The quark model

1964: Gell-Mann and Zweig independently proposed the existence of elementary particles of spin $\frac{1}{2}$ and fractional charge (the quarks). Three types of quarks (up, down and strange) and the corresponding quark-anti-quarks explained the regularities observed in hadrons.

| | <i>d</i> | <i>u</i> | <i>s</i> | <i>c</i> | <i>b</i> | <i>t</i> |
|-------------------------------------|----------------|----------------|----------------|----------------|----------------|----------------|
| Q – electric charge | $-\frac{1}{3}$ | $+\frac{2}{3}$ | $-\frac{1}{3}$ | $+\frac{2}{3}$ | $-\frac{1}{3}$ | $+\frac{2}{3}$ |
| I – isospin | $\frac{1}{2}$ | $\frac{1}{2}$ | 0 | 0 | 0 | 0 |
| I_z – isospin <i>z</i> -component | $-\frac{1}{2}$ | $+\frac{1}{2}$ | 0 | 0 | 0 | 0 |
| S – strangeness | 0 | 0 | -1 | 0 | 0 | 0 |
| C – charm | 0 | 0 | 0 | +1 | 0 | 0 |
| B – bottomness | 0 | 0 | 0 | 0 | -1 | 0 |
| T – topness | 0 | 0 | 0 | 0 | 0 | +1 |

Descriptive and partially predictive model
(e.g. masses, magnetic moments)



Are the quarks real?

Prevailing interpretation (~1965s) :

- The quark model is only a useful organisational scheme for hadron spectroscopy
- Particles have a "diffuse substructure" but no "elementary constituents"
(Nuclear democracy - Bootstrap model)

“...the idea that mesons and baryons are made primarily of quarks and gluons is hard to believe...”

M. Gell-mann 1966

“Additional data are necessary and very welcome to destroy the picture of elementary constituents.”

J. Bjorken 1967

“I think Professor Bjorken and I constructed the sum rules in the hope of destroying the quark model.”

K. Gottfried 1967

“Of course the whole quark idea is ill founded.”

J.J. Kokkedee 1967

SLAC and the “M(onster)-Project”

On 10 April 1956, the Stanford staff met at W. Panofsky's house to discuss R. Hofstadter's proposal to build a linear accelerator 10 times more powerful than Mark III. The project was given the provisional name 'M(onster) Project' because it was estimated that the accelerator should be 2 miles long and reach an energy of 20 GeV!!!

- 1957 a detailed project is presented
- 1959 Eisenhower says yes
- 1961 Congress approves the project (\$114 Million)

1962, construction began



During excavation work, the skeleton of a mammal that lived in the Miocene, (Paleoparadoxia), which populated the region 14 million years ago, was found ...



The (CIT)-SLAC-MIT Collaboration

SLAC began its operational phase in 1966.

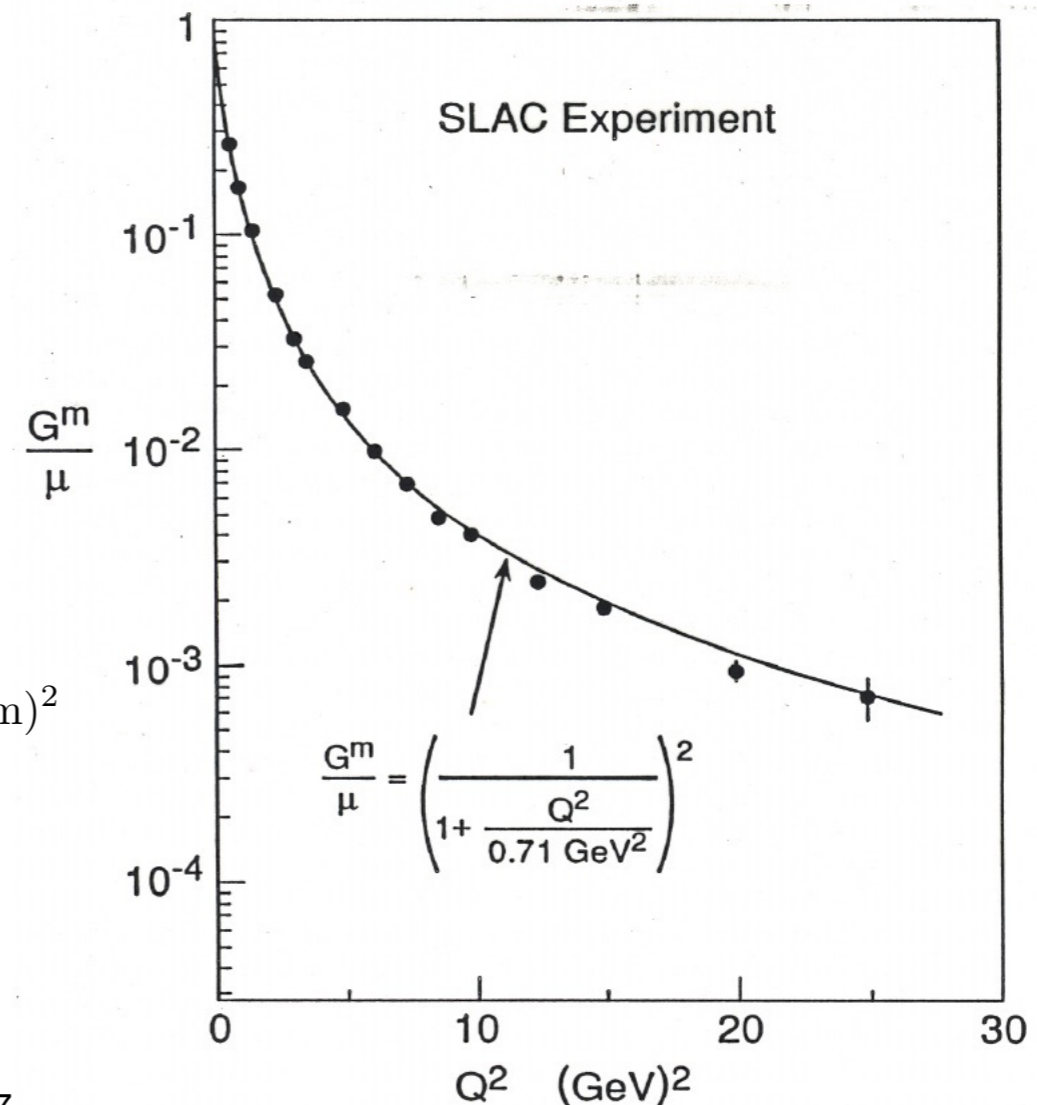
The CIT-SLAC-MIT collaboration built the electron spectrometer to study the structure of the proton through the elastic diffusion process e-p

The electron is an ideal 'probe':

- elementary particle
- interacts electromagnetically (QED)

Magnetic Form Factor \Rightarrow

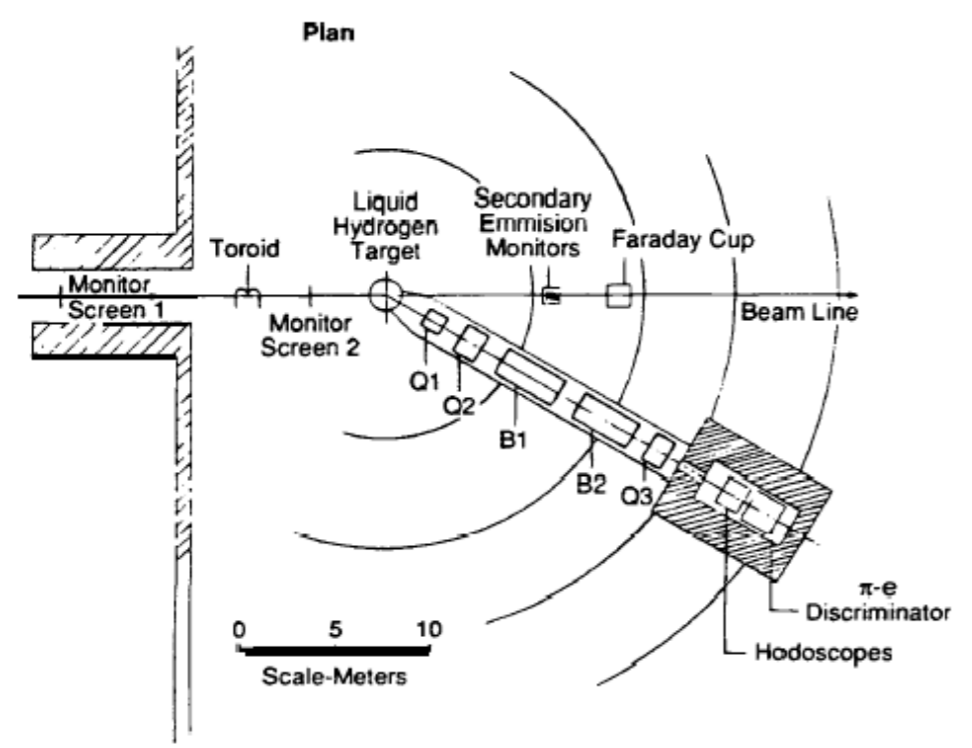
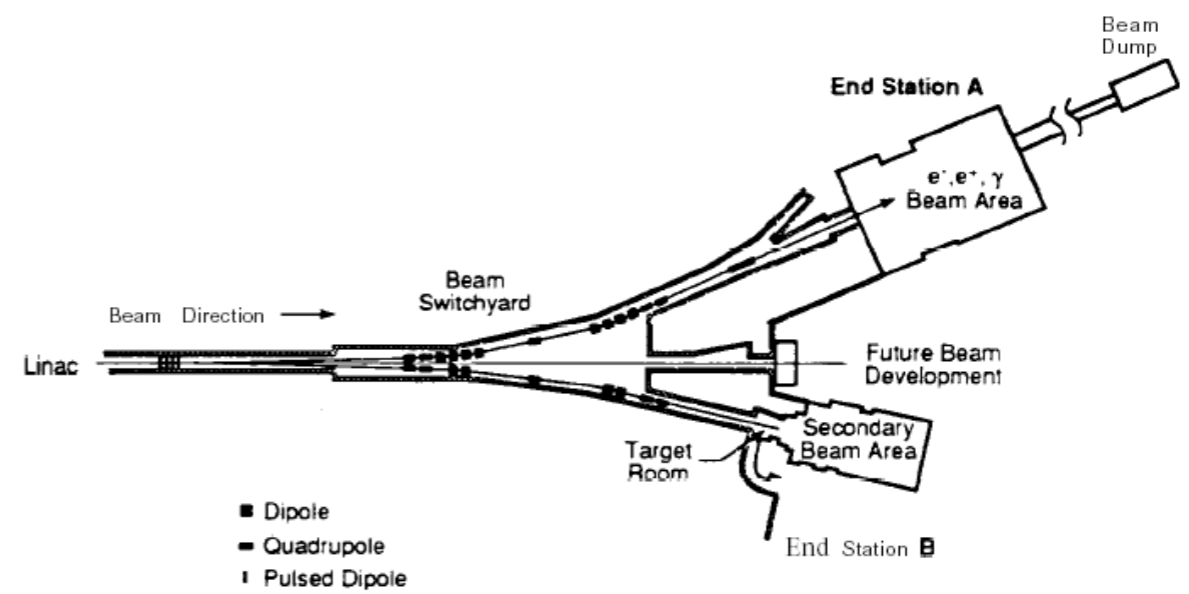
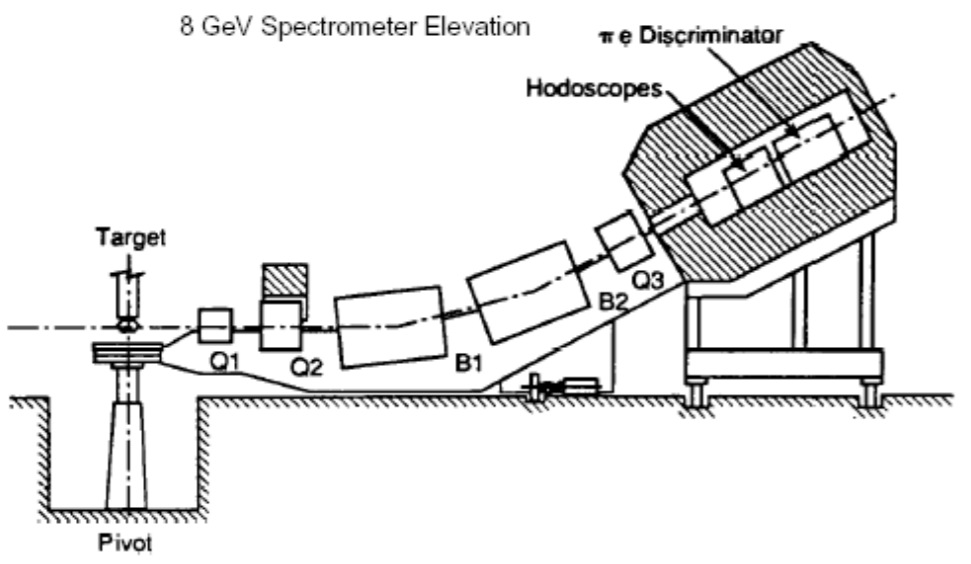
$$\langle r^2 \rangle = \int d^3r r^2 \rho(\mathbf{r}) = -6 \frac{dG_E(q^2)}{dq^2} \Big|_{q^2=0} = ((0.81 \pm 0.04) \cdot 10^{-13} \text{ cm})^2$$





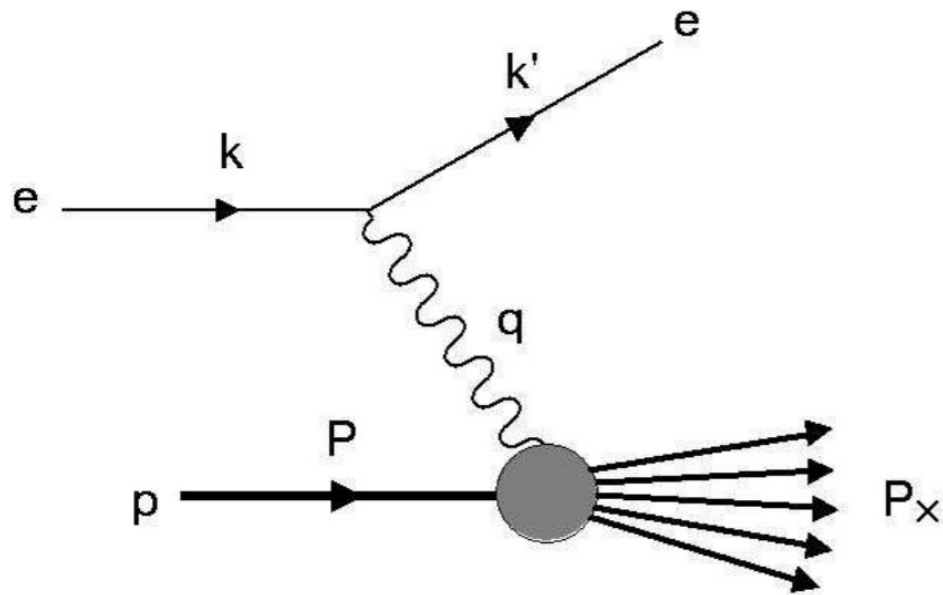
SLAC-MIT

....under the direction of Taylor, Friedman and Kendall



SLAC-MIT

In 1967, the SLAC-MIT collaboration began the systematic study of inelastic scattering:



Elastic vs inelastic scattering:

Elastic scattering provides information on 'time-averaged' electric charge and magnetic moment distributions

Inelastic scattering gives us a 'snapshot' of the proton's structure

$$Q^2 = -(k - k')^2 = 4EE' \sin^2(\theta/2)$$

$$\omega = \frac{1}{x} = \frac{2m_p \nu}{Q^2}$$

$$\nu = \frac{P \cdot q}{m_p} = E - E'$$

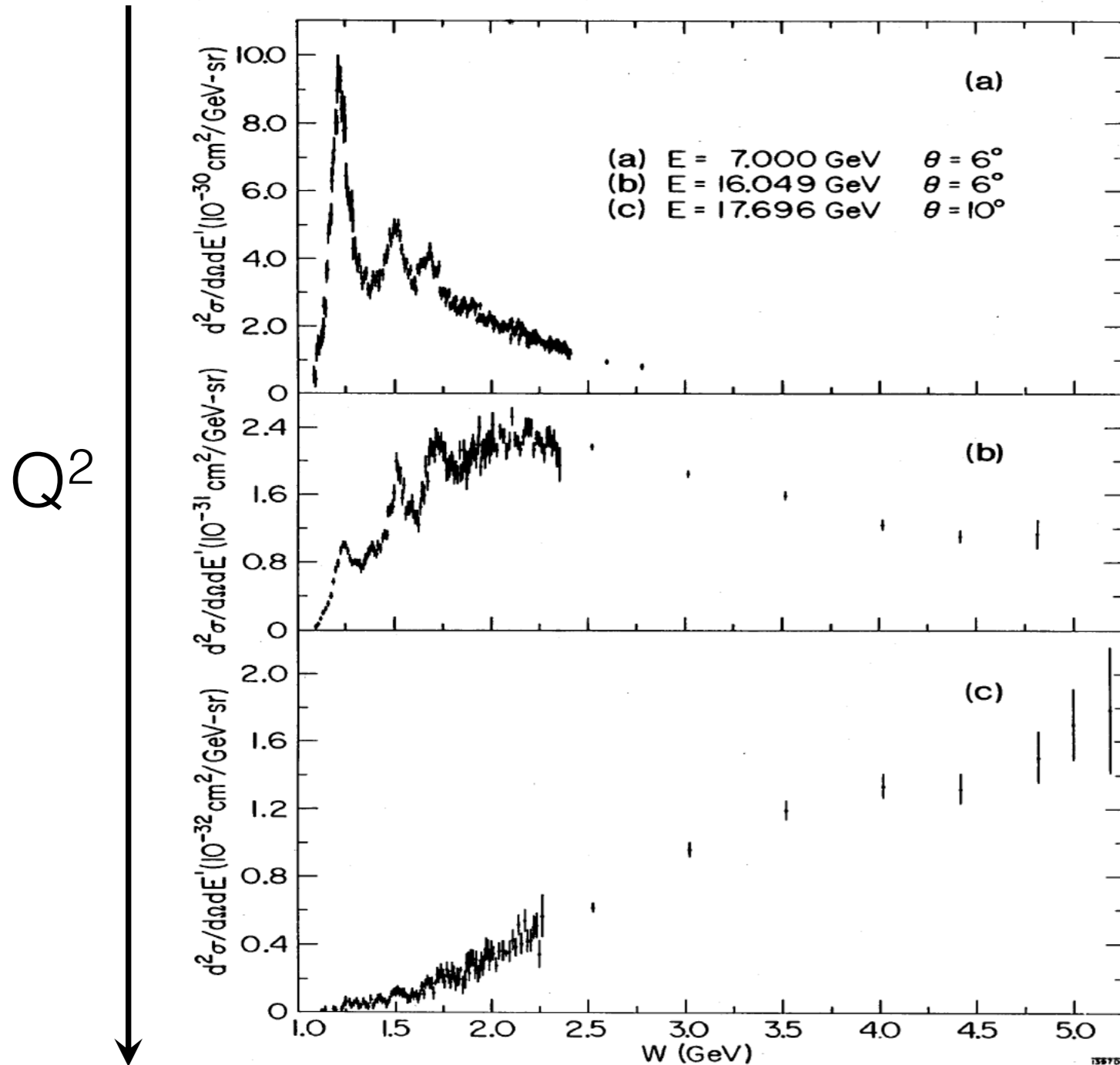
$$W^2 = P_X^2 = 2m_p \nu + m_p^2 - Q^2$$

$$\Delta t = \frac{h}{\Delta E}$$

$$\Delta E = 2 \text{ GeV} \rightarrow \Delta t = 3 \cdot 10^{-25} \text{ s}$$

$$\rightarrow \Delta x \simeq 10^{-16} \text{ m} \quad (v = c)$$

SLAC MIT



It was decided to study the region of the continuum.

Two unexpected results :

- Bjorken scaling
- Slight dependence on Q^2

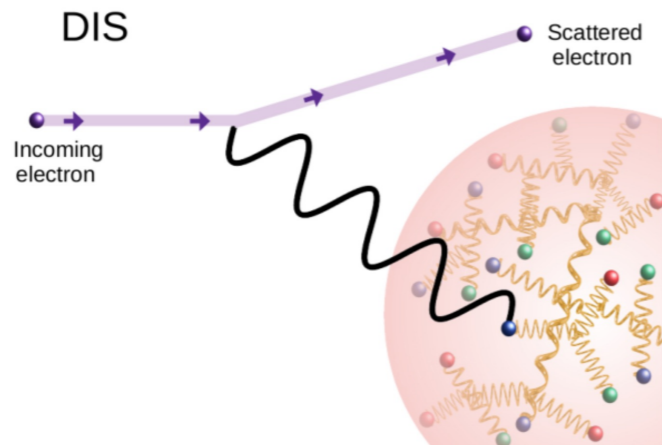
Reminder:

$$Q_{el}^2 = 2E_e E'_e (1 - \cos\theta'_e)$$

Bjorken scaling

$$W > 2.6 \text{ GeV}$$

$$2 < Q^2 < 20 \text{ GeV}^2$$



Differential Cross section:

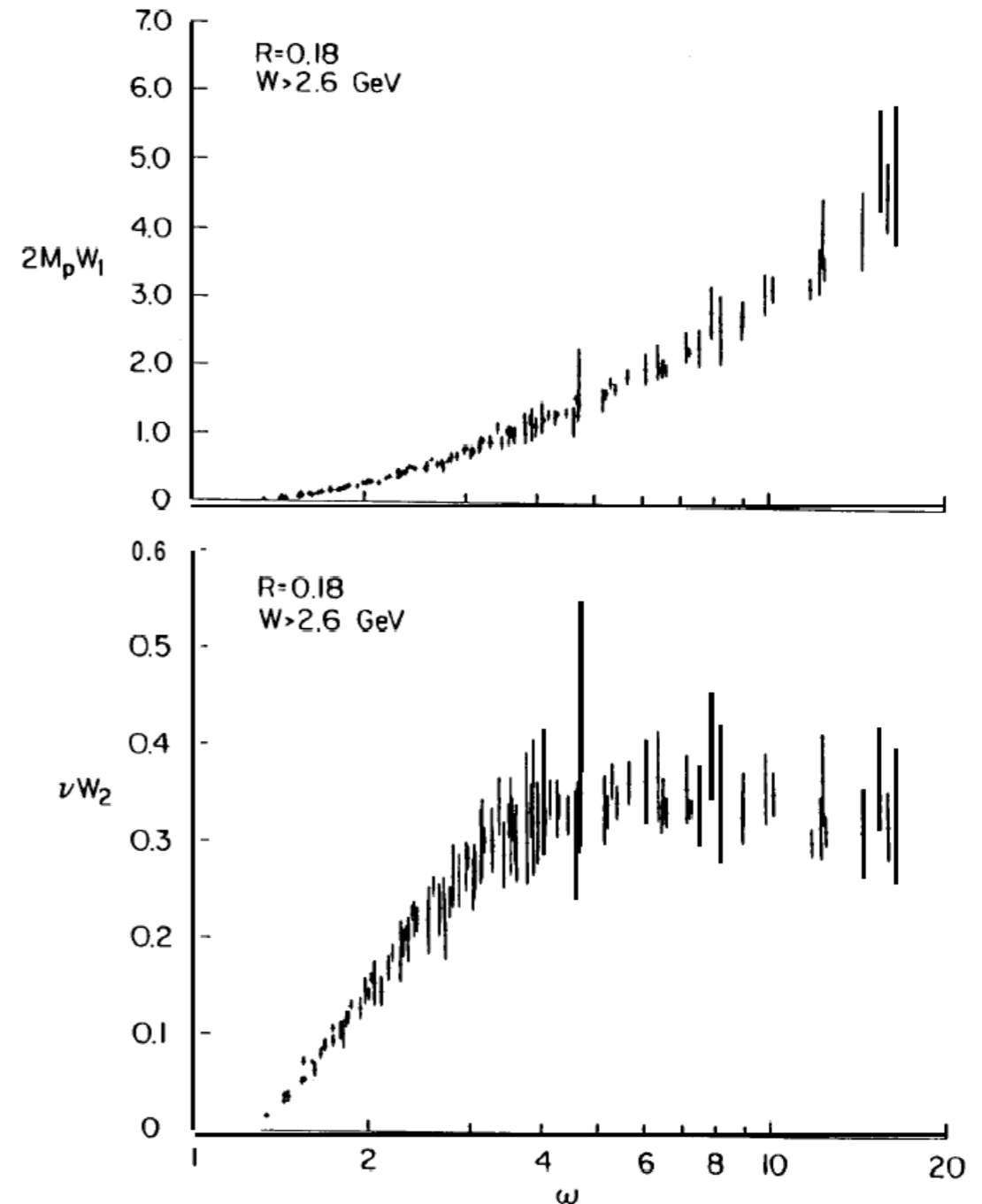
$$\frac{d^2\sigma}{d\Omega dE'} = \sigma_M [W_2(\nu, Q^2) + 2W_1(\nu, Q^2) \tan^2(\theta/2)]$$

Bjorken scaling:

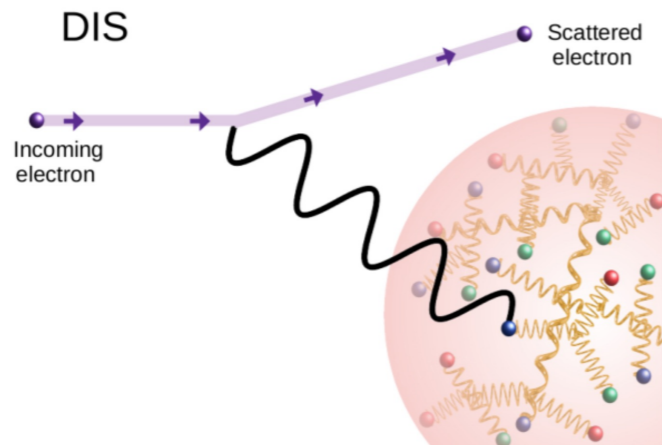
for $\nu \rightarrow \infty$, $Q^2 \rightarrow \infty$ (with $\omega = \frac{2m_p\nu}{Q^2}$ fixed)

$$\nu W_2(\nu, Q^2) \rightarrow F_2(\omega)$$

$$2m_p W_1(\nu, Q^2) \rightarrow F_1(\omega)$$



Bjorken scaling



Differential Cross section:

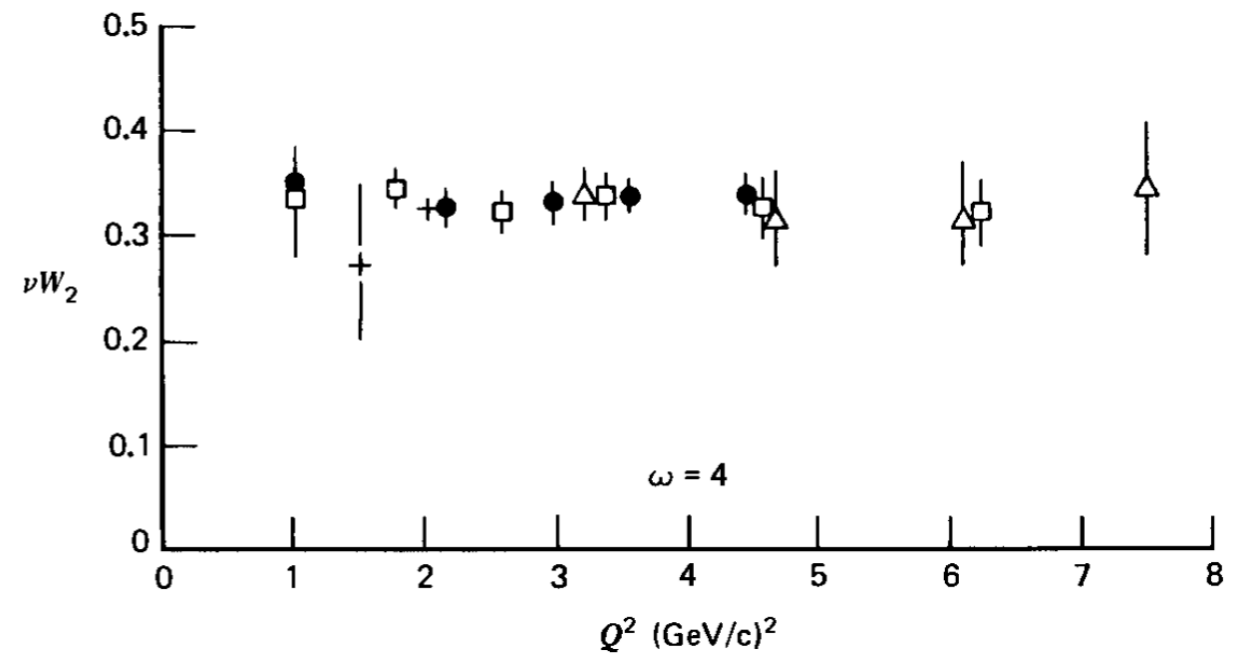
$$\frac{d^2\sigma}{d\Omega dE'} = \sigma_M [W_2(\nu, Q^2) + 2W_1(\nu, Q^2) \tan^2(\theta/2)]$$

Bjorken scaling:

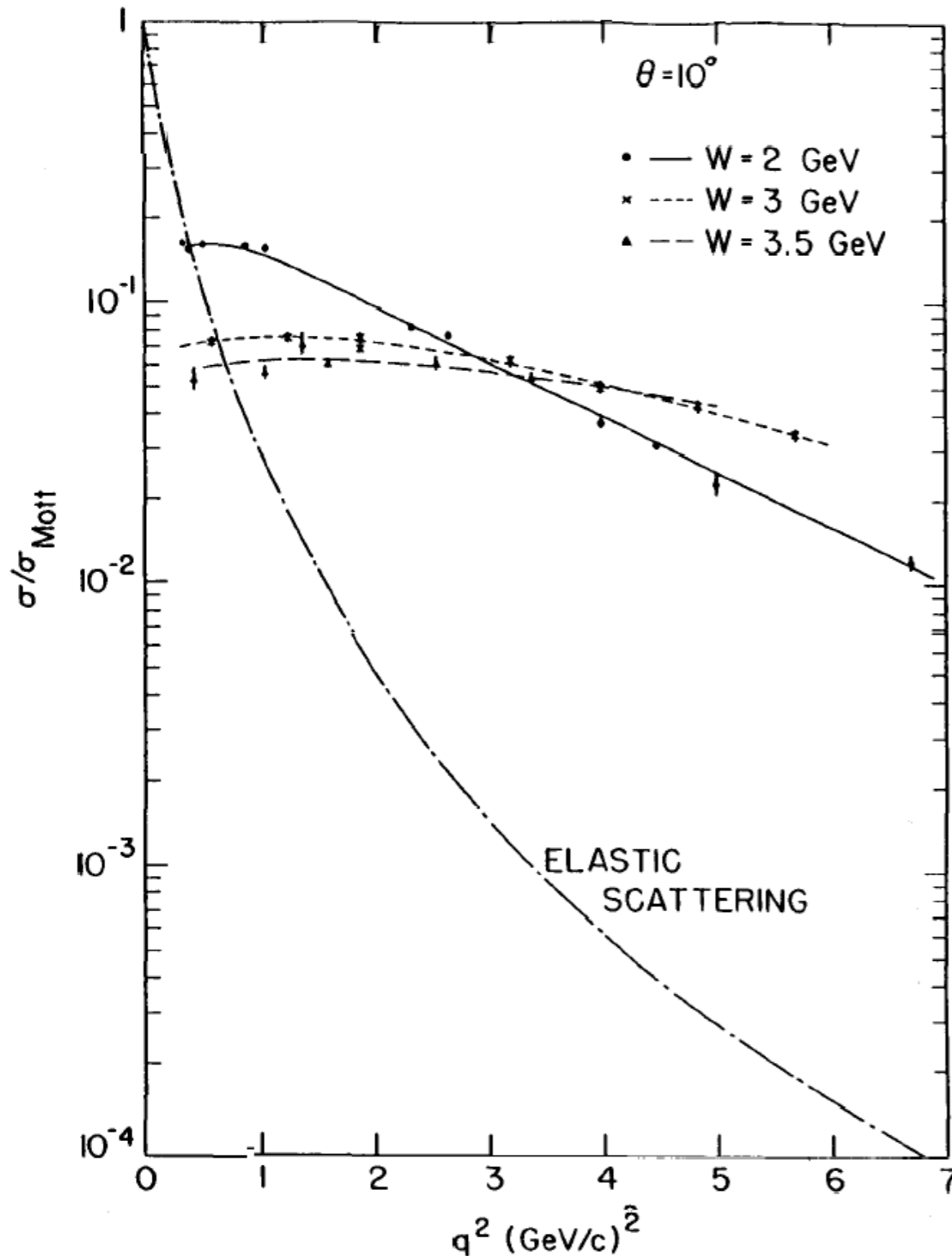
for $\nu \rightarrow \infty$, $Q^2 \rightarrow \infty$ (with $\omega = \frac{2m_p\nu}{Q^2}$ fixed)

$$\nu W_2(\nu, Q^2) \rightarrow F_2(\omega)$$

$$2m_p W_1(\nu, Q^2) \rightarrow F_1(\omega)$$



Q^2 (in)dependence



Slight dependence on Q^2
(compared to elastic scattering)

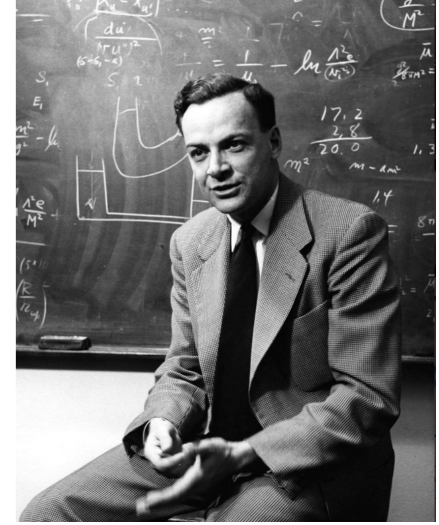
The measurement suggests the possible existence of "point-like" proton constituents

$$F(\mathbf{q}) = \int \rho(\mathbf{r}) e^{i\mathbf{q}\cdot\mathbf{r}} d^3r$$

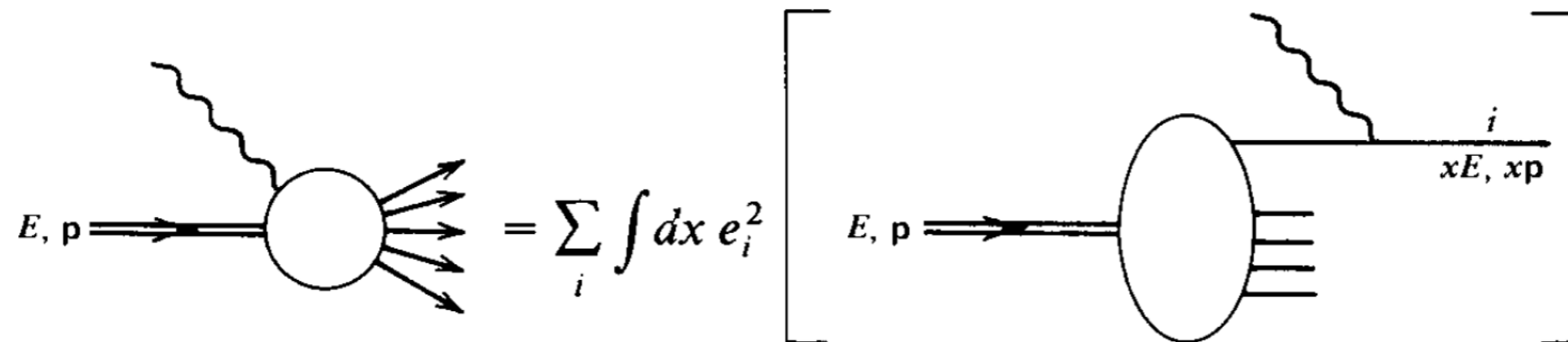
$$\text{if } \rho(\mathbf{r}) = \delta(\mathbf{r}) \rightarrow F(\mathbf{q}) = 1$$

"Pointlike" \Rightarrow weak Q^2 dependence

The Parton Model



Feynman (1969): the proton is a collection of particles (“partons”) and the virtual photon interacts with the single parton. The cross section is the incoherent sum of the photon-particle cross sections.



$$\nu W_2(\nu, Q^2) \rightarrow F_2(x) = \sum_i e_i^2 x f_i(x)$$

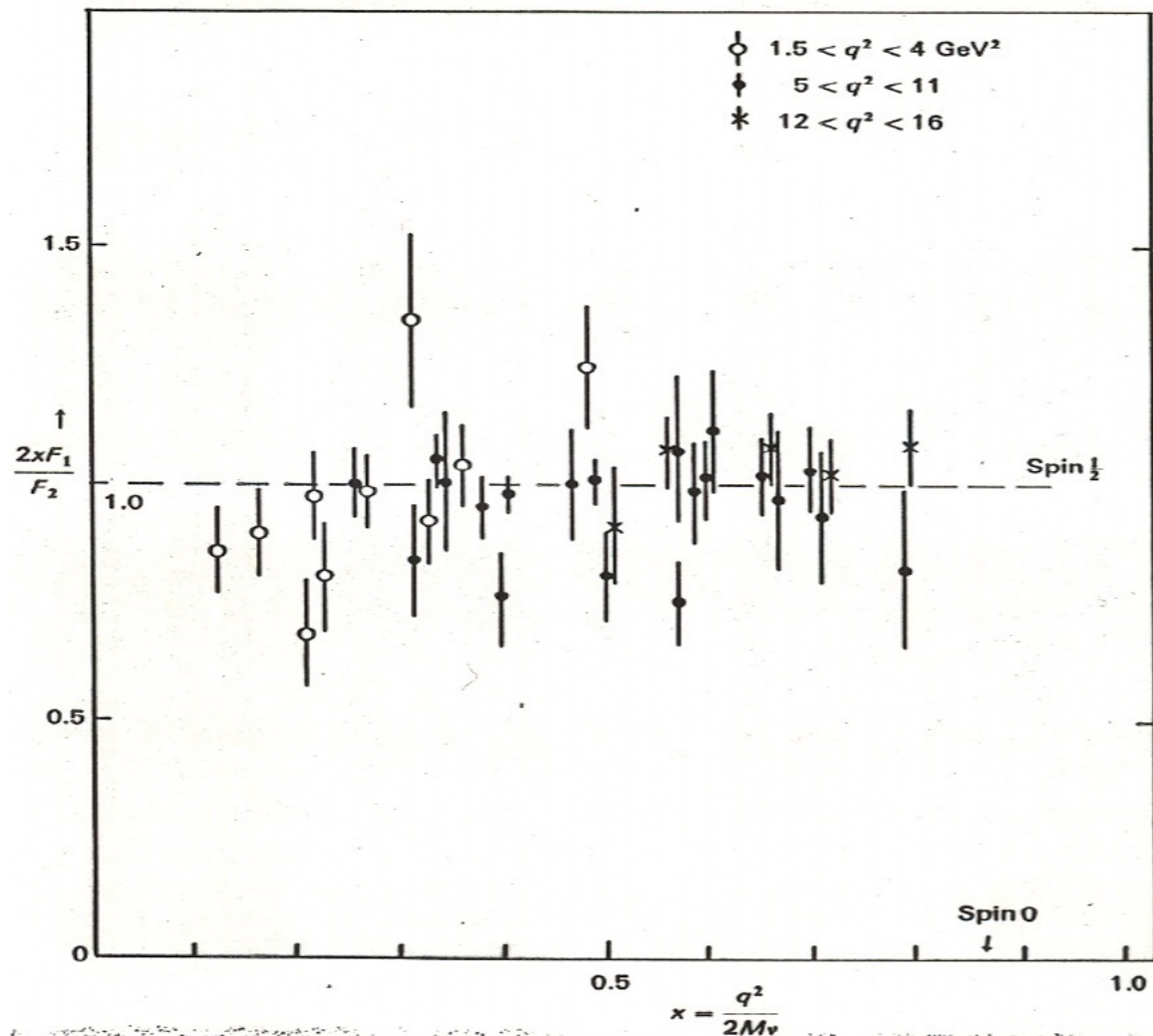
$$m_p W_1(\nu, Q^2) \rightarrow F_1(x) = \frac{1}{2x} F_2(x)$$

Partons and quarks

Can we identify partons with quarks?

- the spin must be 1/2
- the electric charge must be fractional (+2/3 , -1/3)

For spin, a first answer came from the experimental verification of the Callan-Gross relation:



$$R = \frac{\sigma_L}{\sigma_T} = \frac{W_2}{W_1} \left(1 + \frac{\nu^2}{q^2} \right) - 1$$

For spin 1/2 and in the “DIS Region”:

$$R \rightarrow 0 \quad ; \quad F_2(x) = 2xF_1(x)$$

Partons and quarks

For the fractional electric charge (+2/3 , -1/3) the first indications came from the "F₂ sum rule":

$$\frac{1}{2} \int [\nu W_2^p(\omega) + \nu W_2^n(\omega)] d\omega = \frac{1}{2} \int [F_2^p(x) + F_2^n(x)] dx = \frac{Q_u^2 + Q_d^2}{2} \int x[u_p(x) + \bar{u}_p(x) + d_p(x) + \bar{d}_p(x)] dx$$

$$\frac{1}{2} \int [F_2^p(x) + F_2^n(x)] dx = \left(\frac{Q_u^2 + Q_d^2}{2} \right) (?) = \frac{5}{18} \cdot (?) \simeq 0.28 \cdot (?)$$

Experimental result (SLAC-MIT):

$$\frac{1}{2} \int [F_2^p(x) + F_2^n(x)] dx = 0.14 \pm 0.005$$

Conclusion: consistent with the quark model if quarks/antiquarks carry 50% of the proton's momentum. What about the remaining 50%?

Gargamelle

Can we identify partons with quarks?

- the spin must be 1/2
- the electric charge must be fractional (+2/3 , -1/3)

Further confirmation came from initial comparisons of electron and neutrino scattering data :

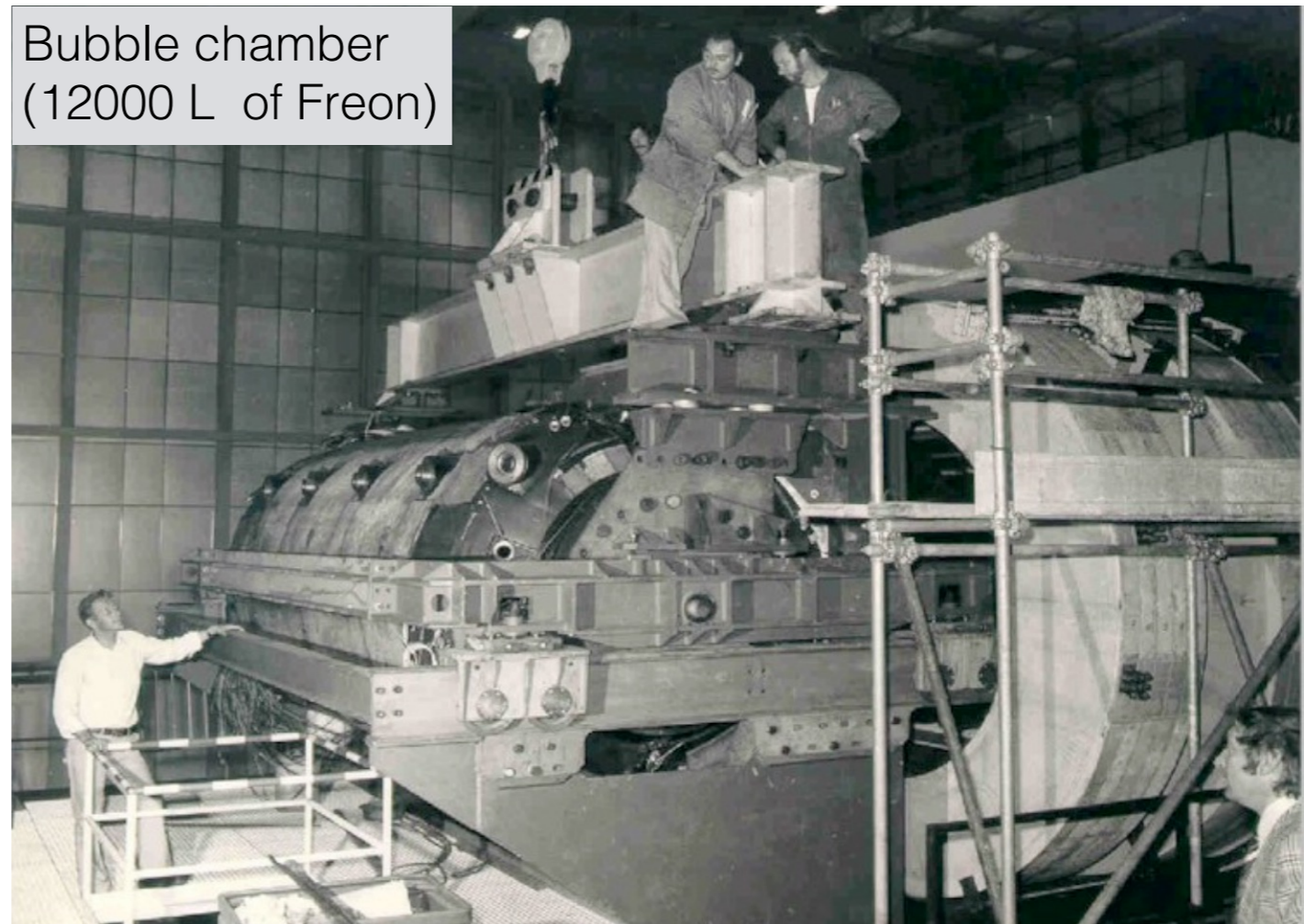
Gargamelle Experiment
(CERN 24 GeV PS Synchrotron)

Processes:

$$\nu_{\mu} + N \rightarrow \mu^{-} + X$$

$$\bar{\nu}_{\mu} + N \rightarrow \mu^{+} + X$$

Bubble chamber
(12000 L of Freon)



Gargamelle

Can we identify partons with quarks?

- the spin must be 1/2
- the electric charge must be fractional (+2/3 , -1/3)

Further confirmation came from initial comparisons of electron and neutrino scattering data :

Gargamelle Experiment
(CERN 24 GeV PS Synchrotron)

Processes:

$$\nu_{\mu} + N \rightarrow \mu^{-} + X$$

$$\bar{\nu}_{\mu} + N \rightarrow \mu^{+} + X$$



Neutrinos

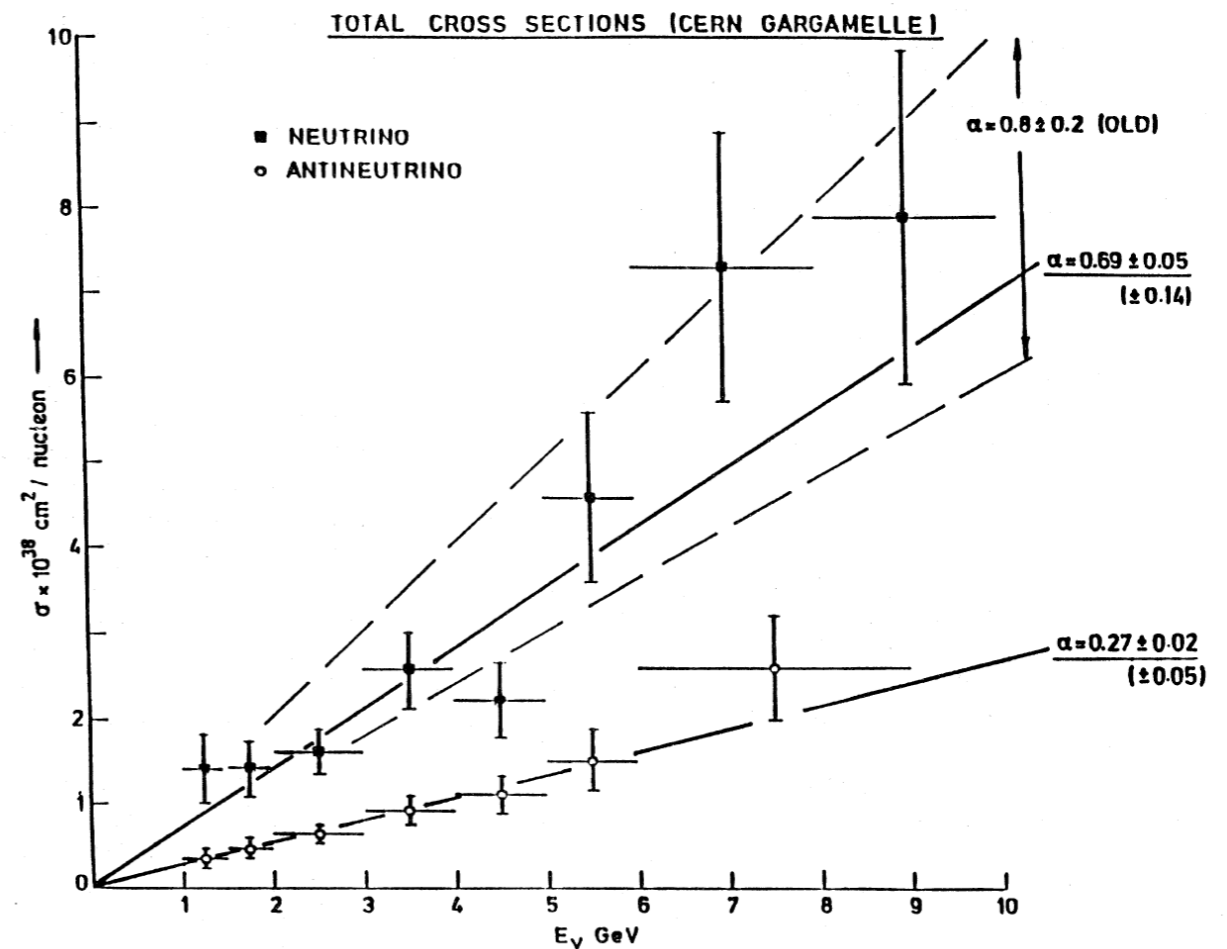
Linear Energy dependence of $\sigma_{tot}(\nu_\mu)$, ($\sigma_{tot}(\bar{\nu}_\mu)$) provides further confirmation of the existence of point constituents in the proton and neutron.

Cross sections ("scaling region"):

$$\frac{d^2\sigma^{\nu,\bar{\nu}}}{dx dy} = \frac{G^2 ME}{\pi} \left[(1-y)F_2(x) + \frac{y^2}{2} [2xF_1(x)] \mp y \left(1 - \frac{y}{2}\right) xF_3(x) \right]$$

$$\sigma_{tot}(\nu_\mu) = \alpha_\nu E$$

$$\sigma_{tot}(\bar{\nu}_\mu) = \alpha_{\bar{\nu}} E$$

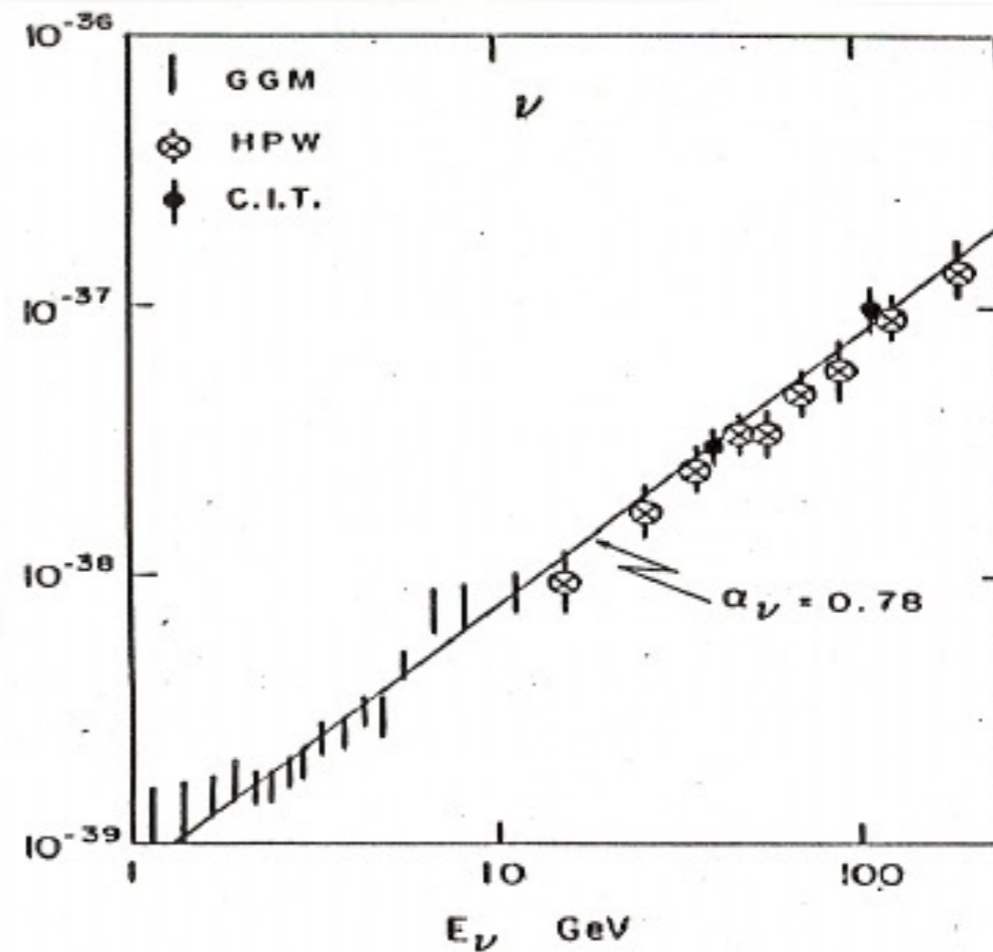
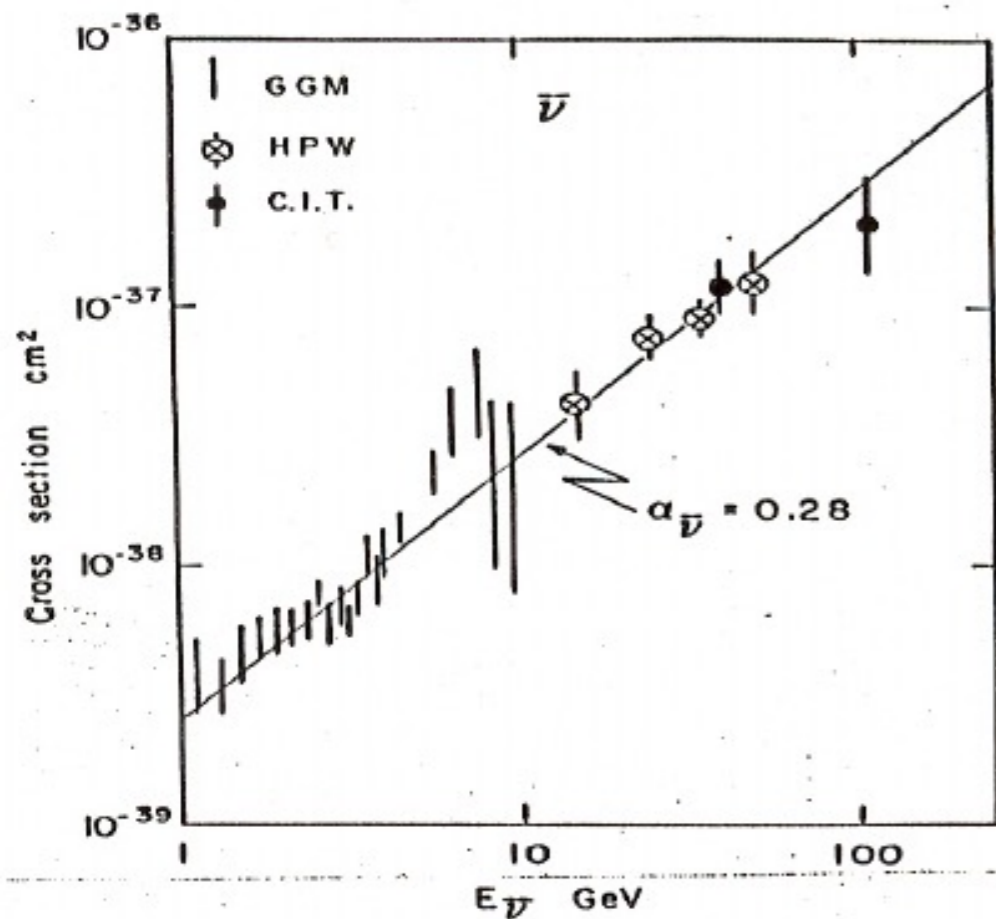


ICHEP 1972

Perkins "...the preliminary data on the cross sections provide an astonishing verification for the Gell-Mann/Zweig quark model of hadrons."

Neutrinos

Linear Energy dependence of $\sigma_{tot}(\nu_\mu)$, ($\sigma_{tot}(\bar{\nu}_\mu)$) provides further confirmation of the existence of point constituents in the proton and neutron.



ICHEP 1972

Perkins "...the preliminary data on the cross sections provide an astonishing verification for the Gell-Mann/Zweig quark model of hadrons."

Partons electric charge

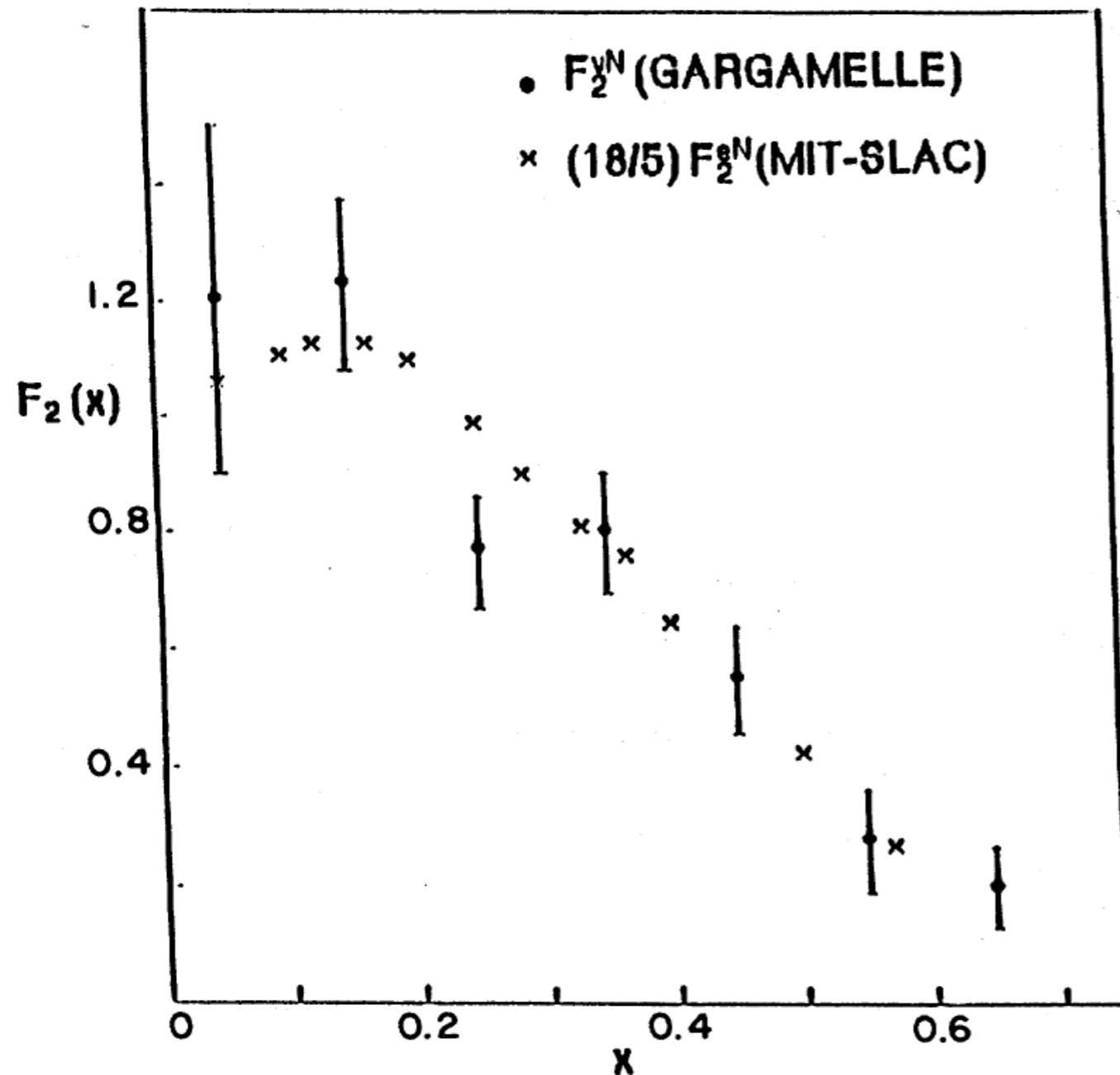
Partons have fractional charge (+2/3 , -1/3) ?

The answer came from the first comparison of electron and neutrino scattering data:

$$\frac{\frac{1}{2} \int [F_2^{\nu n}(x) + F_2^{\nu p}(x)] dx}{\frac{1}{2} \int [F_2^{en}(x) + F_2^{ep}(x)] dx} = \frac{2}{(Q_u^2 + Q_d^2)} = \frac{2}{(2/3)^2 + (1/3)^2} = \frac{18}{5} = 3.6$$

Experimental result (SLAC-MIT, Gargamelle): **3.4 ± 0.7**

Other early results with neutrinos



First comparison of $F_2^{\nu N}$ with F_2^{eN}

$$F_2^{\nu N} \sim \left(\frac{18}{5}\right) F_2^{eN}$$

Other early results with neutrinos

$$\frac{1}{2} \int [F_2^{\nu p}(x) + F_2^{\nu n}(x)] dx = \int x[u_p(x) + \bar{u}_p(x) + d_p(x) + \bar{d}_p(x)] dx$$

Experimental result (Gargamelle): 0.49 ± 0.7

50% of the proton momentum is carried by quarks, in agreement with the SLAC-MIT results

$$\frac{1}{2} \int [F_3^{\nu p}(x) + F_3^{\nu n}(x)] dx = \text{Nr. of valence quarks}$$

Experimental result (Gargamelle): 3.2 ± 0.6

Consistent with the Quark Model

Quantum ChromoDynamics (QCD)

$$\mathcal{L} = -\frac{1}{4} F_{\alpha\beta}^A F_A^{\alpha\beta} + \sum_{\text{flavours}} \bar{q}_a (i\not{D} - m)_{ab} q_b + \mathcal{L}_{\text{gauge-fixing}}$$

$$F_{\alpha\beta}^A = \partial_\alpha \mathcal{A}_\beta^A - \partial_\beta \mathcal{A}_\alpha^A - gf^{ABC} \mathcal{A}_\alpha^B \mathcal{A}_\beta^C$$

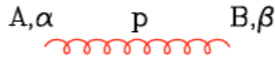
$$(D_\alpha)_{ab} = \partial_\alpha \delta_{ab} + ig (t^C \mathcal{A}_\alpha^C)_{ab}$$

$$\frac{\partial \alpha_S(Q)}{\partial \tau} = \beta(\alpha_S(Q)) \quad \tau = \ln \left(\frac{Q^2}{\mu^2} \right)$$

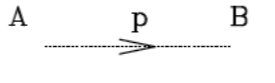
$$\beta(\alpha_S) = -b\alpha_S^2(1 + b'\alpha_S) + \mathcal{O}(\alpha_S^4)$$

$$b = \frac{(11C_A - 2N_f)}{12\pi}, \quad b' = \frac{(17C_A^2 - 5C_A N_f - 3C_F N_f)}{2\pi(11C_A - 2N_f)}$$

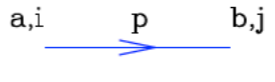
$$\alpha_S(Q) = \frac{1}{b \ln(Q^2/\Lambda^2)} \left[1 - \frac{b'}{b} \frac{\ln \ln(Q^2/\Lambda^2)}{\ln(Q^2/\Lambda^2)} \right] \quad (\text{NLO}).$$



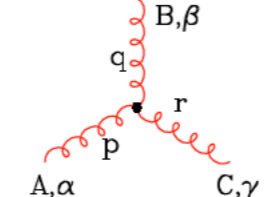
$$\delta^{AB} \left[-g^{\alpha\beta} + (1-\lambda) \frac{p^\alpha p^\beta}{p^2 + i\epsilon} \right] \frac{i}{p^2 + i\epsilon}$$



$$\delta^{AB} \frac{i}{(p^2 + i\epsilon)}$$

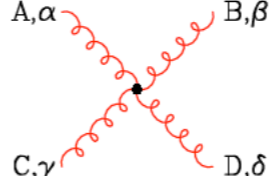


$$\delta^{ab} \frac{i}{(p - m + i\epsilon)_{ji}}$$

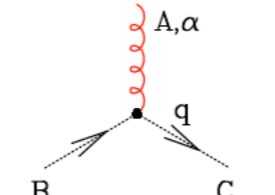


$$-g f^{ABC} [(p-q)^\gamma g^{\alpha\beta} + (q-r)^\alpha g^{\beta\gamma} + (r-p)^\beta g^{\gamma\alpha}]$$

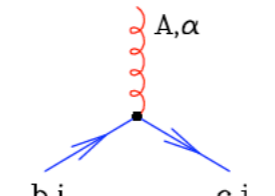
(all momenta incoming)



$$\begin{aligned} & -ig^2 f^{XAC} f^{XBD} [g^{\alpha\beta} g^{\gamma\delta} - g^{\alpha\delta} g^{\beta\gamma}] \\ & -ig^2 f^{XAD} f^{XBC} [g^{\alpha\beta} g^{\gamma\delta} - g^{\alpha\gamma} g^{\beta\delta}] \\ & -ig^2 f^{XAB} f^{XCD} [g^{\alpha\gamma} g^{\beta\delta} - g^{\alpha\delta} g^{\beta\gamma}] \end{aligned}$$



$$g f^{ABC} q^\alpha$$



$$-ig (t^A)_{cb} (\gamma^\alpha)_{ji}$$

DGLAP Equations

Dokshitzer–Gribov–Lipatov–Altarelli–Parisi (DGLAP) evolution equations

$$\frac{dq_i(x, Q^2)}{d \log Q^2} = \frac{\alpha_s}{2\pi} \int_x^1 \frac{dy}{y} \left[q_i(y, Q^2) P_{qq} \left(\frac{x}{y} \right) + g(y, Q^2) P_{qg} \left(\frac{x}{y} \right) \right]$$

$$\frac{dg(x, Q^2)}{d \log Q^2} = \frac{\alpha_s}{2\pi} \int_x^1 \frac{dy}{y} \left[\sum_i q_i(y, Q^2) P_{gq} \left(\frac{x}{y} \right) + g(y, Q^2) P_{gg} \left(\frac{x}{y} \right) \right]$$

Splitting functions:

$$P_{qq}^{(0)}(z) = \frac{4}{3} \left[\frac{1+z^2}{(1-z)_+} + \frac{3}{2} \delta(1-z) \right]$$

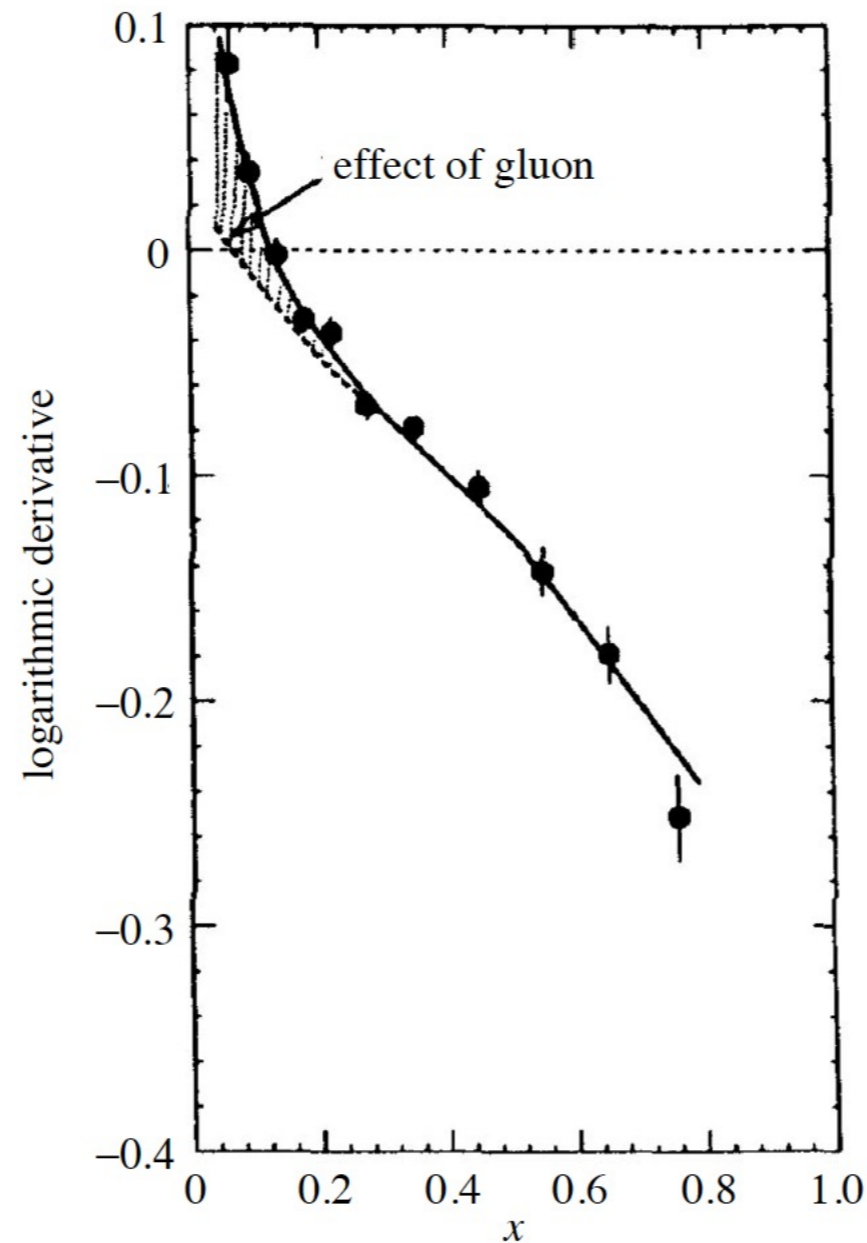
$$P_{qg}^{(0)}(z) = \frac{1}{2} [z^2 + (1-z)^2]$$

$$P_{gq}^{(0)}(z) = \frac{4}{3} \left[\frac{1+(1-z)^2}{z} \right]$$

$$P_{gg}^{(0)}(z) = 6 \left[\frac{z}{(1-z)_+} + \frac{1-z}{z} + z(1-z) + \left(\frac{11}{12} - \frac{n_f}{18} \right) \delta(1-z) \right]$$

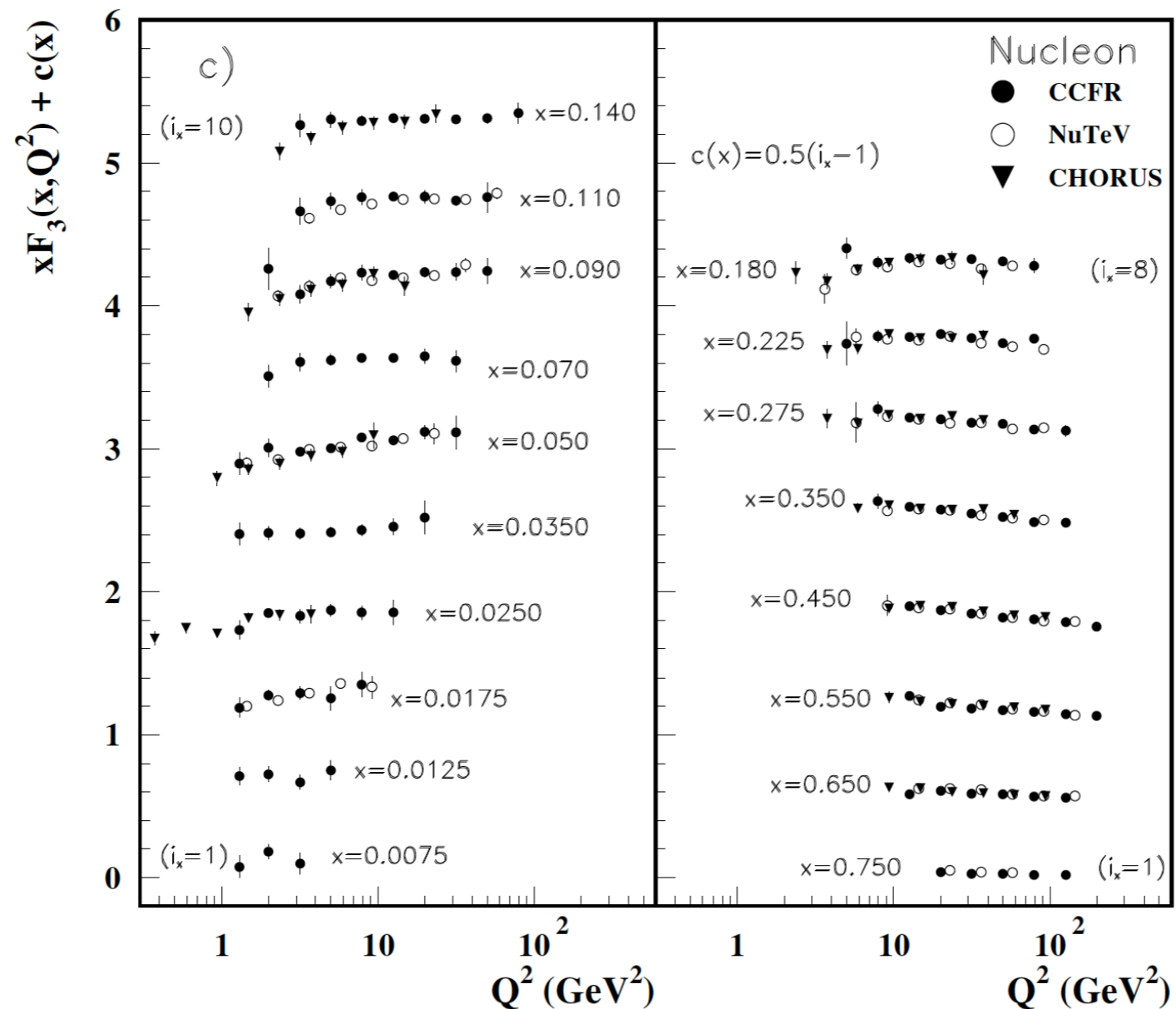
Scaling violation

$$\frac{\partial F_2}{\partial \ln Q^2} = \frac{\alpha_s}{2\pi} \int_x^1 \frac{d\xi}{\xi} \left\{ F_2(\xi, Q^2) P_{qq} \left(\frac{x}{\xi}, \alpha_s \right) + 2f G(\xi, Q^2) P_{qg} \left(\frac{x}{\xi}, \alpha_s \right) \right\}$$



Scaling violation

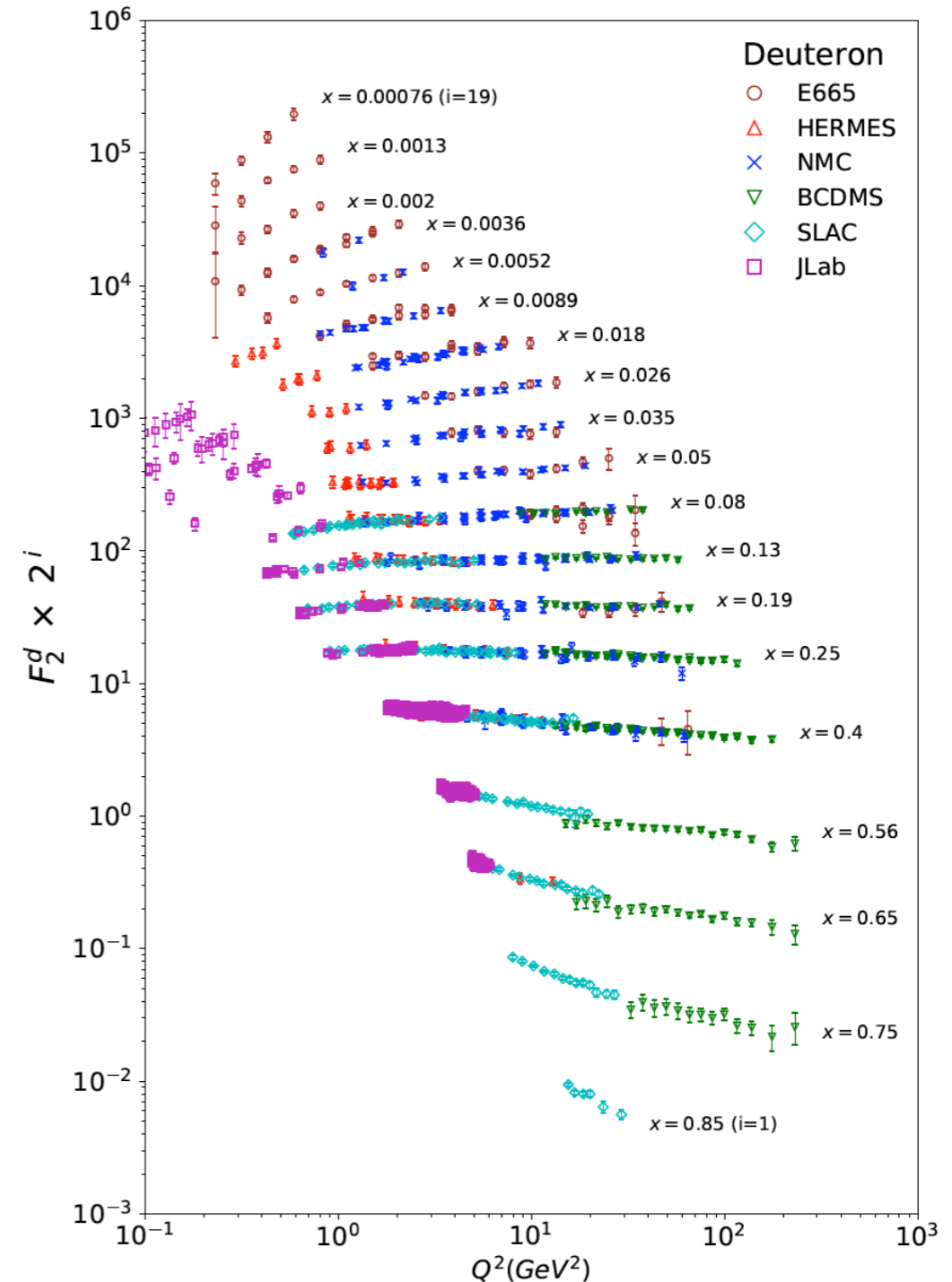
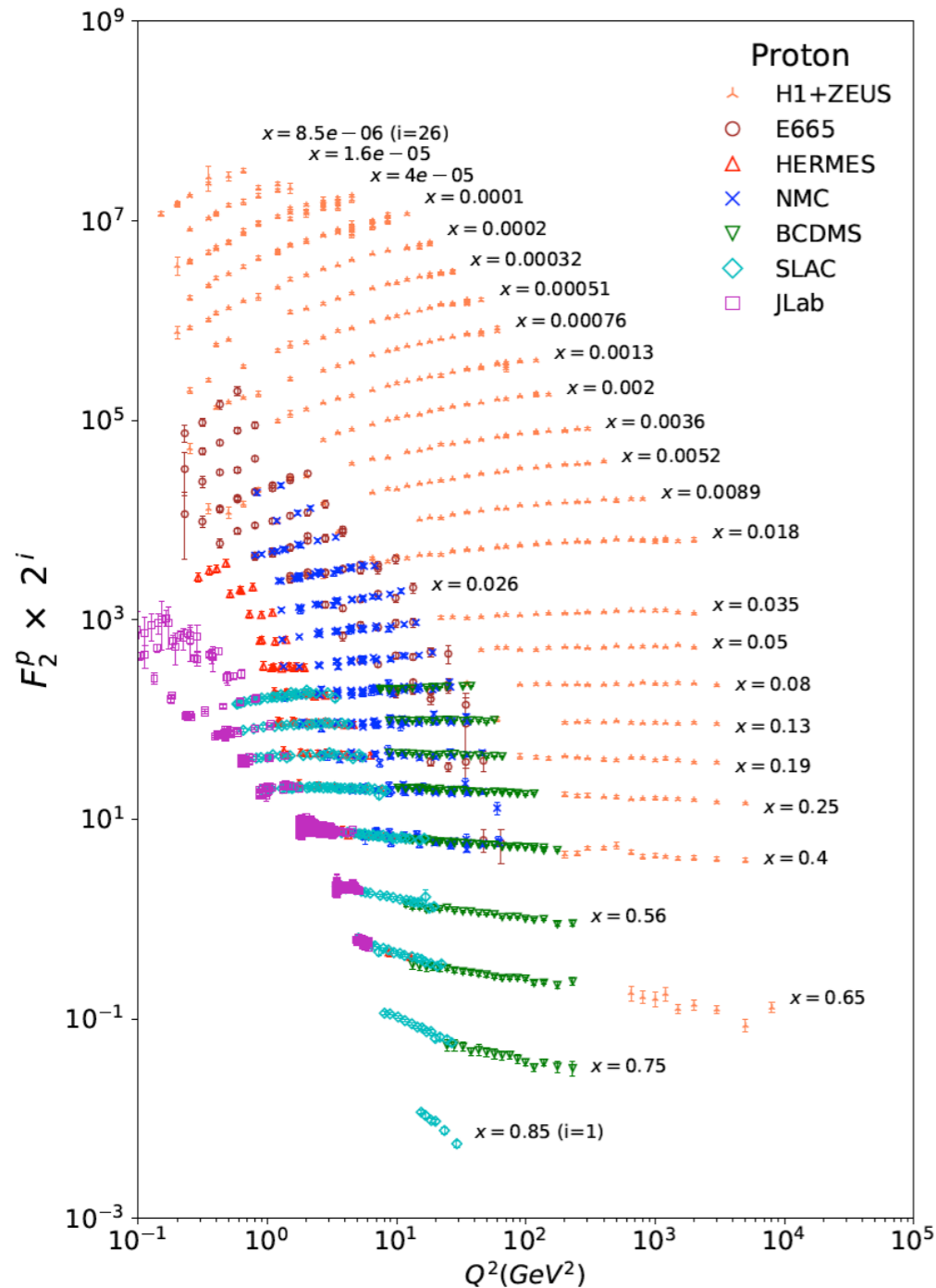
$$\frac{\partial xF_3}{\partial \ln Q^2} = \frac{\alpha_s}{2\pi} \int_x^1 \frac{d\xi}{\xi} \left\{ \xi F_3(\xi, Q^2) P_{qq} \left(\frac{x}{\xi}, \alpha_s \right) \right\}$$



Other Fixed Target Experiments

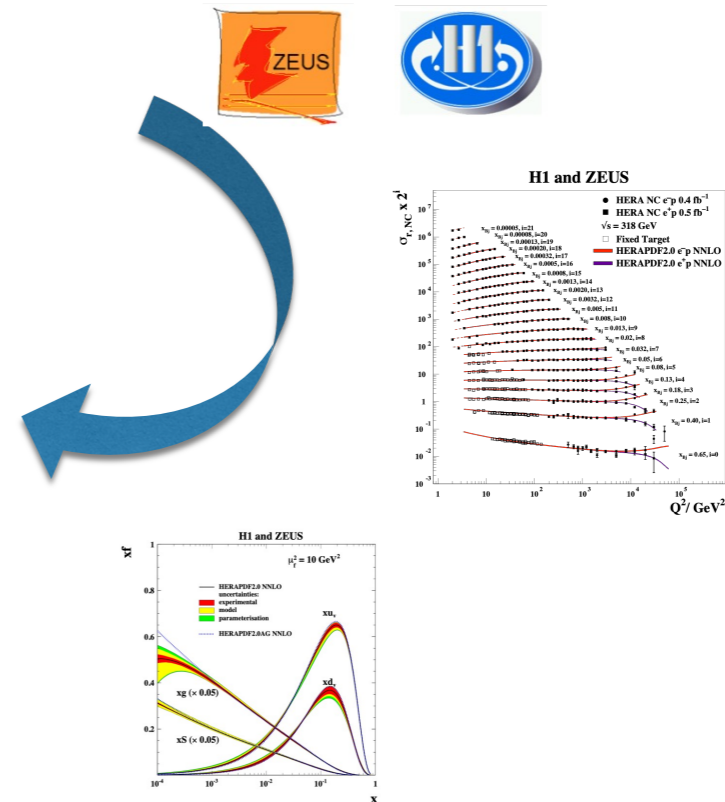
Experiments with muon beams: EMC, BFP, NMC, BCDMS, etc.

Experiments with neutrino beams: CCFR, HPWF, CDHSW, CHARM, WA24, WA21, etc.



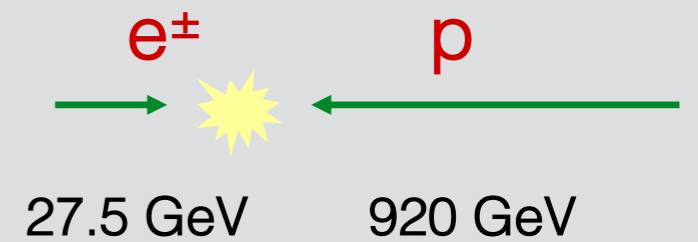
II. HERA

- H1-ZEUS
- High-lights
- LHC & PDFs



HERA

The world's first and only e-p collider



$$\sqrt{s} = 318 \text{ GeV}$$

'Equivalent' to a fixed target experiment with e^\pm of 50 TeV

HERA Operation

HERA-I (1992-2000)

$E_e=27.6$ GeV

$E_p=820$ & 920 GeV

$L_{int} \sim 130$ pb⁻¹ per experiment

Mostly e⁺p

HERA-II (2003-2007)

$E_e=27.6$ GeV

$E_p=920$ GeV

$L_{int} \sim 360$ pb⁻¹ per experiment

Longitudinally polarized lepton beams

Similar amounts of e⁺p and e⁻p

Low Energy Run 2007

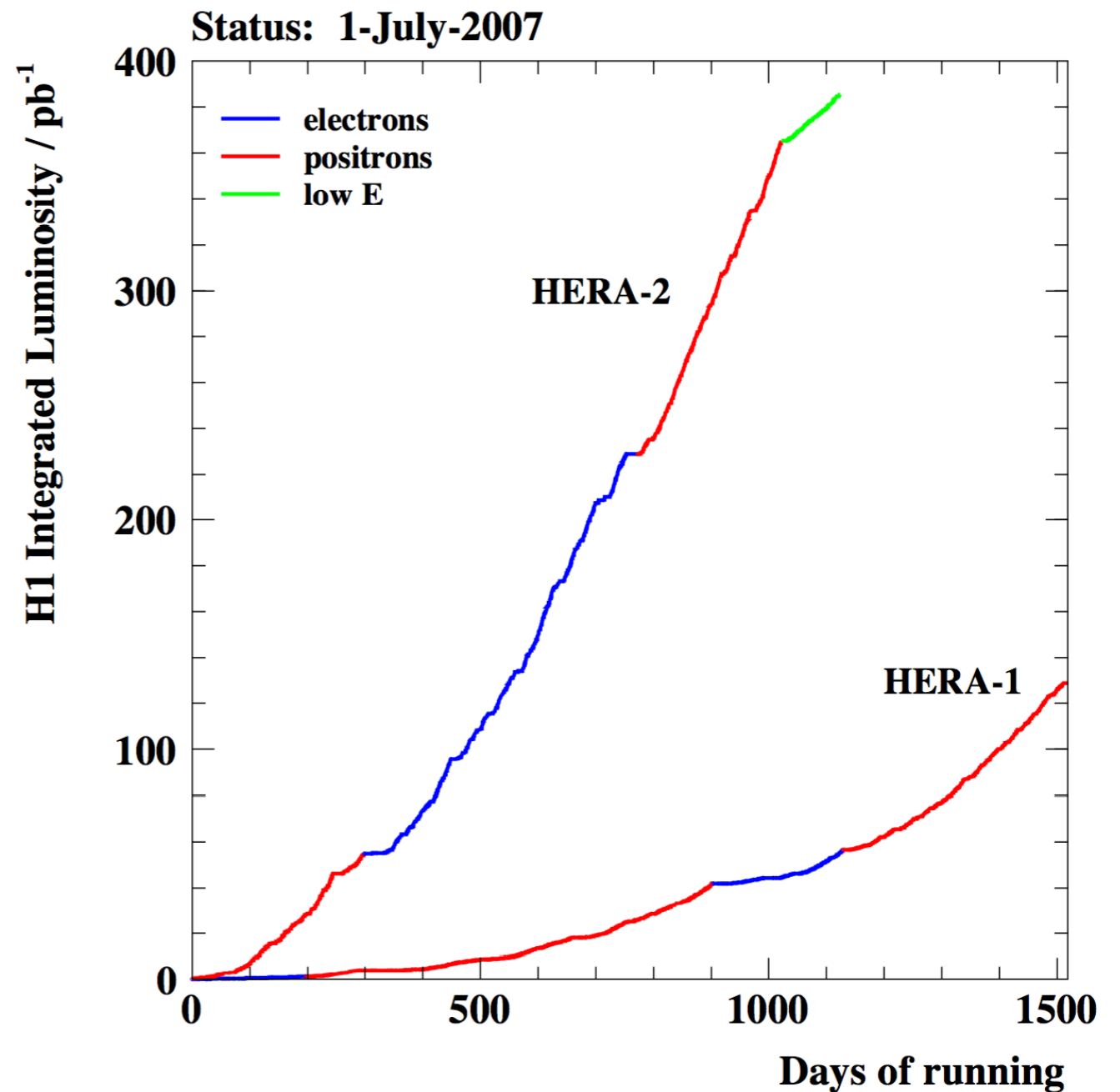
$E_e=27.6$ GeV

$E_p=460$ & 575 GeV

Runs at reduced \sqrt{s} :

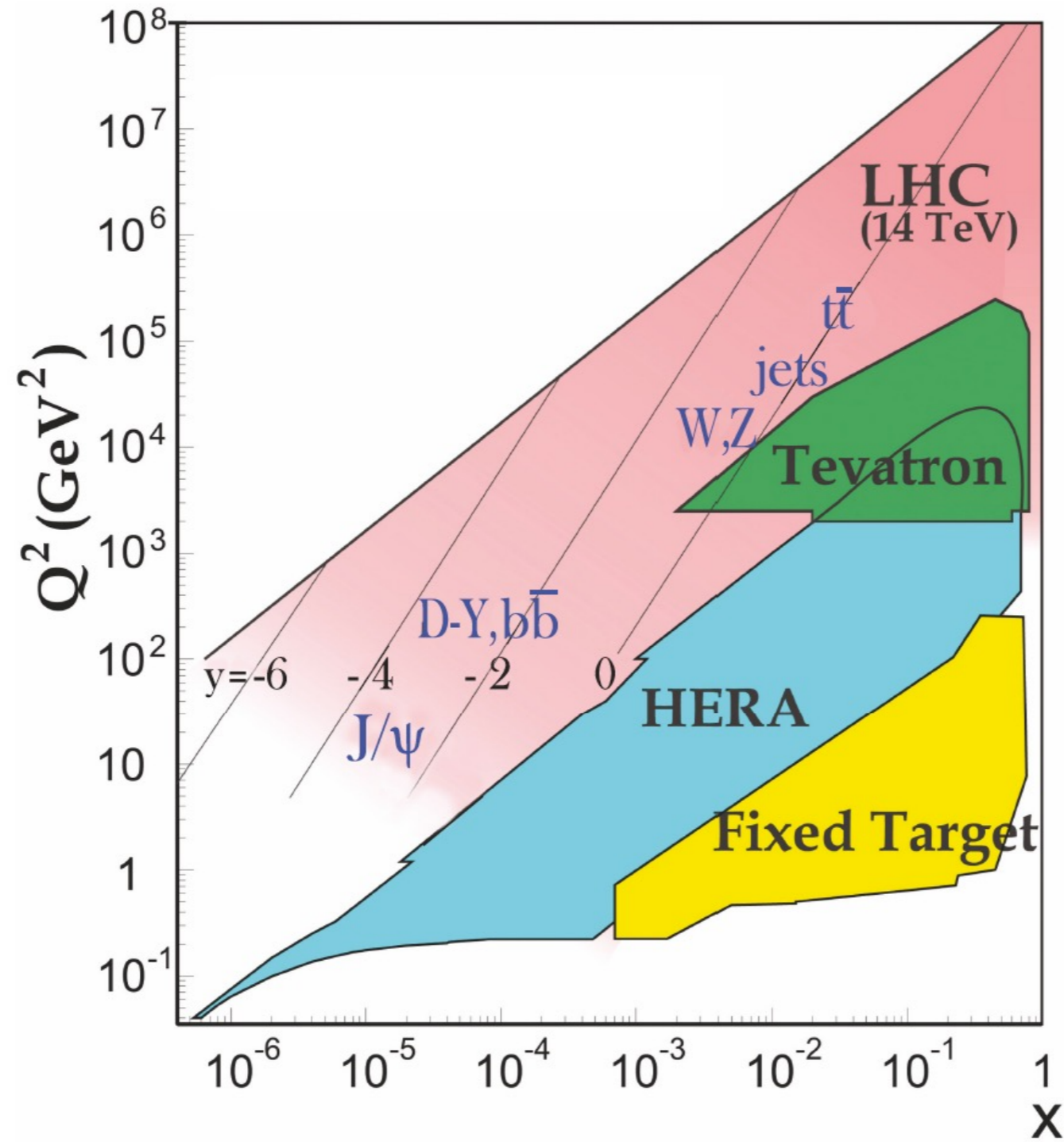
225 GeV (LER), 252 (MER) GeV

Dedicated F_L measurements



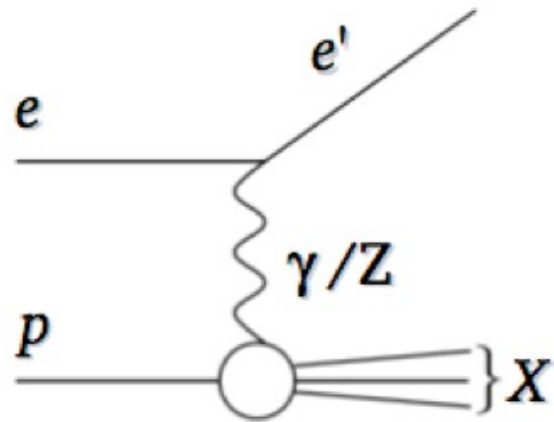
1 fb⁻¹ Integrated lumi, H1+ZEUS

HERA Kinematic domain

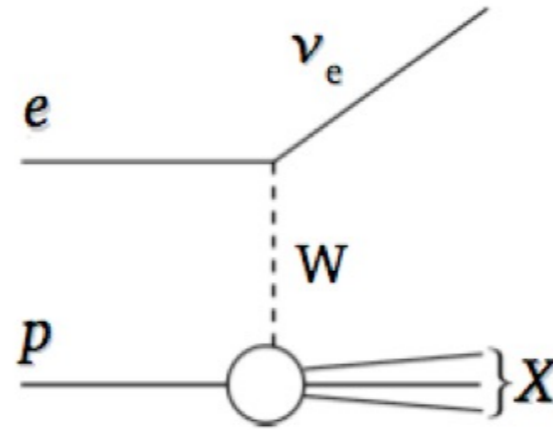


DIS processes and cross sections

NC: $e p \rightarrow e' X$



CC: $e p \rightarrow \nu_e X$



Kinematic variables:

- Virtuality exchanged boson

$$Q^2 = -q^2 = -(k - k')^2$$

- Bjorken scaling variable

$$x = \frac{Q^2}{2p \cdot q}$$

“Reduced” Cross sections

NC:

$$\sigma_{r,\text{NC}}^{\pm} = \frac{d^2 \sigma_{\text{NC}}^{e^{\pm} p}}{dx dQ^2} \cdot \frac{Q^4 x}{2\pi \alpha^2 Y_{\pm}} = F_2 \mp \frac{Y_{-}}{Y_{+}} x F_3 - \frac{y^2}{Y_{+}} F_L$$

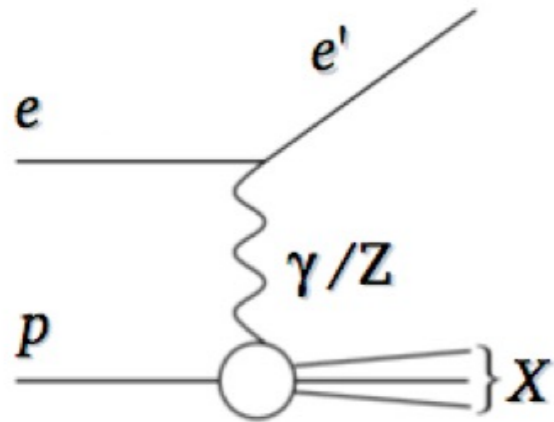
CC:

$$\sigma_{r,\text{CC}}^{\pm} = \frac{d^2 \sigma_{\text{CC}}^{e^{\pm} p}}{dx dQ^2} \cdot \frac{2\pi x}{G_F^2} \left[\frac{M_W^2 + Q^2}{M_W^2} \right]^2 = \frac{1}{2} \left(Y_{+} W_2^{\pm} \mp Y_{-} x W_3^{\pm} - y^2 W_L^{\pm} \right)$$

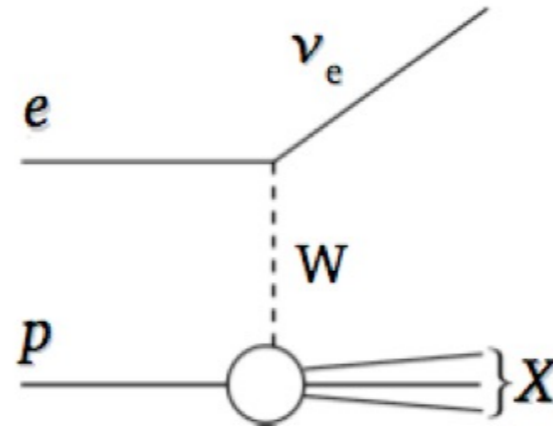
with $Y_{\pm} = 1 \pm (1 - y)^2$

DIS processes and cross sections

NC: $e p \rightarrow e' X$



CC: $e p \rightarrow \nu_e X$



Kinematic variables:

- Virtuality exchanged boson

$$Q^2 = -q^2 = -(k - k')^2$$

- Bjorken scaling variable

$$x = \frac{Q^2}{2p \cdot q}$$

Structure Functions, PDFs and DGLAP evolution equations (LO, NLO and NNLO):

$$x^{-1} F_2(x, Q^2) = \sum_{i=q,g} \int_x^1 \frac{d\xi}{\xi} C_{2,i} \left(\frac{x}{\xi}, \alpha_s(\mu^2), \frac{\mu^2}{Q^2} \right) f_i(\xi, \mu^2)$$

$$\frac{d}{d \ln \mu^2} f_i(\xi, \mu^2) = \sum_k \left[P_{ik}(\alpha_s(\mu^2)) \otimes f_k(\mu^2) \right] (\xi)$$

Combination: Data sets



The HERA Legacy



| Data Set | | x_{Bj} Grid | Q^2 [GeV ²] Grid | \mathcal{L} | e^+/e^- | \sqrt{s} | x_{Bj}, Q^2 from | Ref. |
|--|-------|---------------|--------------------------------|---------------|------------------|------------|--------------------|------------------|
| | from | to | from | to | pb ⁻¹ | GeV | equations | |
| HERA I $E_p = 820$ GeV and $E_p = 920$ GeV data sets | | | | | | | | |
| H1 svx-mb [2] | 95-00 | 0.000005 | 0.02 | 0.2 | 12 | 2.1 | e^+p 301, 319 | [3] |
| H1 low Q^2 [2] | 96-00 | 0.0002 | 0.1 | 12 | 150 | 22 | e^+p 301, 319 | [4] |
| H1 NC | 94-97 | 0.0032 | 0.65 | 150 | 30000 | 35.6 | e^+p 301 | [5] |
| H1 CC | 94-97 | 0.013 | 0.40 | 300 | 15000 | 35.6 | e^+p 301 | [5] |
| H1 NC | 98-99 | 0.0032 | 0.65 | 150 | 30000 | 16.4 | e^-p 319 | [6] |
| H1 CC | 98-99 | 0.013 | 0.40 | 300 | 15000 | 16.4 | e^-p 319 | [6] |
| H1 NC HY | 98-99 | 0.0013 | 0.01 | 100 | 800 | 16.4 | e^-p 319 | [7] |
| H1 NC | 99-00 | 0.0013 | 0.65 | 100 | 30000 | 65.2 | e^+p 319 | [7] |
| H1 CC | 99-00 | 0.013 | 0.40 | 300 | 15000 | 65.2 | e^+p 319 | [7] |
| ZEUS BPC | 95 | 0.000002 | 0.00006 | 0.11 | 0.65 | 1.65 | e^+p 300 | [11] |
| ZEUS BPT | 97 | 0.0000006 | 0.001 | 0.045 | 0.65 | 3.9 | e^+p 300 | [12] |
| ZEUS SVX | 95 | 0.000012 | 0.0019 | 0.6 | 17 | 0.2 | e^+p 300 | [13] |
| ZEUS NC [2] high/low Q^2 | 96-97 | 0.00006 | 0.65 | 2.7 | 30000 | 30.0 | e^+p 300 | [14] |
| ZEUS CC | 94-97 | 0.015 | 0.42 | 280 | 17000 | 47.7 | e^+p 300 | [15] |
| ZEUS NC | 98-99 | 0.005 | 0.65 | 200 | 30000 | 15.9 | e^-p 318 | [16] |
| ZEUS CC | 98-99 | 0.015 | 0.42 | 280 | 30000 | 16.4 | e^-p 318 | [17] |
| ZEUS NC | 99-00 | 0.005 | 0.65 | 200 | 30000 | 63.2 | e^+p 318 | [18] |
| ZEUS CC | 99-00 | 0.008 | 0.42 | 280 | 17000 | 60.9 | e^+p 318 | [19] |
| HERA II $E_p = 920$ GeV data sets | | | | | | | | |
| H1 NC ^{1.5p} | 03-07 | 0.0008 | 0.65 | 60 | 30000 | 182 | e^+p 319 | [8] ¹ |
| H1 CC ^{1.5p} | 03-07 | 0.008 | 0.40 | 300 | 15000 | 182 | e^+p 319 | [8] ¹ |
| H1 NC ^{1.5p} | 03-07 | 0.0008 | 0.65 | 60 | 50000 | 151.7 | e^-p 319 | [8] ¹ |
| H1 CC ^{1.5p} | 03-07 | 0.008 | 0.40 | 300 | 30000 | 151.7 | e^-p 319 | [8] ¹ |
| H1 NC med Q^2 ^{*y.5} | 03-07 | 0.0000986 | 0.005 | 8.5 | 90 | 97.6 | e^+p 319 | [10] |
| H1 NC low Q^2 ^{*y.5} | 03-07 | 0.000029 | 0.00032 | 2.5 | 12 | 5.9 | e^+p 319 | [10] |
| ZEUS NC | 06-07 | 0.005 | 0.65 | 200 | 30000 | 135.5 | e^+p 318 | [22] |
| ZEUS CC ^{1.5p} | 06-07 | 0.0078 | 0.42 | 280 | 30000 | 132 | e^+p 318 | [23] |
| ZEUS NC ^{1.5} | 05-06 | 0.005 | 0.65 | 200 | 30000 | 169.9 | e^-p 318 | [20] |
| ZEUS CC ^{1.5} | 04-06 | 0.015 | 0.65 | 280 | 30000 | 175 | e^-p 318 | [21] |
| ZEUS NC nominal ^{*y} | 06-07 | 0.000092 | 0.008343 | 7 | 110 | 44.5 | e^+p 318 | [24] |
| ZEUS NC satellite ^{*y} | 06-07 | 0.000071 | 0.008343 | 5 | 110 | 44.5 | e^+p 318 | [24] |
| HERA II $E_p = 575$ GeV data sets | | | | | | | | |
| H1 NC high Q^2 | 07 | 0.00065 | 0.65 | 35 | 800 | 5.4 | e^+p 252 | [9] |
| H1 NC low Q^2 | 07 | 0.0000279 | 0.0148 | 1.5 | 90 | 5.9 | e^+p 252 | [10] |
| ZEUS NC nominal | 07 | 0.000147 | 0.013349 | 7 | 110 | 7.1 | e^+p 251 | [24] |
| ZEUS NC satellite | 07 | 0.000125 | 0.013349 | 5 | 110 | 7.1 | e^+p 251 | [24] |
| HERA II $E_p = 460$ GeV data sets | | | | | | | | |
| H1 NC high Q^2 | 07 | 0.00081 | 0.65 | 35 | 800 | 11.8 | e^+p 225 | [9] |
| H1 NC low Q^2 | 07 | 0.0000348 | 0.0148 | 1.5 | 90 | 12.2 | e^+p 225 | [10] |
| ZEUS NC nominal | 07 | 0.000184 | 0.016686 | 7 | 110 | 13.9 | e^+p 225 | [24] |
| ZEUS NC satellite | 07 | 0.000143 | 0.016686 | 5 | 110 | 13.9 | e^+p 225 | [24] |

H1 & ZEUS have now published all their inclusive measurements (1992-2007)

- HERA-I
- HERA-II measurements at high- Q^2
- HERA-II measurements at reduced \sqrt{s}

$$0.6 \times 10^{-6} < x_{Bj} < 0.65, \quad 0.045 < Q^2 < 50000$$

41 data sets are combined:

- NC & CC cross sections
- e^+p and e^-p scattering
- 4 different \sqrt{s} (318, 301, 252 and 225 GeV)

2927 data points



1307 combined points

In typical cases 3 to 6 measurements contribute to a combined result

NC e^+p accuracy reaches ~1%

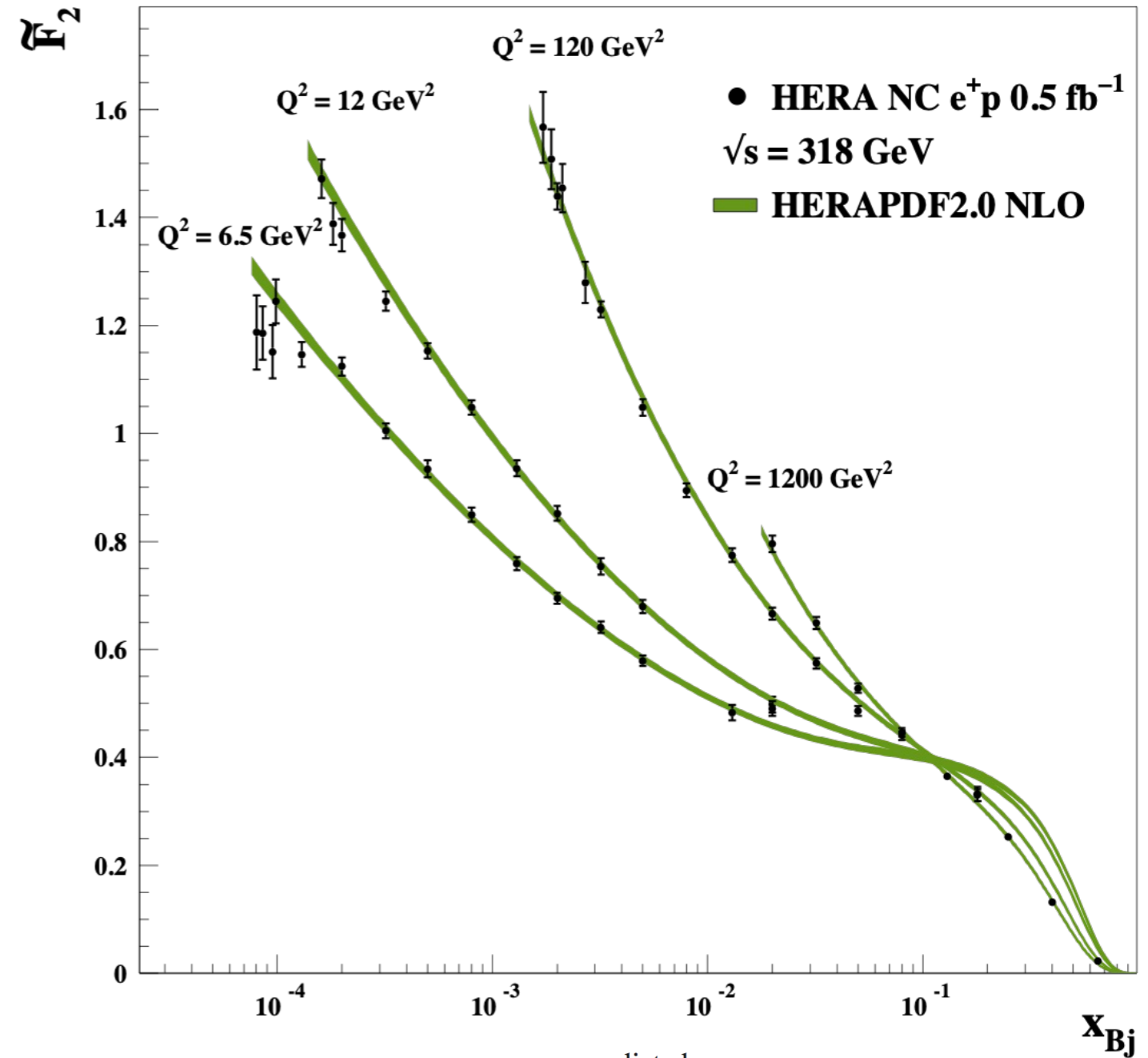
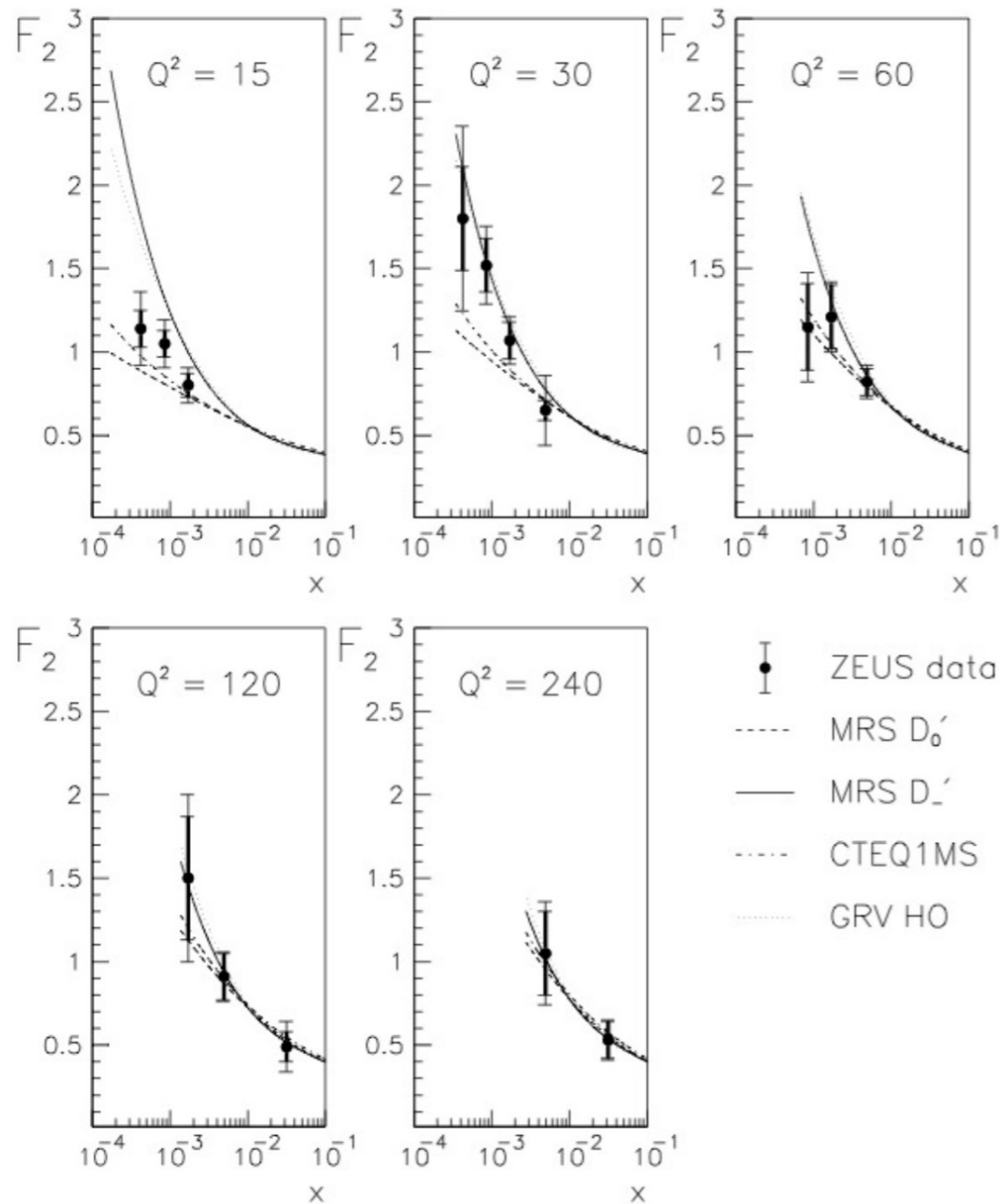
The usage of different reconstruction techniques and the differences in the strengths of the detector components of the two experiments lead to a substantial reduction of the systematic uncertainties of the combined cross sections.

Rise of F_2

HERA F_2 (1993)

HERA F_2 (2015)

H1 and ZEUS



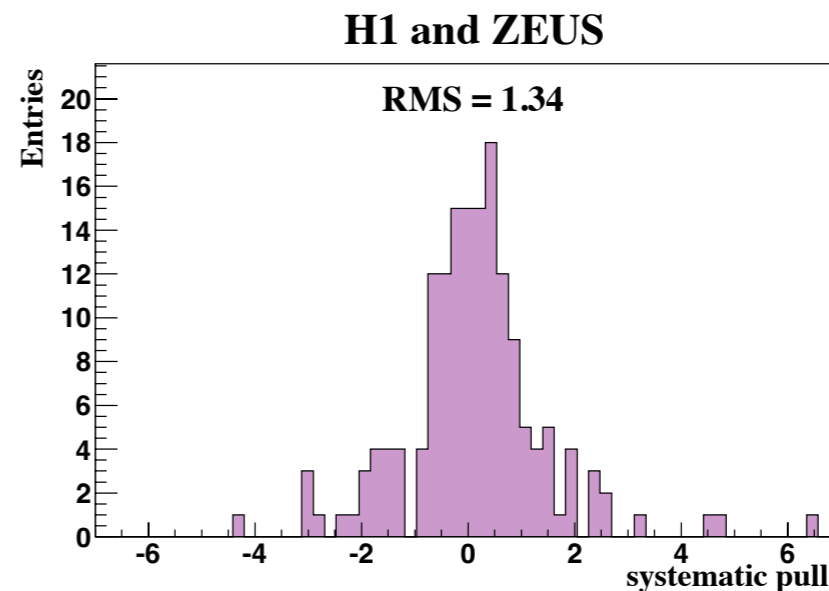
$$\tilde{F}_2 = \sigma_{r,\text{NC}}^\pm \cdot \frac{\tilde{F}_2^{\text{predicted}}}{\sigma_{r,\text{NC}}^\pm} = \sigma_{r,\text{NC}}^\pm \cdot (1 + C_F)$$

Combination: Averaging Method

- Combination performed using the [HERAverager](#) package
- Averaging procedure take correlations of systematic unc. fully into account
- Multiplicative treatment of the systematic uncertainties (as a default choice)
- Minimisation procedure based on the following χ^2 definition:

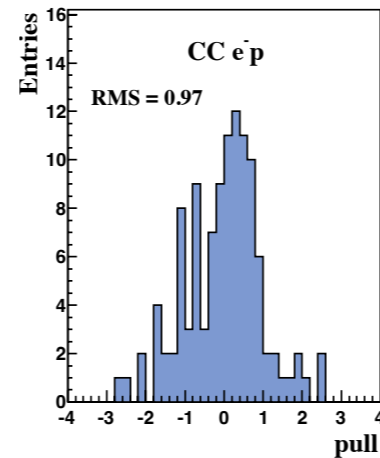
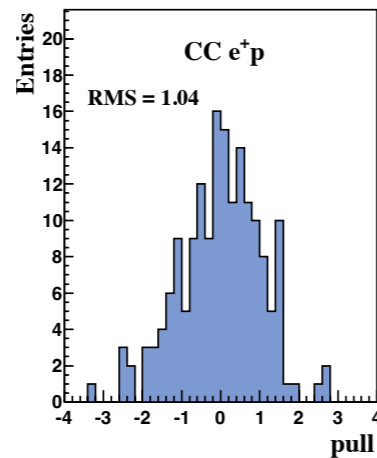
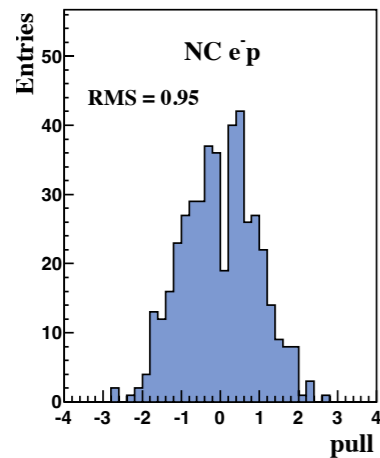
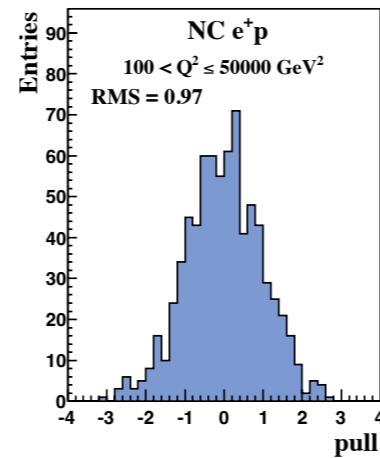
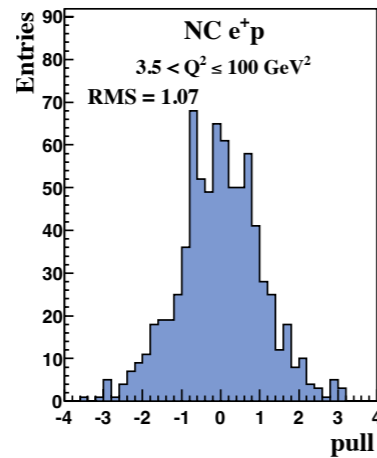
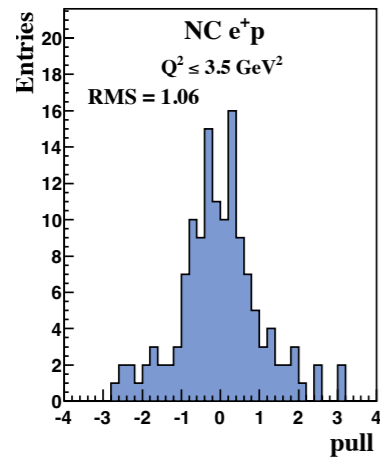
$$\chi_{\text{exp,ds}}^2(\mathbf{m}, \mathbf{b}) = \sum_i \frac{[m^i - \sum_j \gamma_j^i m^i b_j - \mu^i]^2}{\delta_{i,\text{stat}}^2 \mu^i (m^i - \sum_j \gamma_j^i m^i b_j) + (\delta_{i,\text{uncor}} m^i)^2} + \sum_j b_j^2$$

- **Procedural uncertainties:**
 - Multiplicative vs additive nature of the systematic error sources
 - Correlations in photo-production background and hadronic energy scale across H1 and ZEUS measurements
 - Large pulls in correlated syst. uncert.



Combination: Pulls

H1 and ZEUS



χ^2 of the combination:

$$\frac{\chi^2}{d.o.f} = \frac{1687}{1620}$$

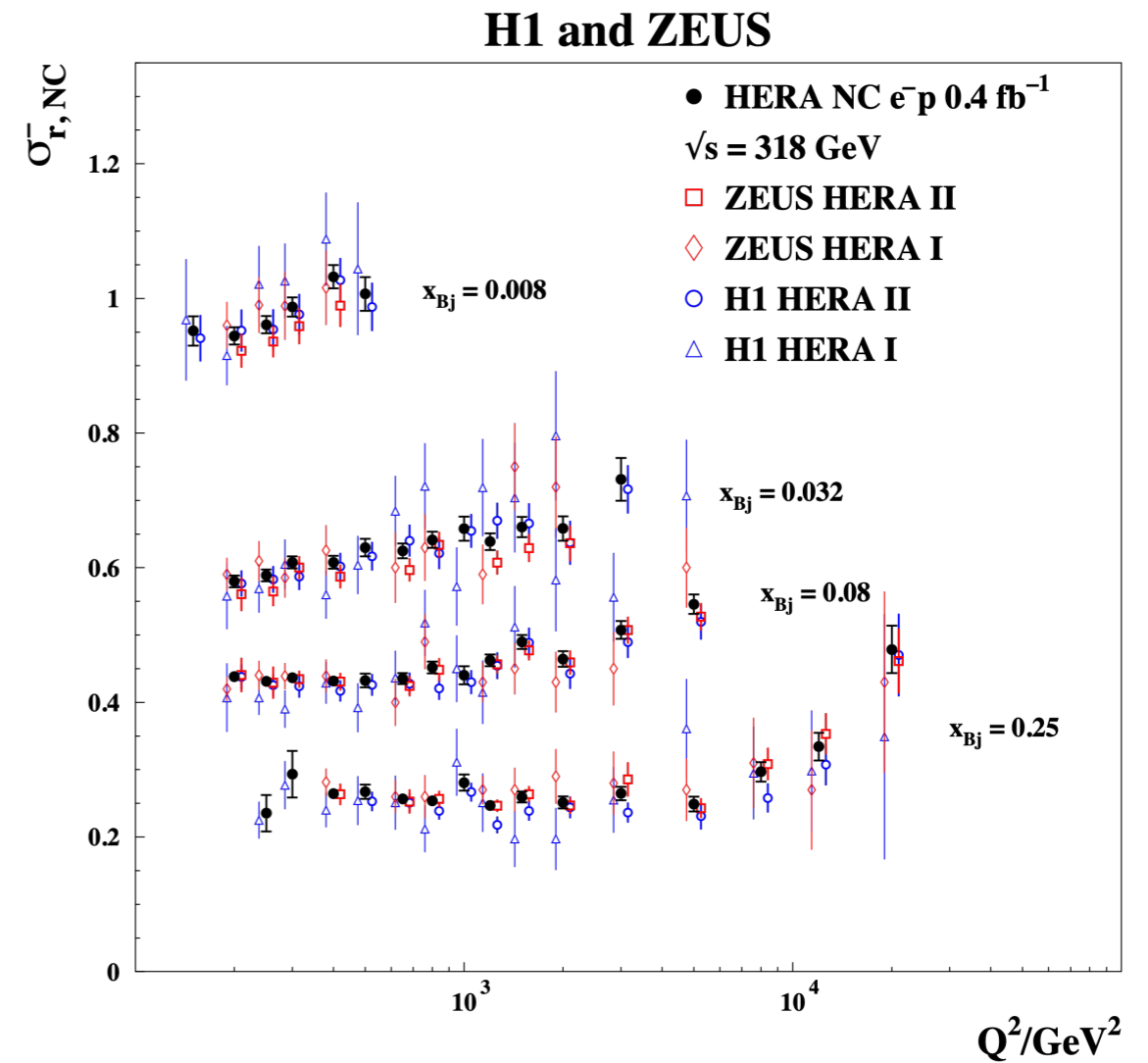
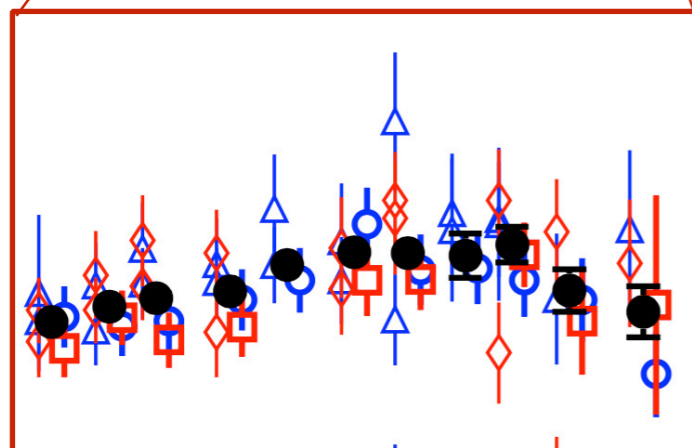
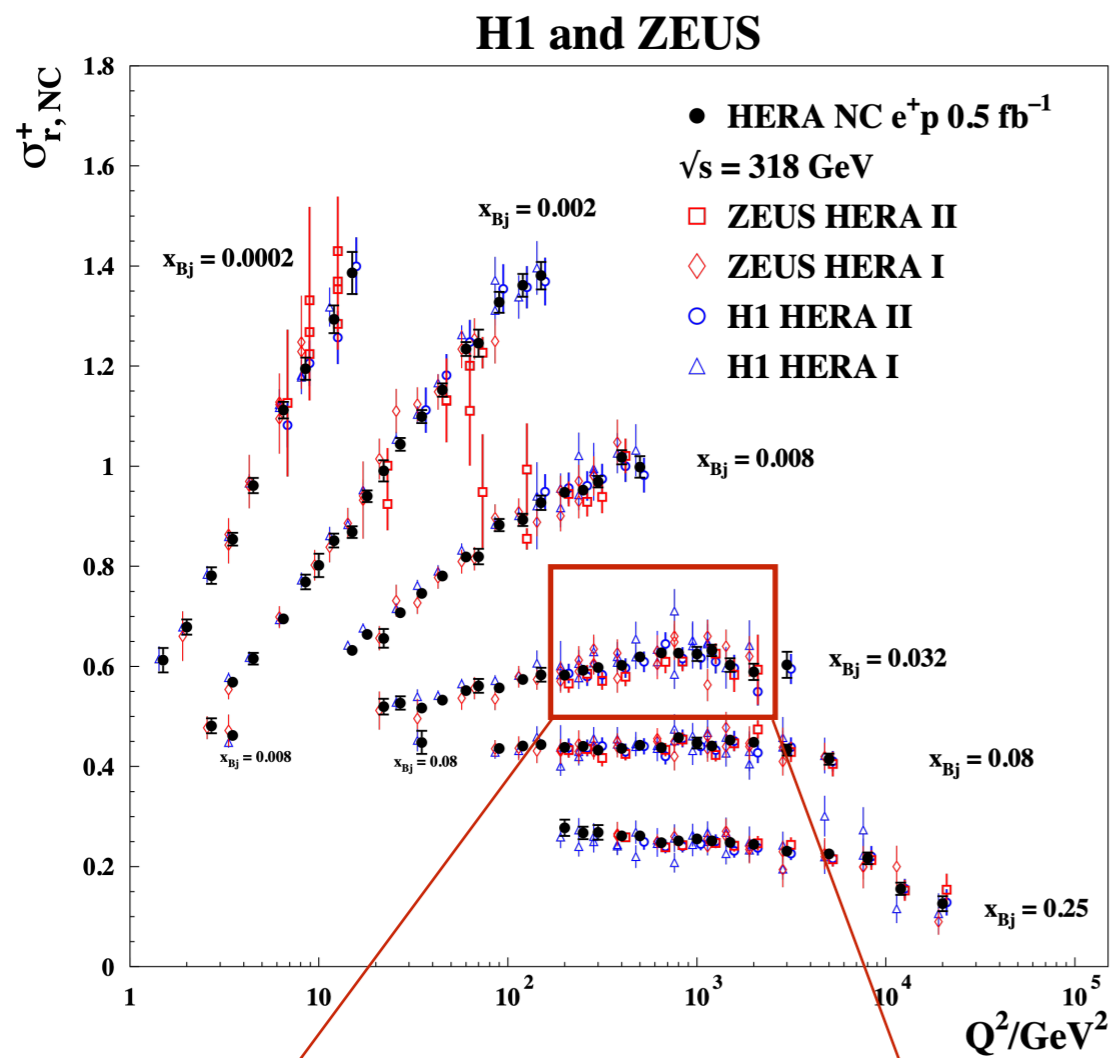
Pull definition:

$$p^{i,k} = \frac{\mu^{i,k} - \mu^{i,ave} (1 - \sum_j \gamma_j^{i,k} b_{j,ave})}{\sqrt{\Delta_{i,k}^2 - \Delta_{i,ave}^2}}$$

For each process pulls centred at zero with ~ unit width

Combination: Results

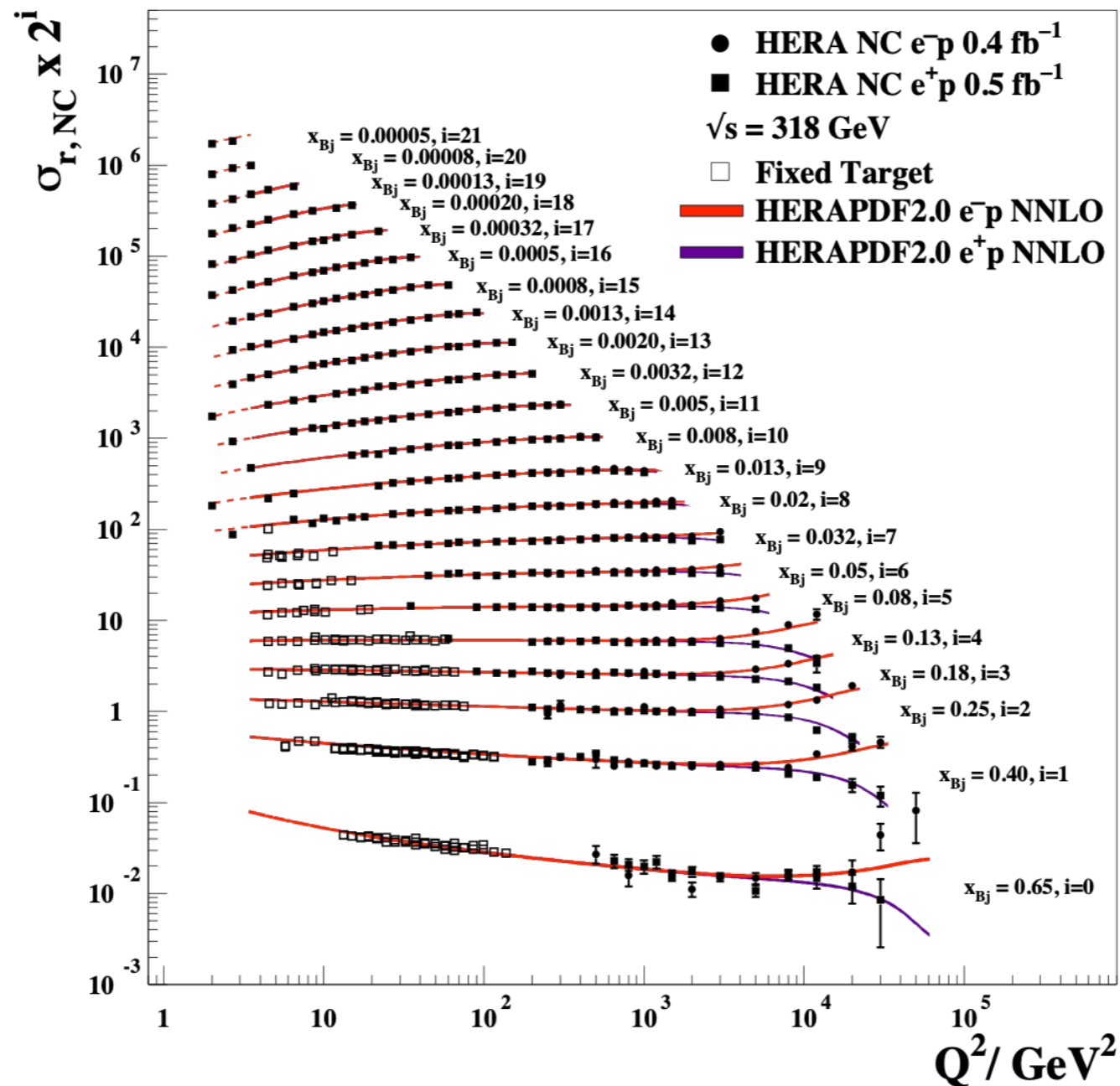
NC $e^\pm p$, $\sqrt{s} = 318$ GeV



N.B. only a few representative x_{Bj} bins are shown

Scaling violations

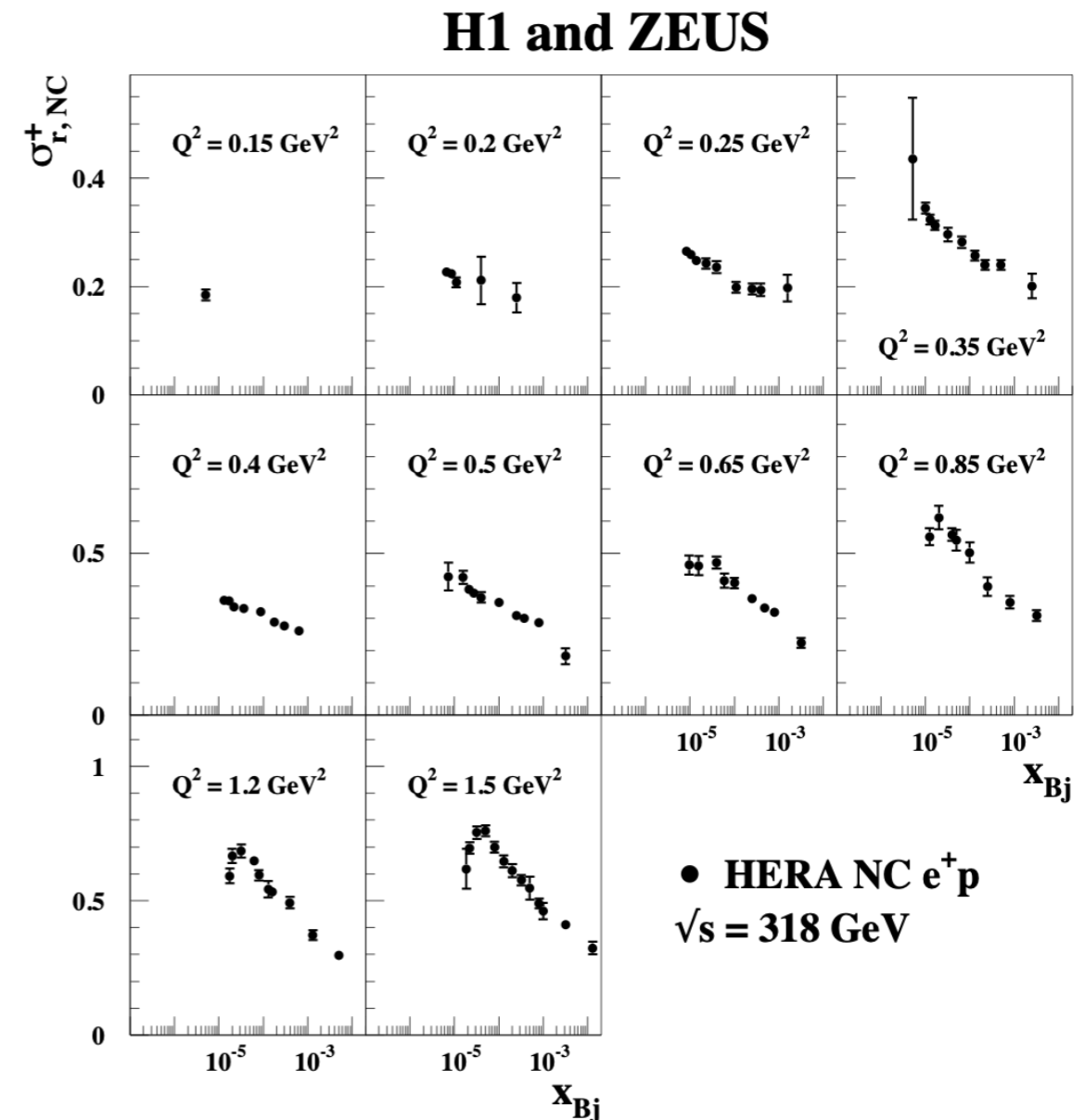
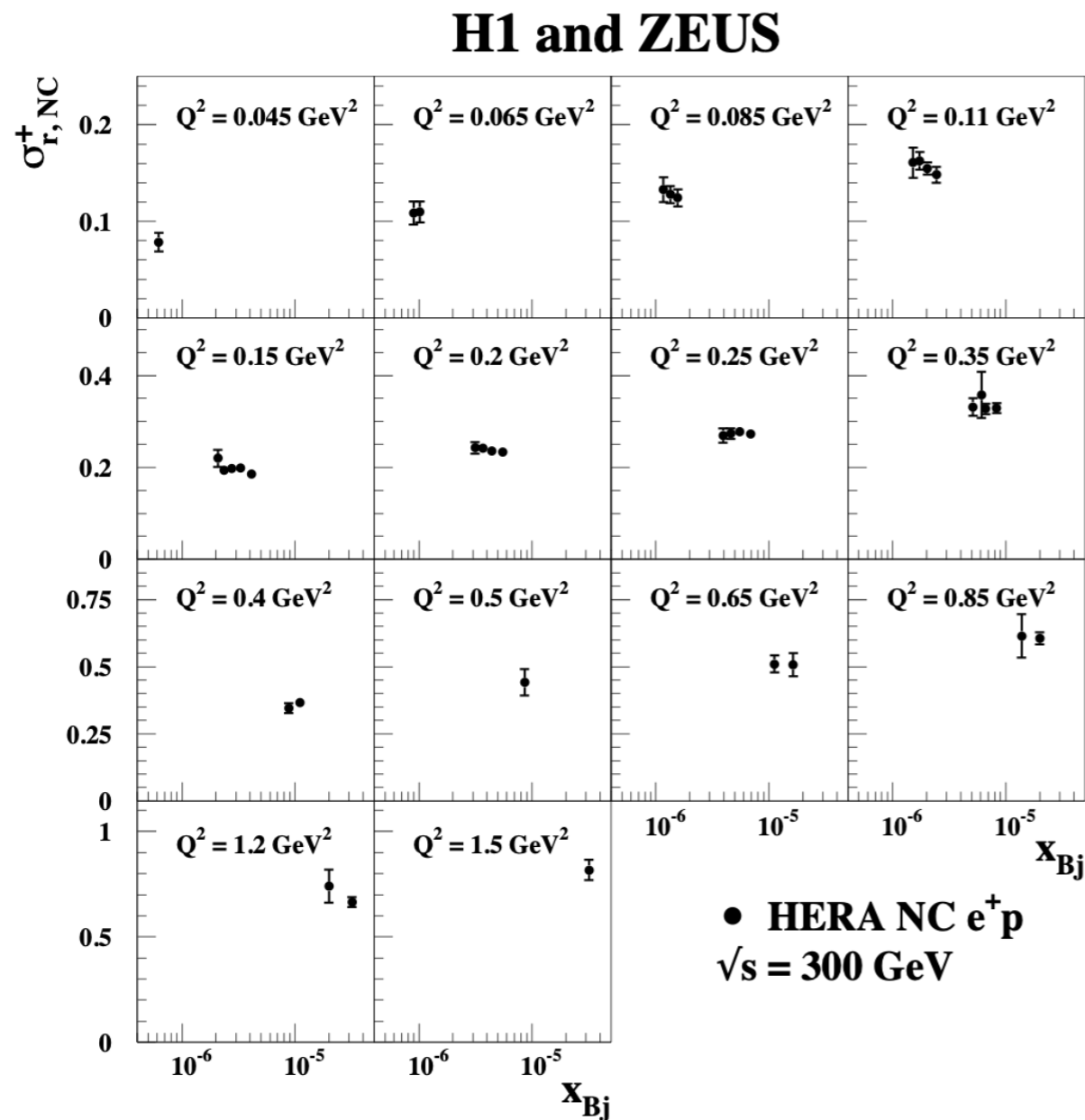
H1 and ZEUS



Textbook plots showing with great precision scaling violations patterns (and EW effects at high- Q^2 and high- x)

Combination: Results

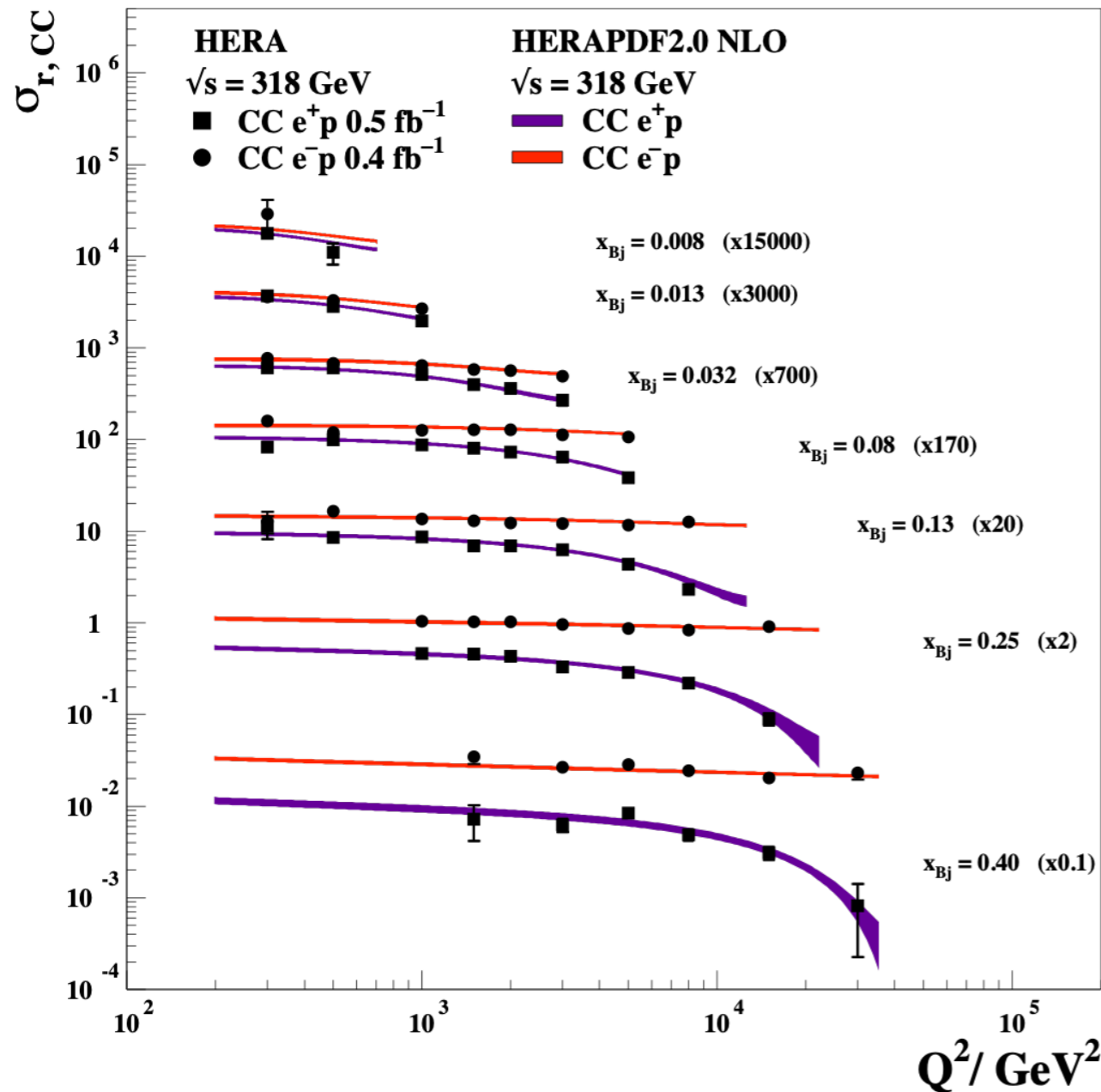
Very low Q^2 and low x_{Bj} data $\sqrt{s} = 300, 318$ GeV



- A very important data sample for QCD studies at low- x_{Bj}
- Interesting also for dipole/saturation models and higher-twist studies

Helicity effects in CC interactions

H1 and ZEUS



Reminder:

$$\sigma_{r,CC}^+ \approx (x\bar{U} + (1-y)^2 xD)$$

$$\sigma_{r,CC}^- \approx (xU + (1-y)^2 x\bar{D})$$

The helicity factor $(1-y)^2$ affects differently the $e^\pm p$ CC cross sections:

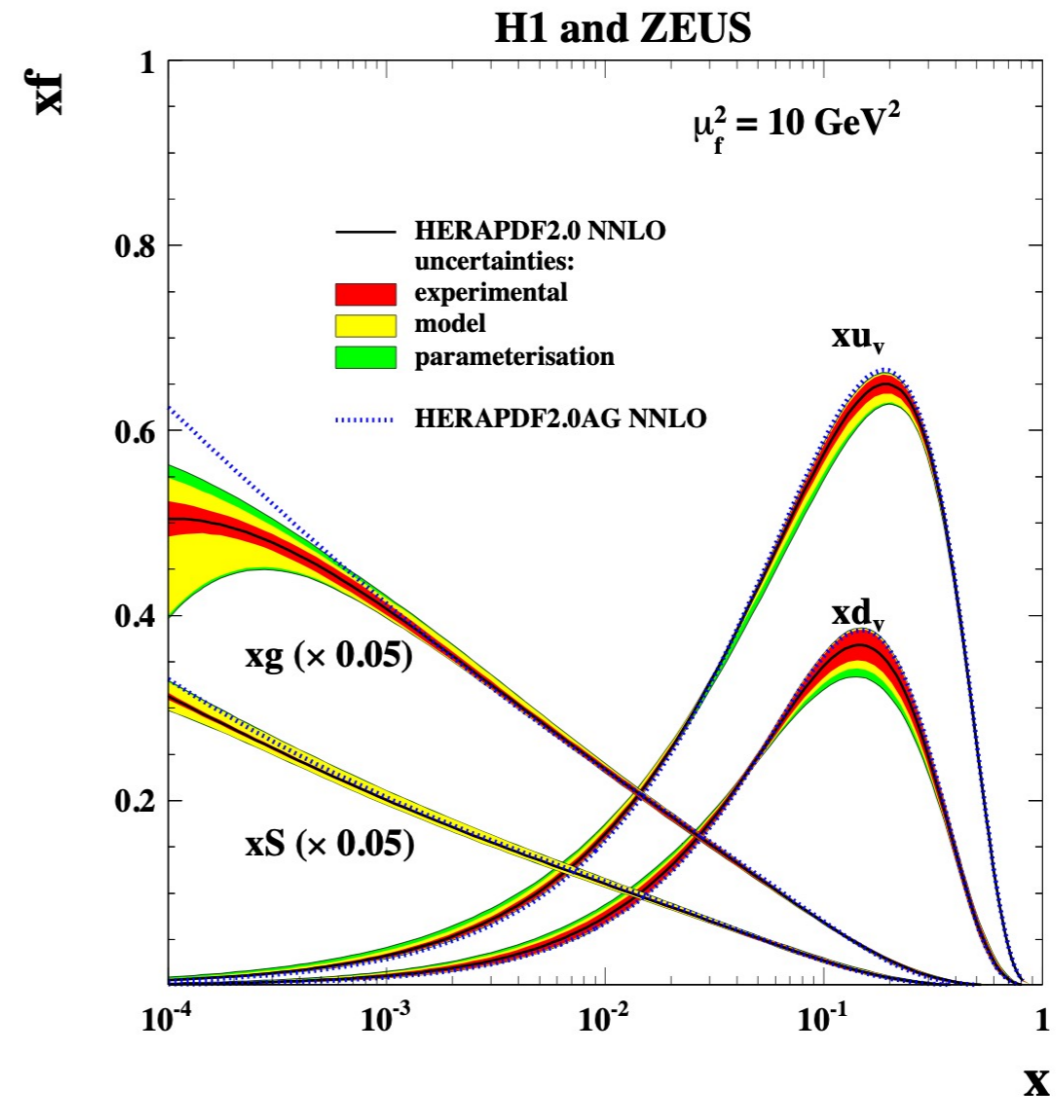
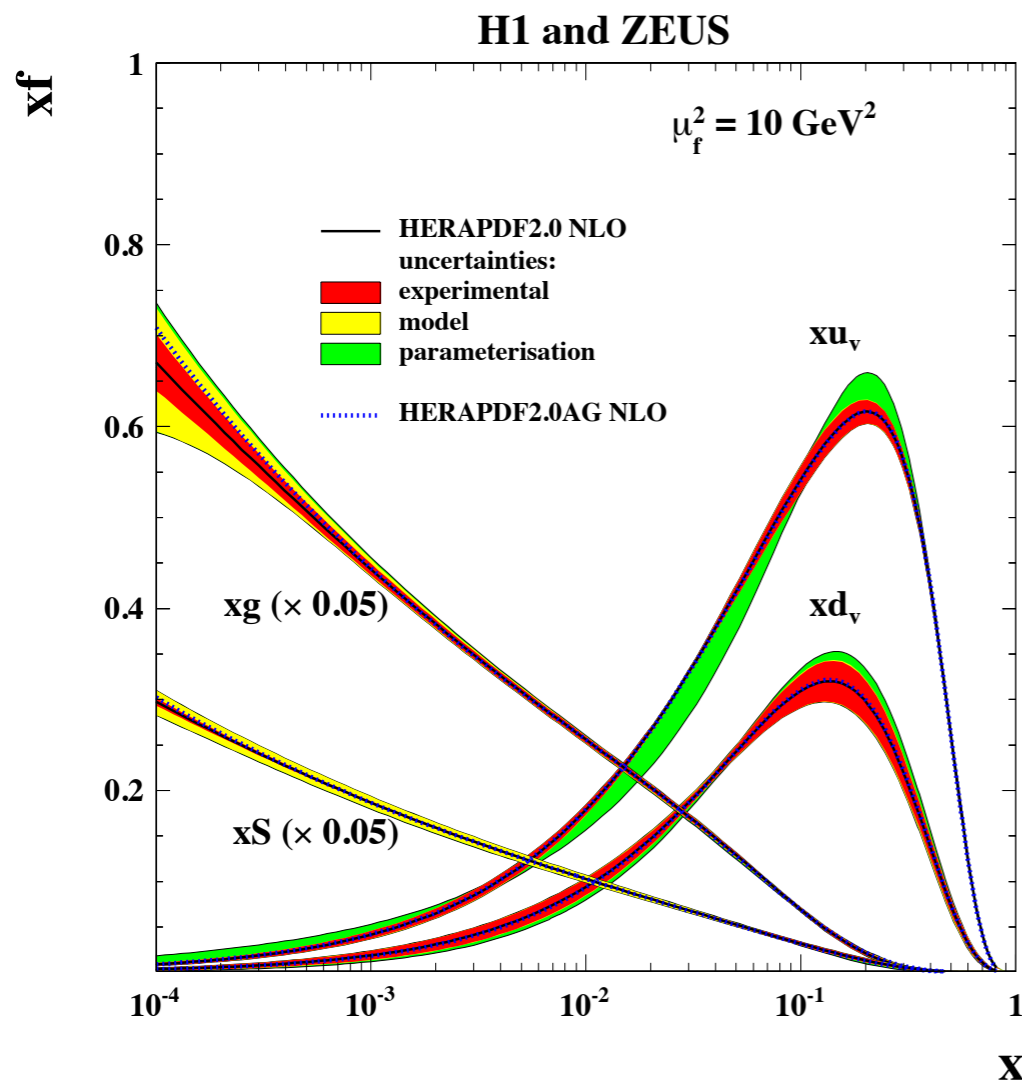
- The e^+p cross section is suppressed at high- y (high- Q^2)
- The e^-p cross section is almost unaffected

The precision of the CC cross sections at high- Q^2 allow the study of these helicity effects.

HERAPDF2.0: NLO and NNLO PDFs

NLO

NNLO

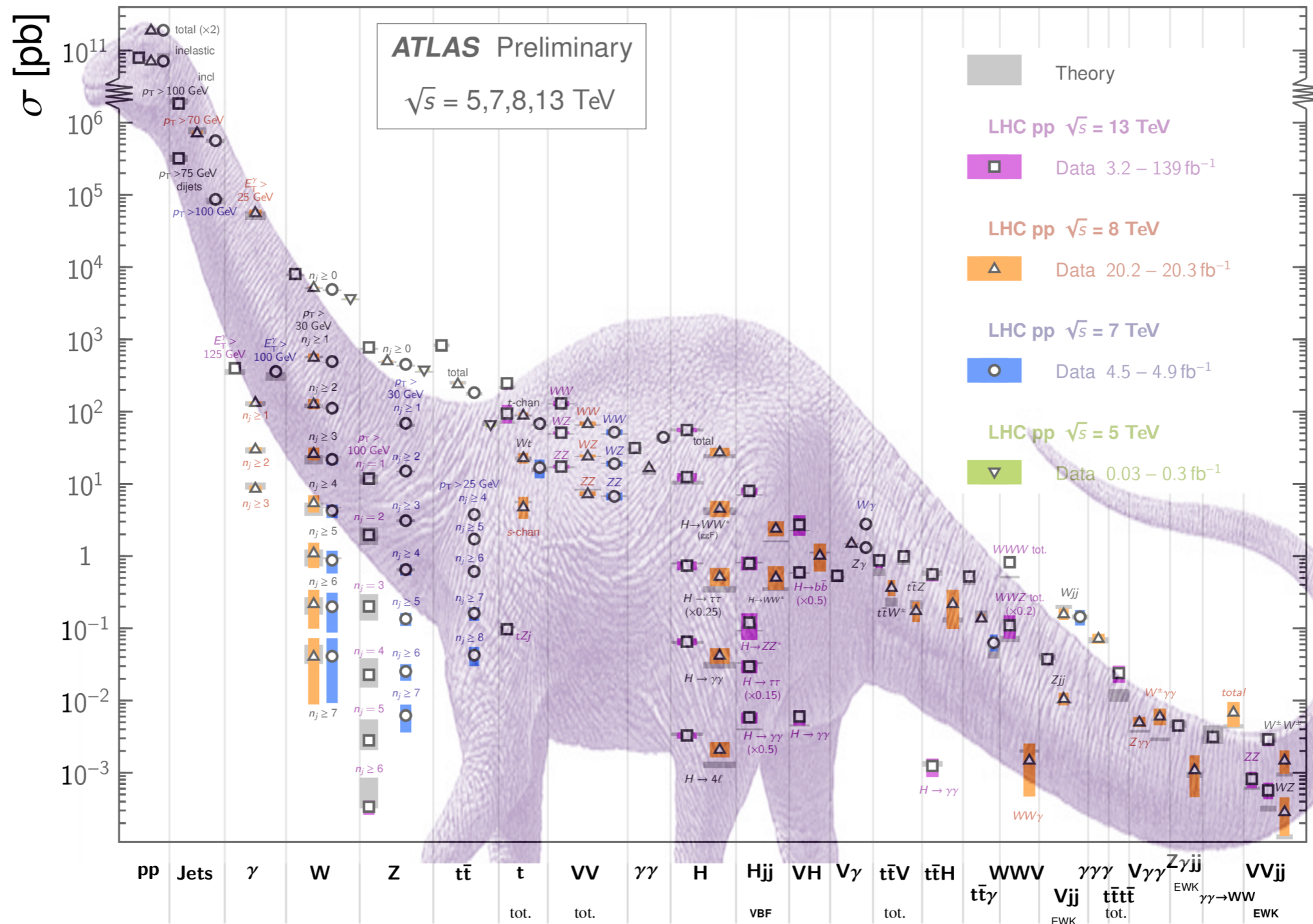


NNLO vs NLO: - gluon ceases to rise at low- x
 - sea at low- x somewhat steeper w.r.t. NLO

Measurements at LHC and PDFs

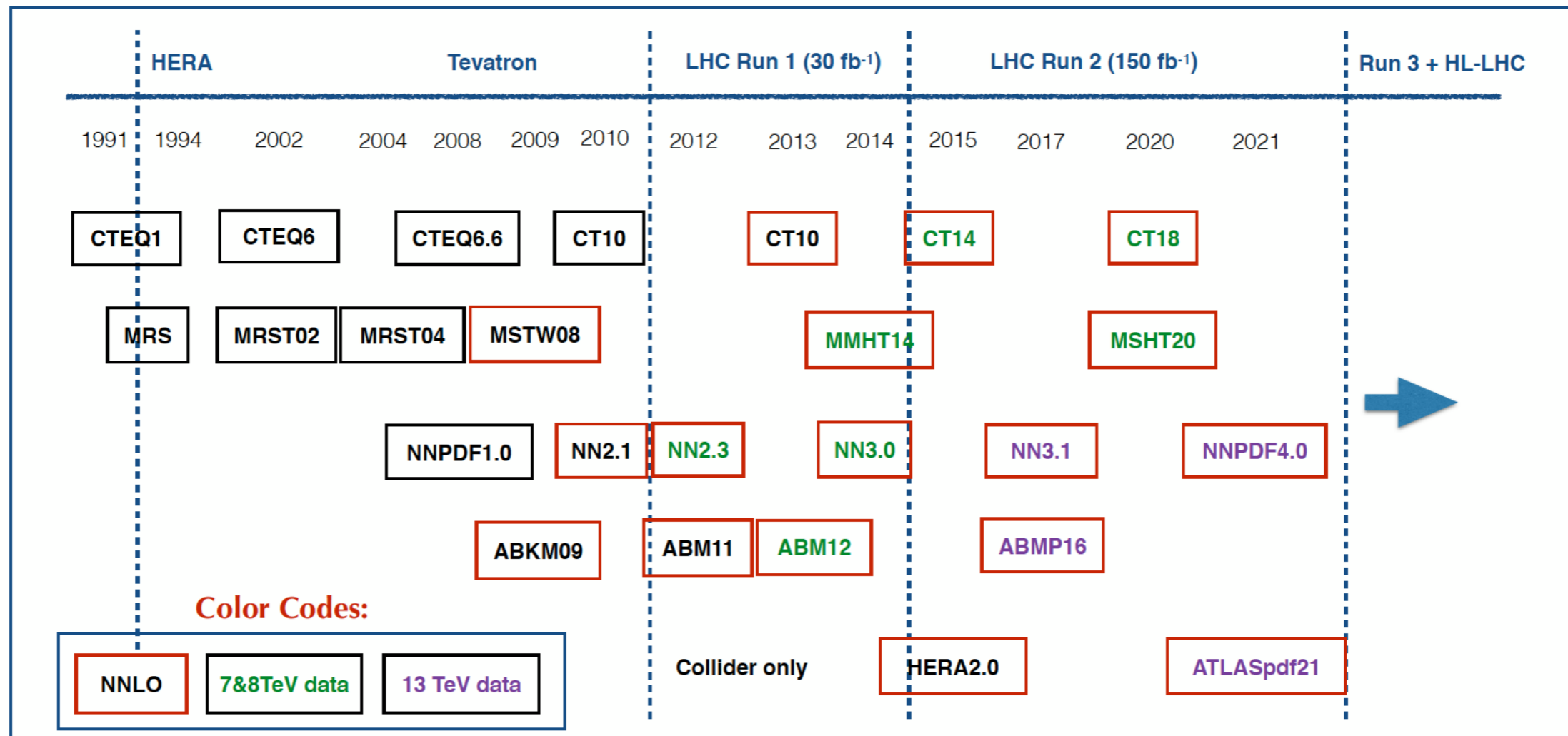
Standard Model Production Cross Section Measurements

Status: February 2022



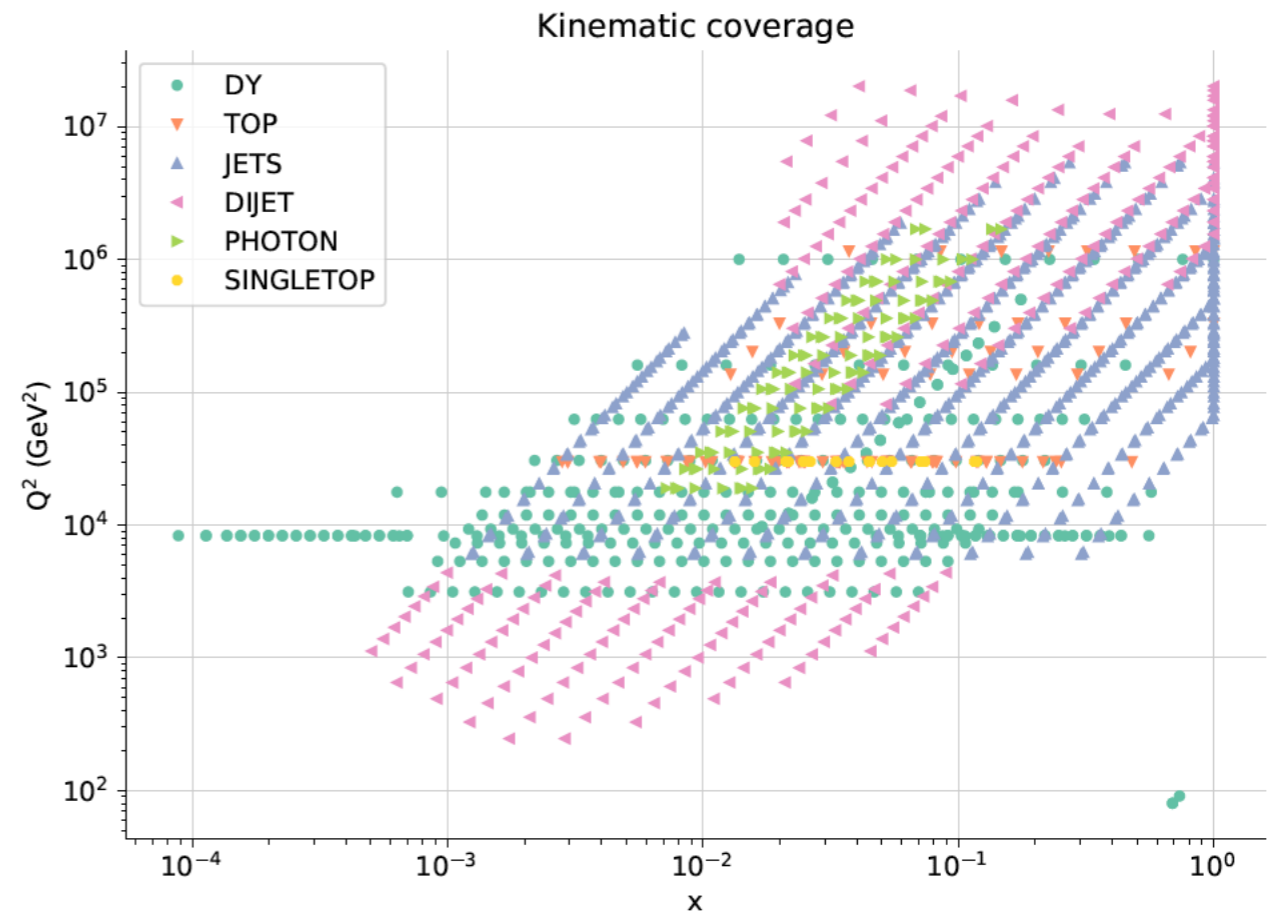
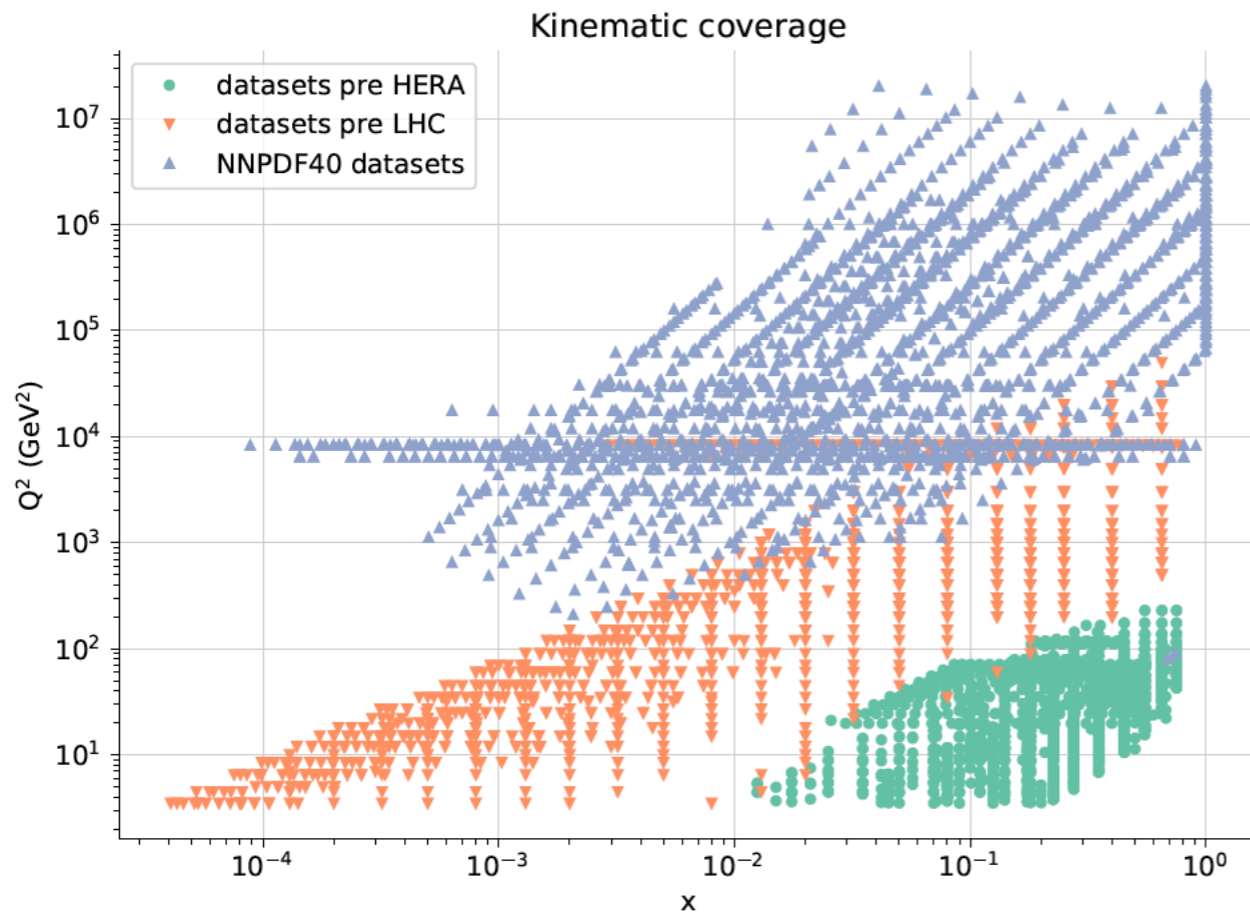
PDF Groups

Collaborations/Groups active in DGLAP analyses and PDFs determinations:



NNPDF4.0

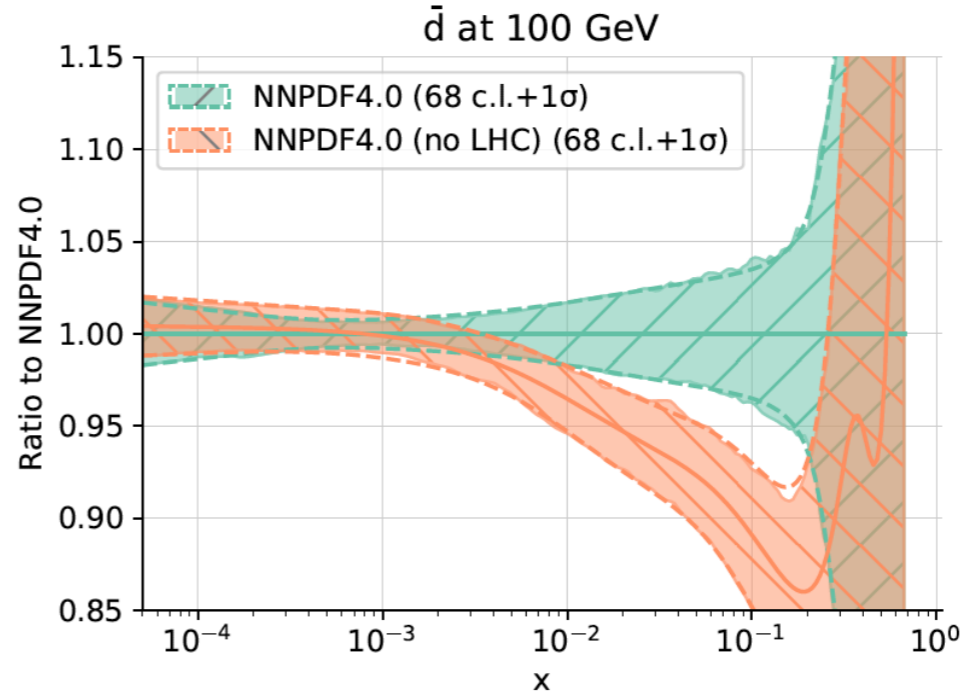
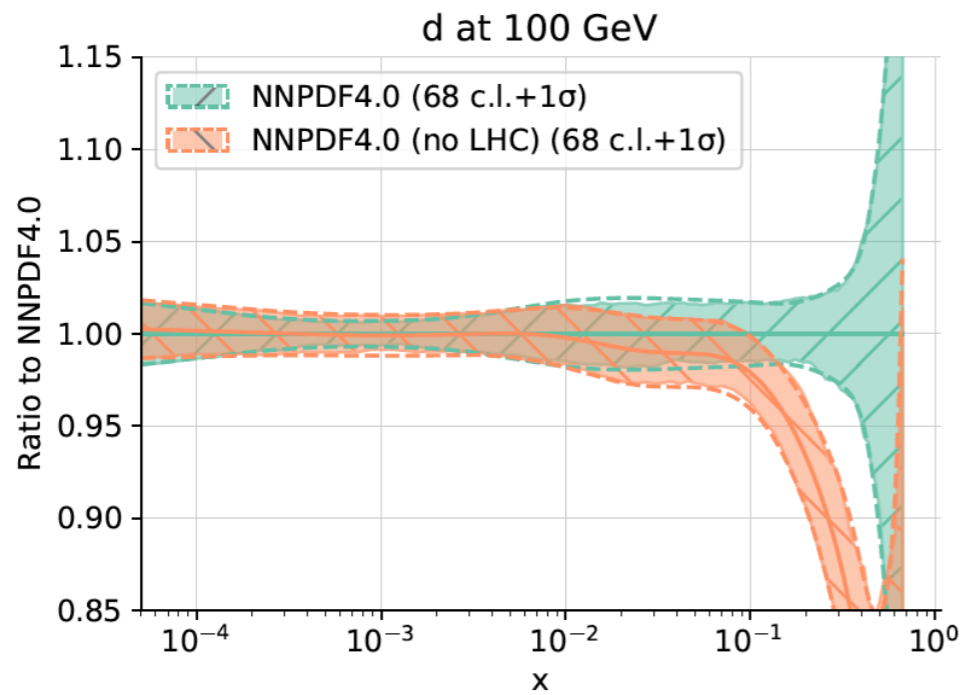
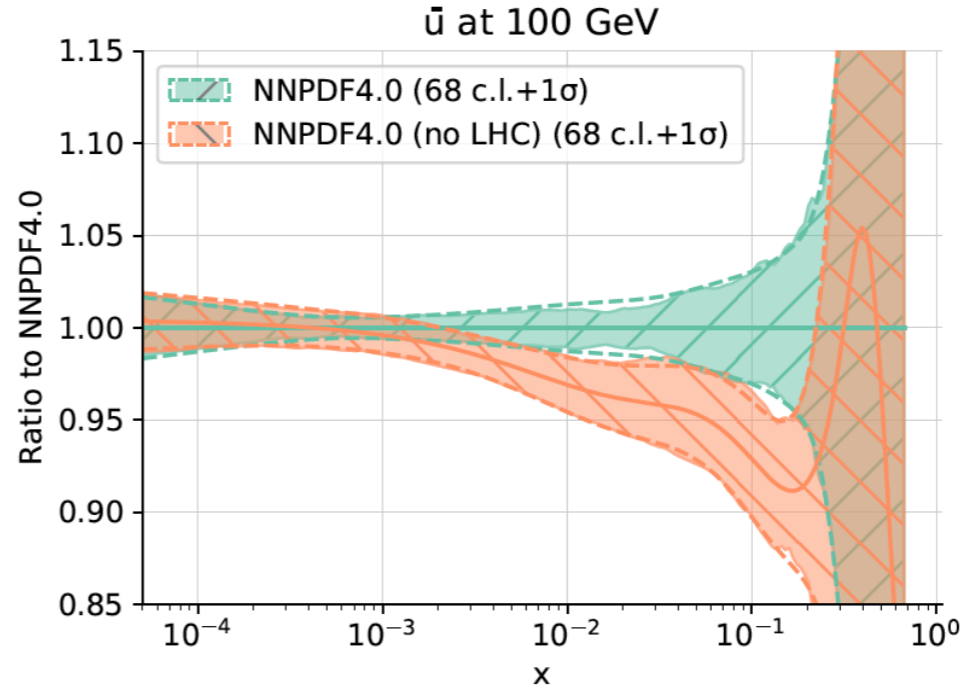
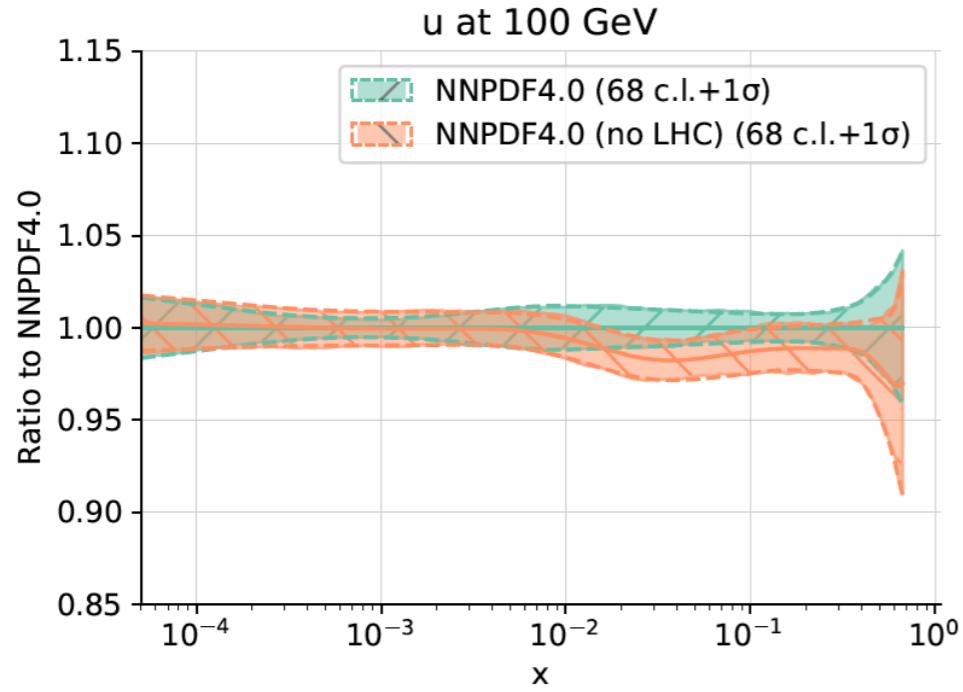
Kinematic regions and observables:



<https://arxiv.org/abs/2109.02653>

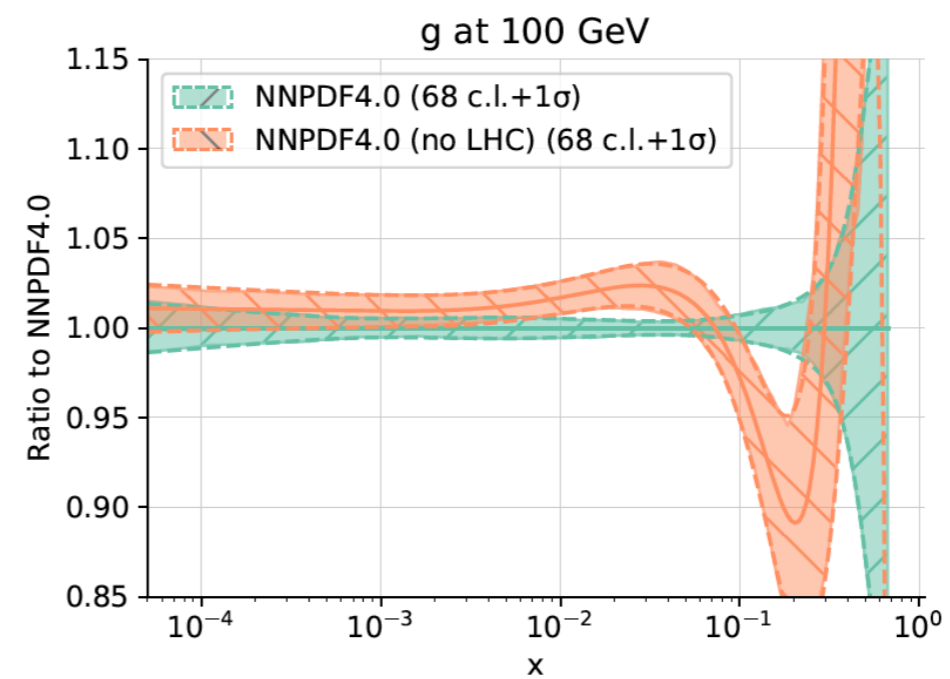
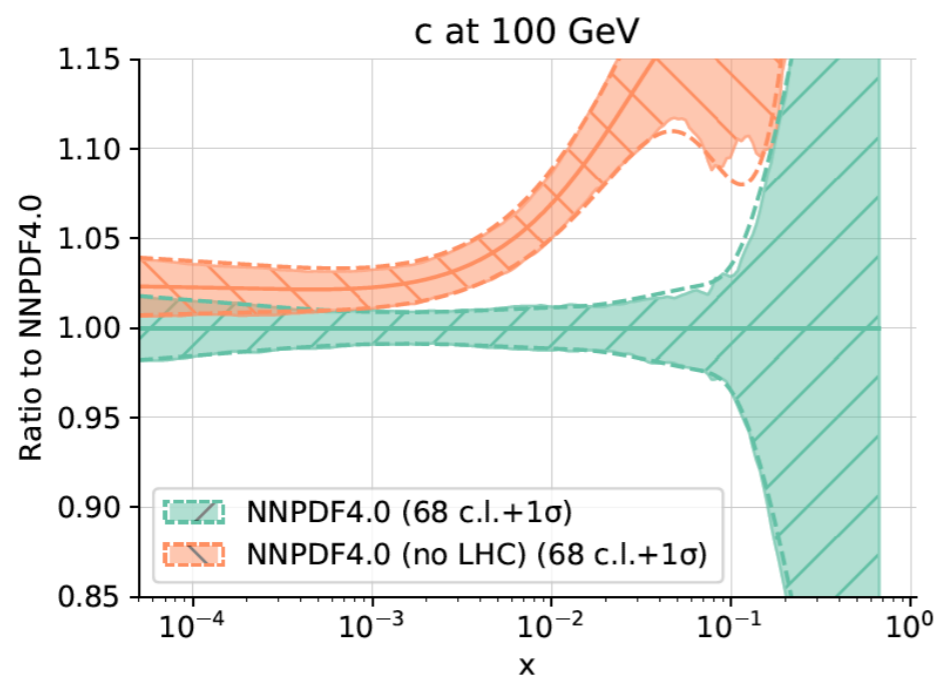
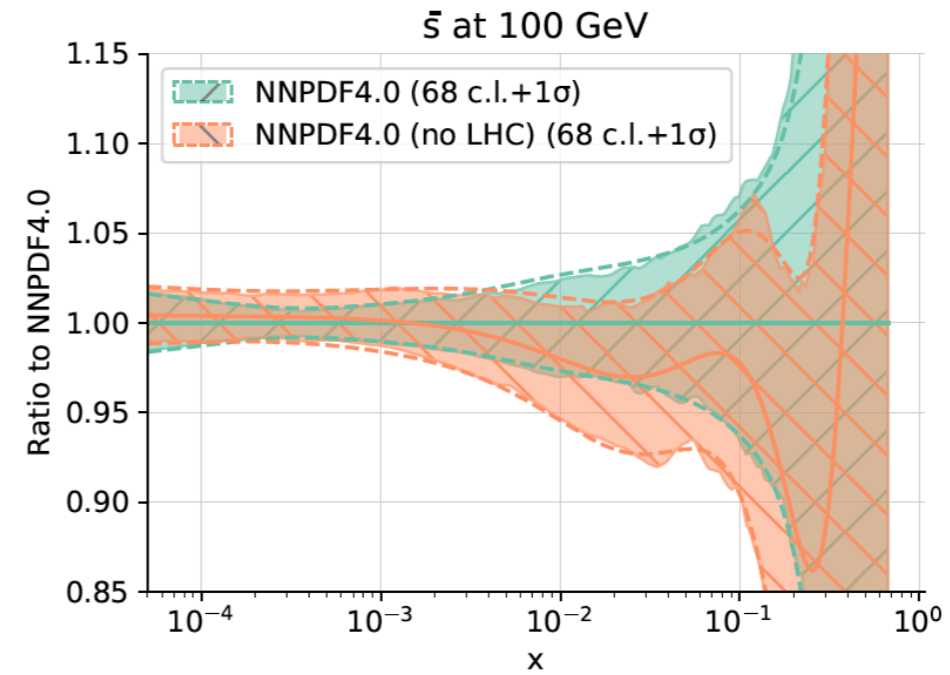
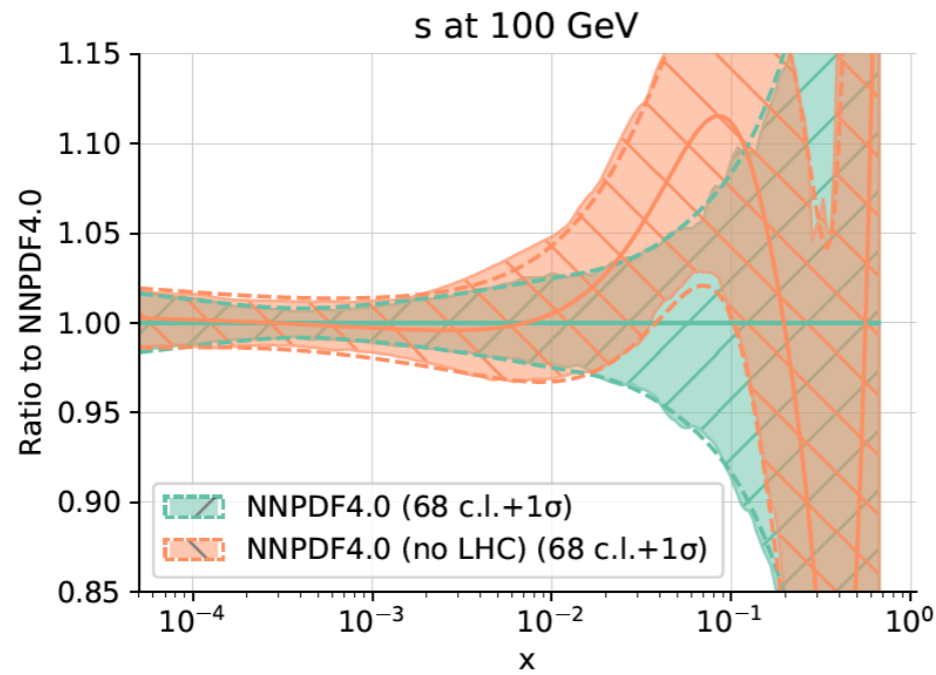
NNPDF4.0

Impatto dati LHC:

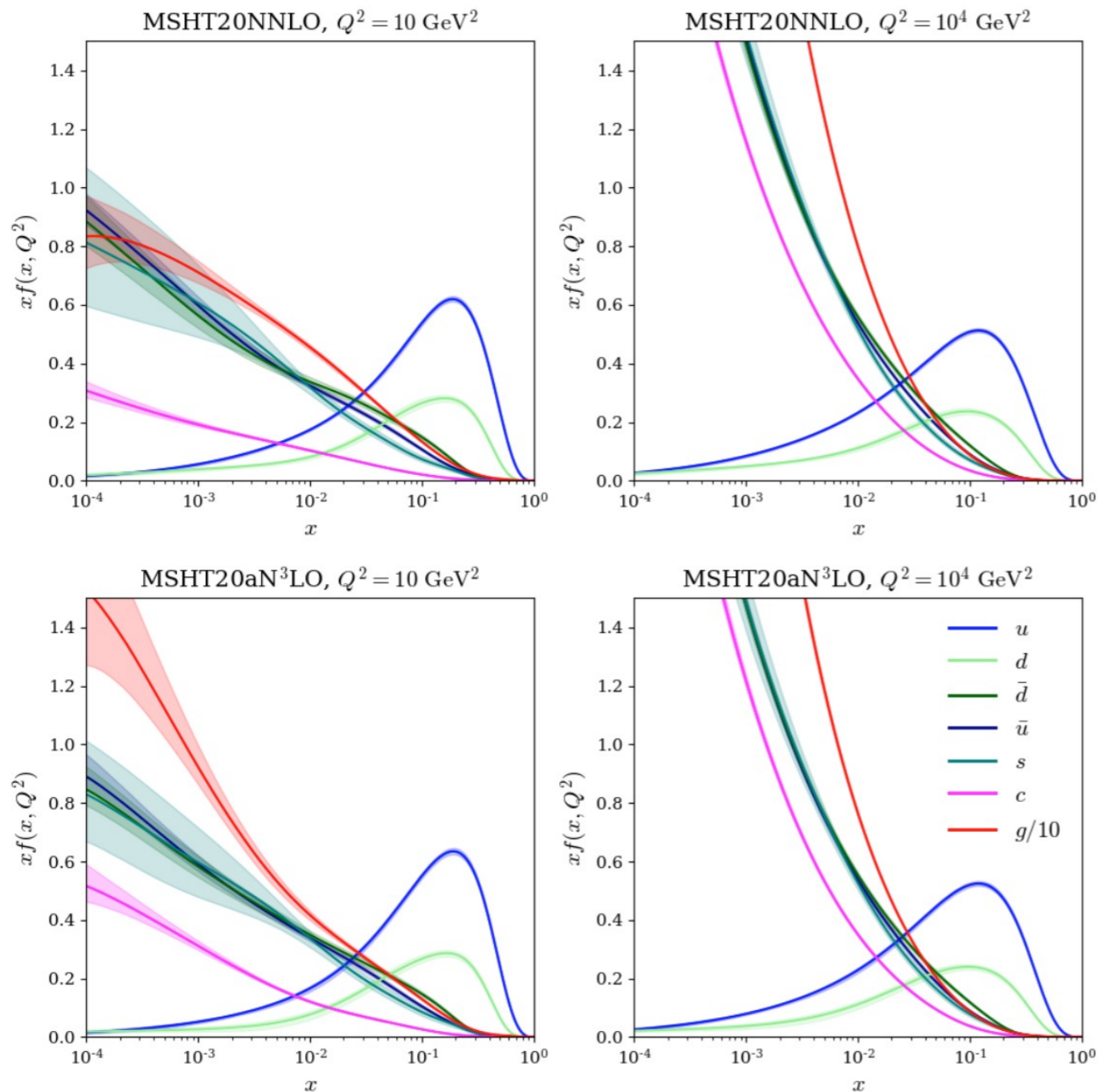


NNPDF4.0

Impatto dati LHC:



MSHT: Approximate N³LO PDFs



First approximate N3LO PDFs

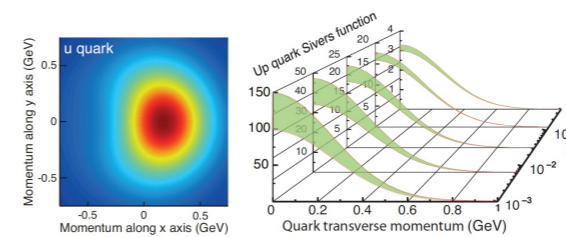
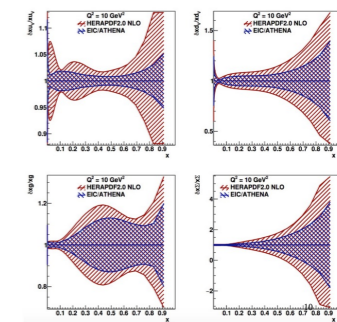
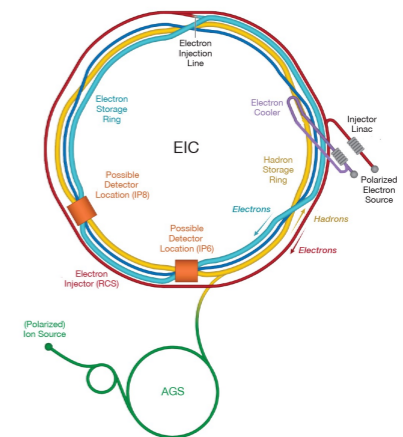
Glucan rises significantly at low

First attempt to quantify theoretical uncertainties

arXiv:2207.04739

III. EIC

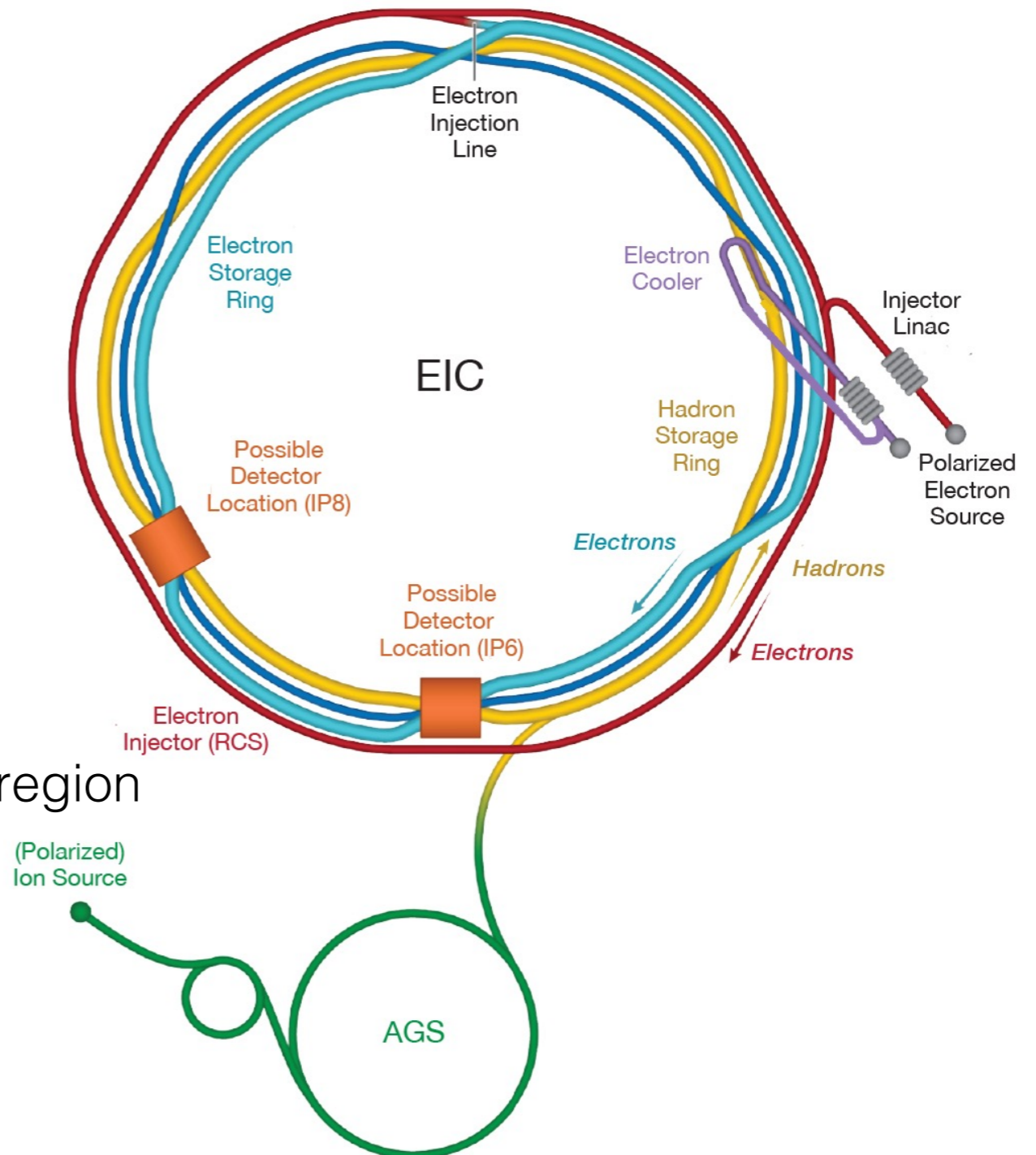
- Accelerator
- Scientific goals
- PDFs



EIC

The main design requirements of the EIC:

- Highly polarized electron (70%) and proton (70%) beams
- Ion beams from deuterons to heavy nuclei
- Variable e+p center-of-mass energies from 20-100 GeV, upgradable to 140 GeV
- High collision electron-nucleon luminosity 10^{33} - 10^{34} cm⁻² s⁻¹
- Possibility to have more than one interaction region



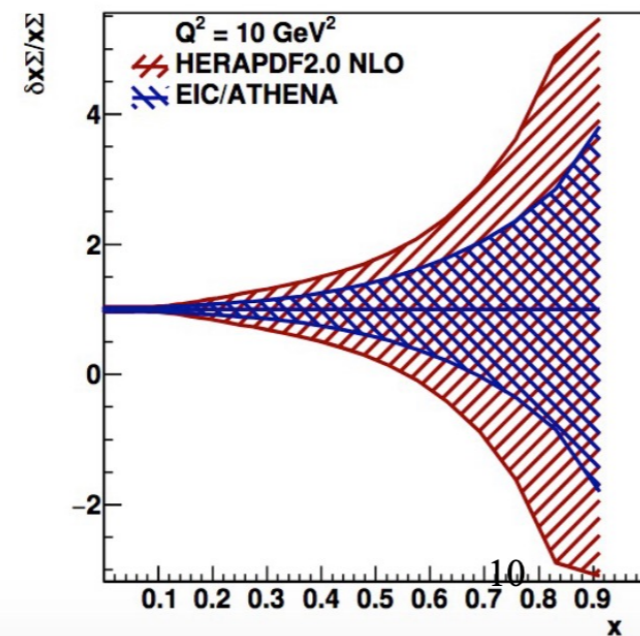
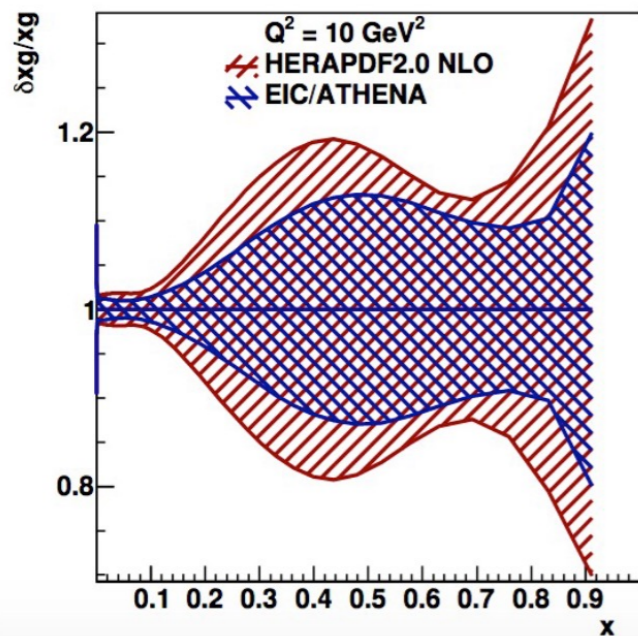
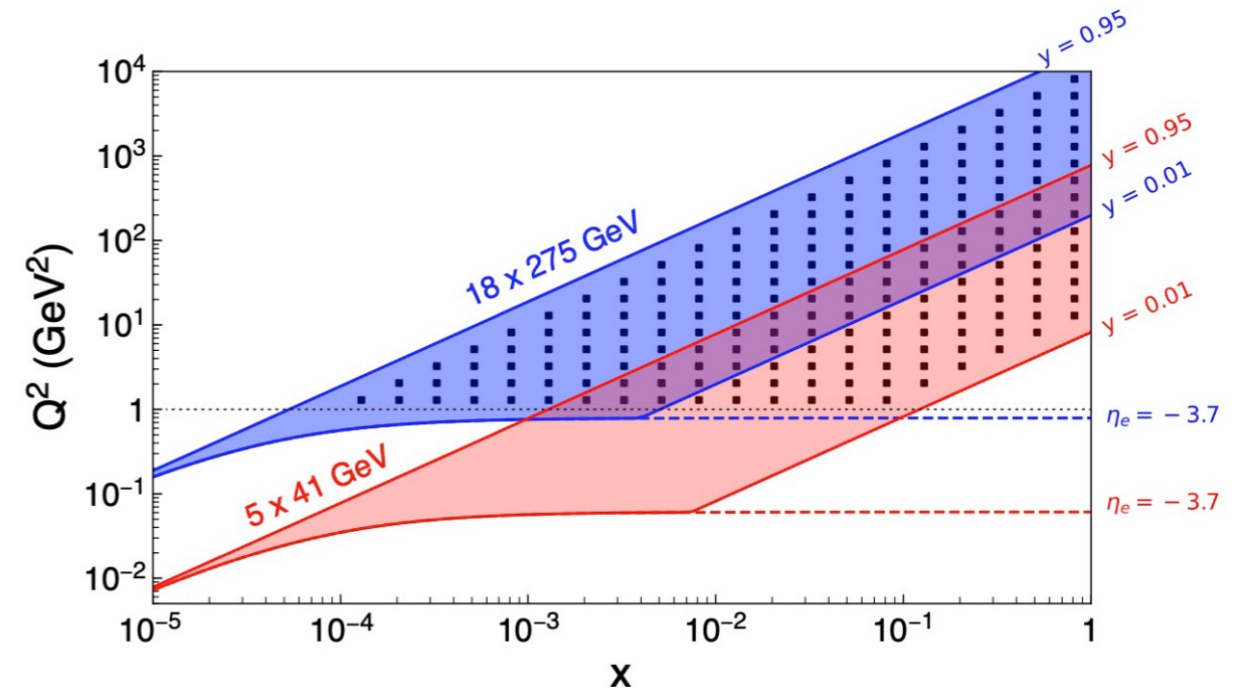
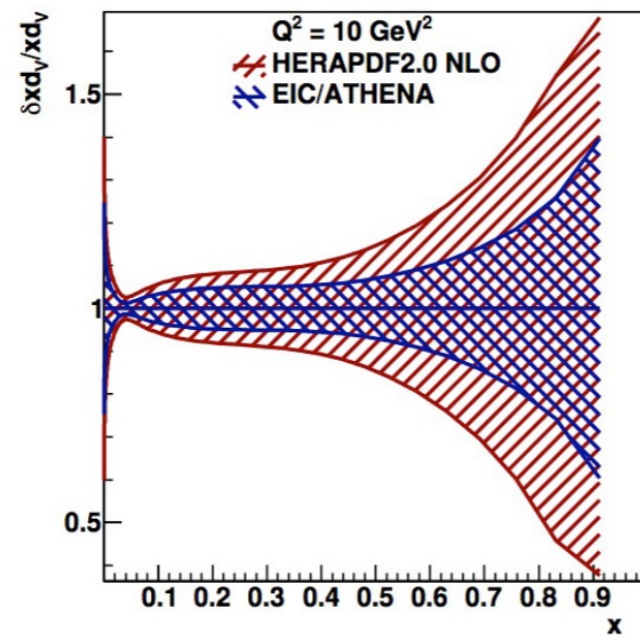
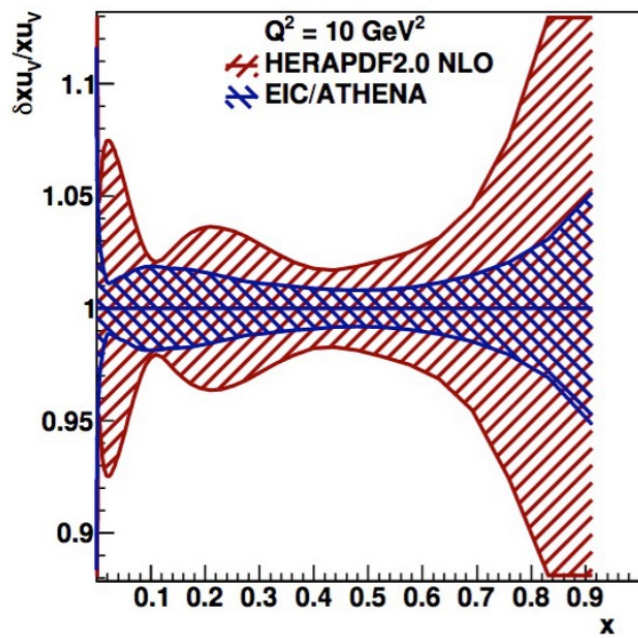
EIC Scientific Goals

Give answers to the 'key scientific questions' of the Yellow Report :

- How do nucleonic properties such as mass and spin emerge from the partons and their interactions?
- How are the partons distributed within the nucleon both in momentum and in spatial position?
- How are the partons distributed within the nucleon both in momentum and in spatial position?
How do confined hadronic states emerge from these quarks and gluons?
How do quark-gluon interactions create nuclear binding?
- How does a dense nuclear medium affect the dynamics of quarks and gluons and their correlations and interactions? What happens to the gluon density in the nuclei?

EIC: Collinear PDFs

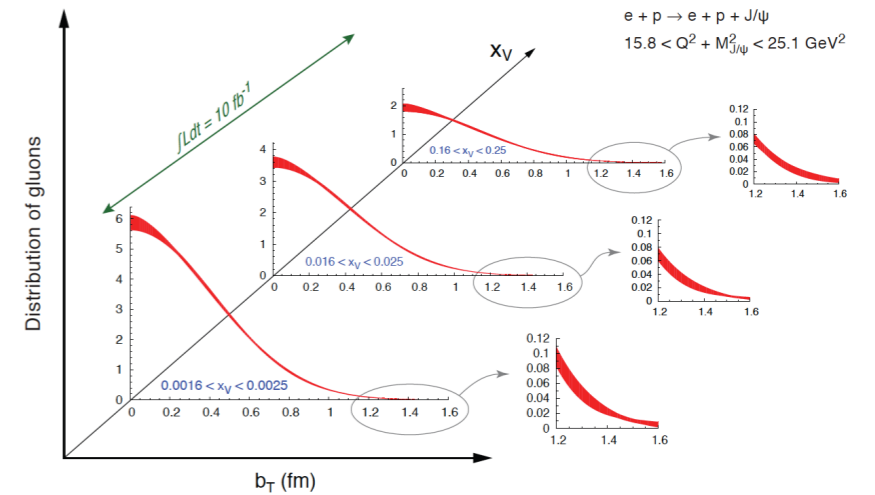
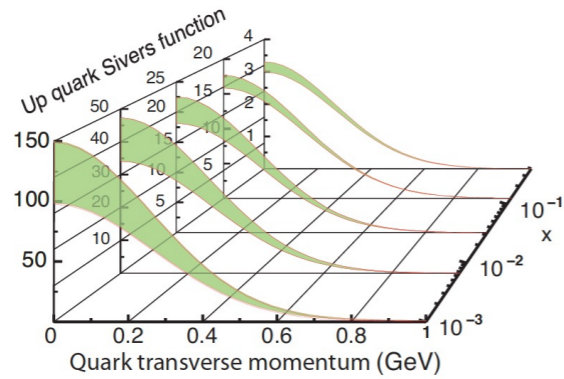
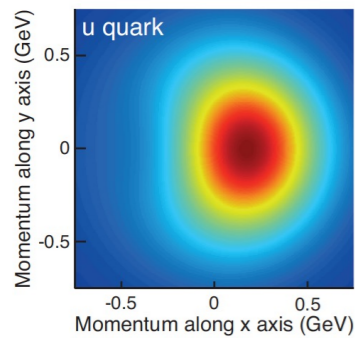
Improved PDFs (simulated data (YR)):



| e-beam E | p-beam E | \sqrt{s} (GeV) | inte. Lumi. (fb^{-1}) |
|----------|----------|------------------|----------------------------------|
| 18 | 275 | 140 | 15.4 |
| 10 | 275 | 105 | 100.0 |
| 10 | 100 | 63 | 79.0 |
| 5 | 100 | 45 | 61.0 |
| 5 | 41 | 29 | 4.4 |

P. Newman et al.
DIS workshop 2022

3D Nucleon Imaging: Wigner functions, TMDs & GPDs



Wigner Distributions

